To the Graduate Council:

I am submitting herewith a thesis written by Scott Allen Stafford entitled "Investigation of the Nonlinear Behavior of a Weakly-Ionized Plasma." I have examined the final copy of this thesis for form and content and recommend that it be accepted in partial fulfillment of the requirements for the degree of Master of Science, with a major in Electrical Engineering.

J. Reece Roth, Major Professor

We have read this thesis
and recommend its acceptance:

Accepted for the Council:

Vice Provost
and Dean of the Graduate School

STATEMENT OF PERMISSION TO USE

In presenting this thesis in partial fulfillment of the requirements for a Master's degree at the University of Tennessee, Knoxville, I agree that the Library shall make it available to borrowers under rules of the library. Brief quotations from this thesis are allowable without special permission, provided that accurate acknowledgement of the source is made.

Permission for extensive quotation from or reproduction of this thesis may be granted by my major professor, or in his absence, by the Head of Interlibrary Services when, in the opinion of either, the proposed use of this material is for scholarly purposes. Any copying or use of the material in this thesis for financial gain shall not be allowed without my written permission.

Signature Scott A. Stafford

Date 4/27/89

INVESTIGATION OF THE NONLINEAR BEHAVIOR OF A WEAKLY-IONIZED PLASMA

A Thesis
Presented for the
Master of Science
Degree
The University of Tennessee, Knoxville

Scott Allen Stafford

May 1989

ACKNOWLEDGMENTS

The author wishes to express his sincere appreciation to Dr. J. R. Roth for his patience, financial support, and helpful advice throughout the course of this research.

The author also extends his gratitude to the remaining members of his committee, Dr. Mark Kot and Dr. Igor Alexeff. Dr. Kot's input was especially helpful in gaining a better understanding of the mathematics involved.

A special thanks is also extended to Roberta L. Campbell and Jenny Daniel for their help with the typing and figure preparation of this thesis.

Finally, the author wishes to express his appreciation to his family and friends for their support and encouragement throughout his academic career.

This work was supported by both the Office of Naval Research and the Air Force Office of Scientific Research. The respective contract numbers are ONR N00014-88-K-0174 and AFOSR-86-0100.

ABSTRACT

The nonlinear behavior of plasmas has been studied by conventional time series methods for many years. Since the advent of the concept of chaotic dynamics in the early 1960's, many new theoretical approaches to turbulence have been developed. In the past ten years these methods have been applied to plasma fluctuations. In the last two or three years, commercial computer software has become available which allows the ready application of a wide range of analytical methods from nonlinear dynamics to laboratory plasmas. Most applications thus far have been to pulsed or unmagnetized plasmas. This report will describe the application of chaos theory to a steady-state, magnetized plasma.

TABLE OF CONTENTS

LIST OF TABLES

LIST OF FIGURES

FIGURE PAGE

CHAPTER I

INTRODUCTION

In the past twenty-five years, research in nonlinear dynamics has flourished. In particular, new concepts have been developed to quantify chaotic behavior. Many of these concepts had their origin in the work of Edward Lorenz, a meteorologist interested in the behavior of a simplified set of equations which model convection in the atmosphere (Lorenz, 1963). Since then these concepts have been applied to fluid flow (Brandstater et al., 1983), chemical reactions (Simoyi et al., 1982), the spreading of diseases (Schaffer, 1985), and biological rhythms (Glass, 1983).

The purpose of this thesis research is to apply the various tools of nonlinear dynamics to potential fluctuations measured in a steady-state, magnetized plasma. The plasmas generated in the UTK Plasma Science Laboratory do not allow us to examine a well-defined transition from coherence to turbulence. Therefore, this leaves two main goals: to look for evidence of low-dimensional chaos; and to look for a trend, or lack of trend, in the parameters which describe the state of turbulence. Chaos-related concepts which were used in this study are reconstructed phase portraits, Poincare sections, correlation dimensions and Lyapunov exponents.

This report will consist of eleven chapters, including this one. Chapter II is a general overview of chaotic dynamics. Chapters III and IV are an introduction to the fundamental mathematical concepts of chaotic dynamics for those readers new to this topic. In Chapter V a brief discussion of the effects of noise is given. Chapter VI is for those readers wanting to learn more about previous applications of nonlinear dynamics to plasmas. In Chapter VII the experimental apparatus and data handling system are described. Chapter VIII gives a brief description of the software package that was used to study the nonlinear behavior of the plasma fluctuations. Chapter IX consists of a comparison of two known reference cases to a particularly interesting set of plasma data. Chapter X is comprised of the results of parametric variation on the state of turbulence. Finally, conclusions and suggestions for future work are discussed in Chapter XI.

CHAPTER II

SURVEY OF CHAOTIC DYNAMICS

There are two ways in which one can define the term chaos. One being in a scientific sense and the other general. Using a dictionary as the source for the general concept yields the following definition: great confusion or complete disorder. The more scientific definition might be: random, unpredictable behavior of deterministic systems. These two definitions are not totally unrelated, but the latter appears to be contradictory. By definition, a deterministic system is predictable; but it is a sensitive dependence upon initial conditions that leads to this random-like behavior. Chaotic dynamics was pioneered by such individuals as Poincare and Smale, but Lorenz reestablished this exciting field of study while studying a simple set of equations he had developed to model air flow in the atmosphere. These equations exhibited what is now known as chaotic behavior. This observation appears to go directly against Isaac Newton's belief that the deterministic equations of classical mechanics imply a regular, ordered universe (Koyre and Cohen, 1972). Therefore, it is no wonder that this field of study has grown so rapidly.

A. Why Study Chaos?

One might ask: beyond the fact that the subject is interesting, what practical reasons are there for studying chaos? First, there is the possibility of gaining an understanding of the source of apparently random behavior, and maybe even being able to control it. Another reason is that greater knowledge of the field brings new tools for detecting and quantifying chaos. In addition, there is the question of the usefulness of numerical simulation of nonlinear systems. Perhaps one of the most important reasons for studying chaotic behavior is the need to understand turbulence.

There are several reasons why researchers have an interest in applying chaos theory to plasma turbulence. In this application, turbulence implies a random-like fluctuation of the electric field and particle number densities. The issue of turbulence is of extreme importance in the fusion community. It is generally accepted that turbulence is the likely origin of anomalous particle and energy losses that are the main obstacle to the success of the tokamak concept. These losses are due to particle transport across the confining magnetic field lines and are much higher than that predicted by neoclassical transport theory. It is the traditional assumption that turbulence consists of infinitely many degrees of freedom, each corresponding to an independent oscillator. When determining the effects of turbulence on energy transport, it is very important to know whether only a few frequency components dominate or if there is actually an infinite number of them. This is a principal motivation for looking for chaotic behavior in a plasma. Another might be to learn about the reproducibility of plasma conditions during laboratory experiments.

B. Systems That Produce Chaotic Behavior

The concepts of chaotic dynamics have been around for approximately 25 years. Initially most of the work done in this area dealt with systems of mathematical equations. More recently, methods have been devised to apply these concepts to actual physical systems which exhibit nonlinear behavior.

Chaotic behavior has been observed in numerous experiments. Much of this research has been done in the field of fluid dynamics, while studying the transition from laminar to turbulent flow. Chaos is known to occur in Taylor-Couette flow, (Brandstater et al., 1983) which is flow between two concentric, rotating cylinders; Rayleigh-Benard convection (Malraison et al., 1983), which is flow created by a thermal gradient; and open flow systems, such as wakes (Sreenivasan, 1985).

Fluid dynamics is not the only field of study in which physical evidence of chaos has been found. Some other applications which have produced this type of behavior are: buckled beams (Moon and Holmes, 1979), nonlinear electrical circuits (Chua and Madan, 1988), chemical reactions (Simoyi et al., 1982), nonlinear optical systems (Ikeda et al., 1980), electrical discharges (Brown et al., 1987), solid-state plasmas (Held and Jeffries, 1986), and unmagnetized plasmas (Cheung et al., 1988). There exist many other nonlinear systems which exhibit complicated, unpredictable behavior that could be chaotic in the precise, mathematical sense. Some of these are: The changing weather, the rise and fall of the economy, the interaction of biological populations, the response of cardiac cells to electrical impulses, and fluctuations in a magnetized plasma.

CHAPTER III

BASIC PRINCIPLES OF NONLINEAR DYNAMICS

Before describing the experimental program, it will be necessary to discuss a few basic concepts.

A. Types Of Dynamical Systems

There are two fundamental types of dynamical systems, stochastic and deterministic. A stochastic system is one that can only be described using statistics. Deterministic systems are completely predictable, in the sense that given the initial conditions and equations of motion, the behavior of such a system can be determined for all time. Chaotic systems are a class of deterministic systems which may produce very irregular behavior, and also lack long-term predictability as a result of their extremely sensitive dependence upon initial conditions.

B. Phase Space

In order to gain information about dynamical behavior, it usually is best to think in terms of phase space. In this multidimensional space, a single point describes the system for an instant of time. For dynamical systems governed by a set of equations, the coordinates are the state variables. The coordinates often used for mechanical systems are the position and velocity for each independent degree of freedom in the system. However, the position and momentum are sometimes used for mechanical systems instead. For an experiment, this is often a formidable task. When studying a complex system, one would not only have to measure numerous signals, but one would also be required to incorporate some type of differentiation or integrator circuit.

A simpler alternative was suggested by Packard (Packard et al., 1980), and later proved by Takens (Takens, 1981). They showed that after transients die out, it is possible to reconstruct a phase portrait from the measurement of a single variable. This reconstructed phase portrait may not look exactly like the original, but the dynamical properties are the same. The method of reconstruction is straightforward; given the initial time series, say $X(t)$, a time delay, τ, is chosen and introduced in order to get coordinates of $X(t)$, $X(t + \tau)$, $X(t + 2\tau) \ldots X(t + (p-1)\tau)$, where p represents the number of dimensions. Since $X(t)$ is made up of discrete points, a series of p-dimensional vectors will be obtained.

For an infinite set of noise-free data the value of τ that is used is almost arbitrary, but for actual data it is necessary to select the time delay within a certain range. If τ is chosen too small, the resulting phase portrait will be greatly compressed. On the other hand, if τ is too large the area in phase space will be completely filled. This is due to the fact that points far apart on the trajectory are essentially uncorrelated.

For quasi-periodic signals, it has been found expedient to use a value of τ that is between ten and thirty percent of the period (Schaffer et al., 1988). In the case of broadband fluctuations, it is better to consider the e-folding time of the autocorrelation function (Simm et al., 1987). In the work that follows, the time lag was taken to be approximately twenty-five percent of the "period".

C. Attractors

There are four types of steady-state motion associated with dynamical systems. They are equilibrium, periodic motion, quasi-periodic motion, and chaotic motion. Each of these forms of motion is considered to have an attractor associated with it. An attractor is a bounded region in phase space towards which a time history approaches after transients die out. One of the four kinds of attractors will be present for any dissipative system. An example of each type of attractor can be found in Figure III-1.

The first three forms of motion mentioned above have been understood for many years. These result in relatively simple attractors. The attractor associated with equilibrium is called a fixed, or equilibrium, point. A damped harmonic oscillator has this type of attractor. Periodic motion results in what is called a limit cycle. This is just a simple, closed curve in phase space. The third classic type of motion is quasi-periodic. The simplest example is a system that has two incommensurate frequencies associated with it; one being its natural frequency and the other a forcing frequency. This system's attractor would be what is called a two-torus.

The attractor for a chaotic system is much more complicated. While the first three cases mentioned above are all simple geometric objects, this is not true of chaotic attractors. For this reason, they have come to be known as strange attractors. An interesting property of strange attractors is that they have a sensitive dependence on initial conditions. This is due to the "stretching and folding" that occurs in phase space. While volume is being contracted in some directions, it may be stretched in others. In order to remain within the bounded region, the volume element will also be folded.

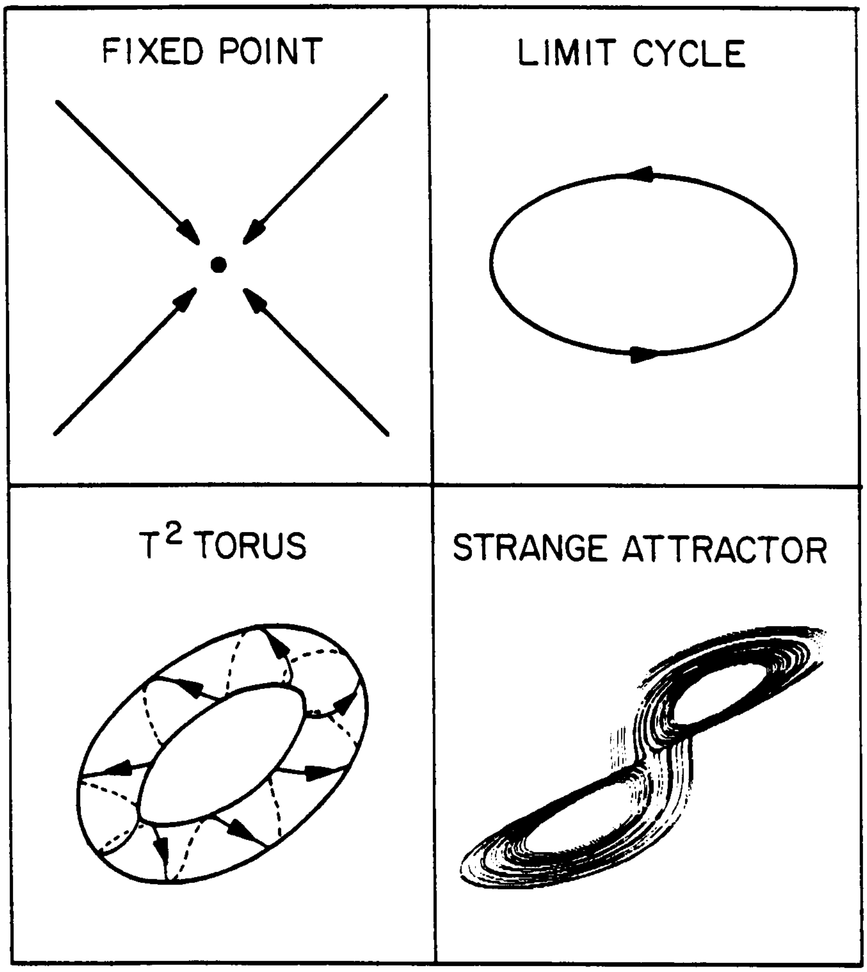

Figure III-1. Types of attractors

Even though the total volume contracts, lengths will not necessarily shrink in all directions. Therefore, points on the attractor that are initially arbitrarily close will begin to diverge at an exponential rate. This leads to what Lorenz called the "Butterfly Effect" (Gleick, 1987). With just an infinitesimal uncertainty in initial conditions, one will be unable to predict the system's future.

D. Fractals

As mentioned in the previous section, a strange attractor arises from the process of stretching and folding. This results in a multisheeted structure which exhibits self-similarity. This type of object has been referred to as a fractal (Mandelbrot, 1983). The following will be a description of two of the simplest examples of fractal objects.

The first example is known as the Cantor set (Moon, 1987). It is illustrated in Figure III-2. The construction of the Cantor set begins with a line segment one unit long. This is divided into three equal sections and the middle one is then removed. This leaves two line segments, each one-third of a unit long. This process is repeated for each remaining line segment and so on. What results is an infinite set of disconnected points that display the concept of self-similarity. As will be seen below, the fractal dimension of this set of points lies between zero and one. This may be understood on the basis that it is more than a point, yet less than a line.

A second example is the Koch curve, or snowflake (Moon, 1987). The construction process is depicted in Figure III-3. One begins with an equilateral triangle. After dividing each side into thirds, attach smaller equilateral triangles to the central third. There are now twelve sides. Once

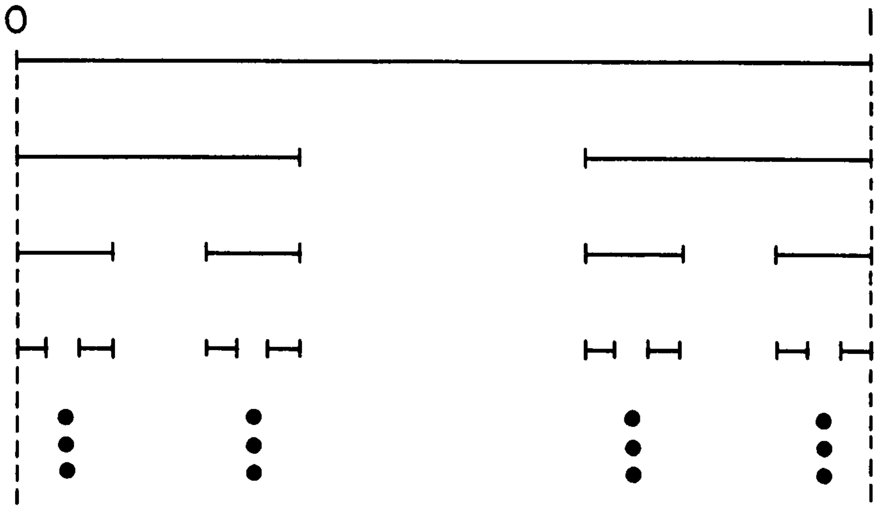

Figure III-2. Construction of the Cantor set

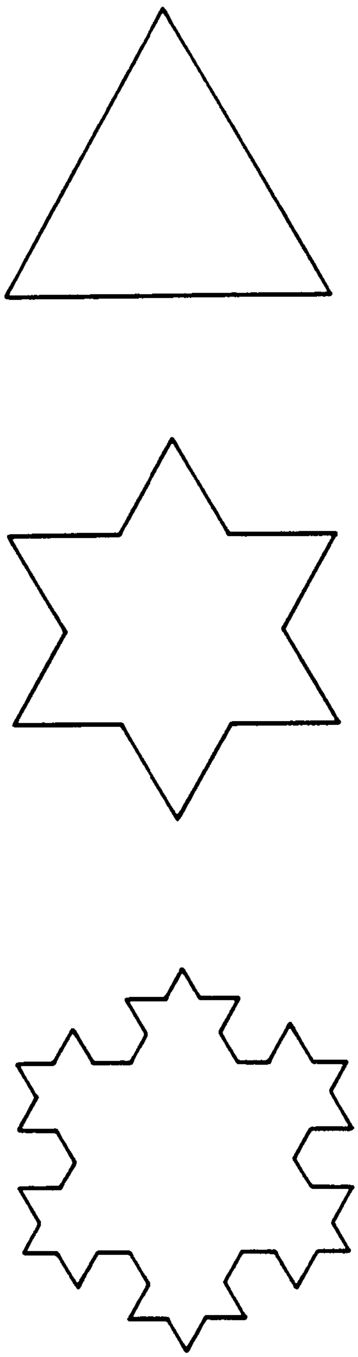

Figure III-3. Construction of the Koch curve

again, each side is divided into thirds and a smaller equilateral triangle is attached to the middle third. This procedure is repeated indefinitely. In the limit, one obtains a curve that has an infinite length while occupying only a finite region of the plane. This property is typical of many strange attractors. The dimension of the Koch curve will be shown to have a value between one and two. This also can be understood on the basis that it is more than a line, but less than a plane.

E. Routes To Chaos

There are four principal theories for the manner in which chaos evolves. Two of these are named after their developers; the Landau turbulence theory and the Ruelle-Takens route to chaos. The other two theories are best known by terms that describe the behavior observed as chaos develops. These two routes are called period-doubling, and intermittency. Each of these will be described briefly.

An early theory on turbulence was put forth by Landau (Landau, 1944). He felt that successive bifurcations would lead to increasingly complex behavior; where bifurcation denotes a sudden change in behavior as a parameter or set of parameters is varied. This theory implies that: a system becomes chaotic gradually, and that only systems with a large number of degrees of freedom can exhibit chaotic behavior. As it has turned out, the Landau theory has been shown to be insufficient and does not occur for any known system (Eckmann, 1981).

A more recent theory developed by Ruelle and Takens (Ruelle and Takens, 1971) states that a small number of bifurcations can produce chaos. In actuality only two, or at most three, bifurcations are necessary. This route to chaos has been verified experimentally numerous times (e.g. Swinney and Gollub, 1978). Figure III-4 is a simple representation of the evolution of the power spectrum of a system that follows this theory.

The period-doubling, or Feigenbaum, route to chaos has also been well studied (e.g. Feigenbaum, 1978). In this route, a system will start out with a periodic motion. As a parameter is varied, the motion will undergo a bifurcation. The period will become twice its original value. As the parameter is changed more, the system may continue to experience bifurcations. After each, the period will be twice its previous value. Once the parameter reaches a certain value, the motion may become chaotic. This period-doubling sequence has been observed in quite a few systems. Some of these are the Lorenz equations (Sparrow, 1982), the Henon map (Eckmann, 1981) and Rayleigh-Benard convection (Libchaber, 1983).

Another way in which chaos has been observed to develop is called the intermittency route to chaos. This route was predicted by Pomeau and Manneville (Manneville and Pomeau, 1980). The motion is originally quite regular, but as a control parameter is varied, short bursts of chaos are seen. As the parameter is varied more, the motion may become completely chaotic. This road to chaos is also exhibited by the Lorenz equations (Pomeau and Manneville, 1980) as well as in some types of fluid flow (e.g. Sreenivasan, 1985).

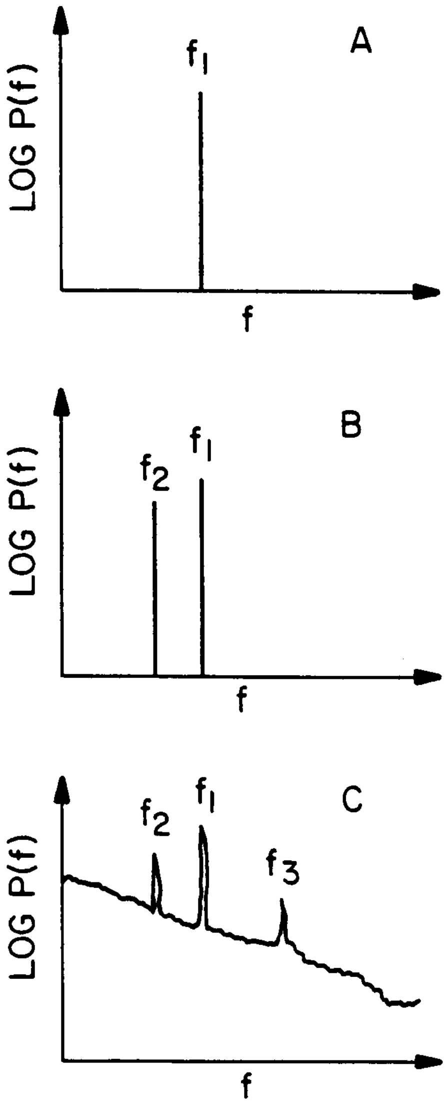

Figure III-4. Representation of the Ruelle-Takens route to chaos

CHAPTER IV

METHODS OF IDENTIFYING CHAOTIC BEHAVIOR

There are several ways to determine whether experimental data exhibit chaotic behavior, and to characterize this behavior. These methods, both qualitative and quantitative, will be discussed in this chapter.

A. Qualitative

1. Time Series

The first place to look for evidence of chaos is the time history of the signal. If it is not periodic, it could be either random or chaotic. Since it is possible for a signal to have more than one associated frequency, this method is not very conclusive. A signal that is typical of plasma fluctuations is shown in Figure IV-1.

2. Fourier Power Spectra

Another source of information is the Fourier spectrum of the measured signal. Fourier spectra are useful to distinguish between periodic, quasi-periodic, and chaotic signals. A characteristic of chaos is that it produces a broadband power spectrum. One must be careful when stating that a continuous power spectrum impies chaos. This is not necessarily true. A continuous spectrum is also characteristic of a system with a large number of degrees of freedom. Figure IV-2 is the Fourier power spectrum associated with the signal in Figure IV-1.

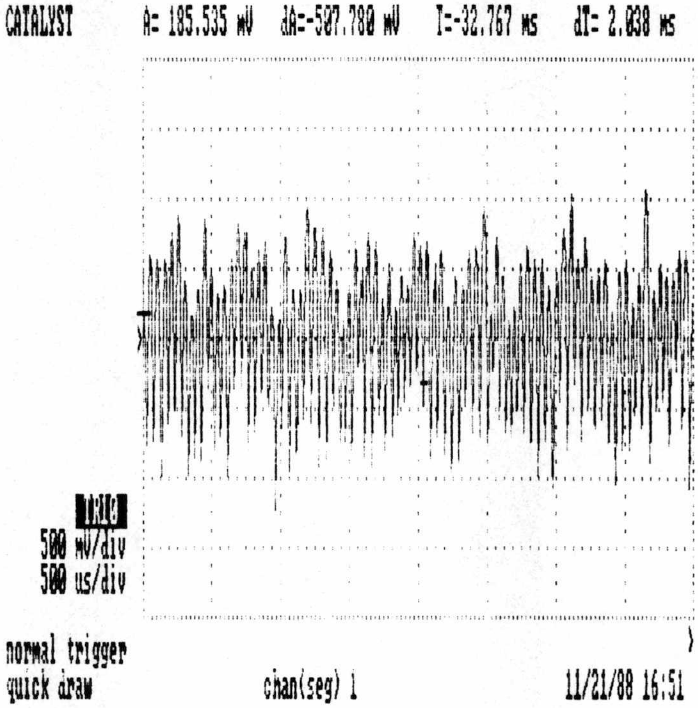

Figure IV-1. Characteristic plasma fluctuation signal

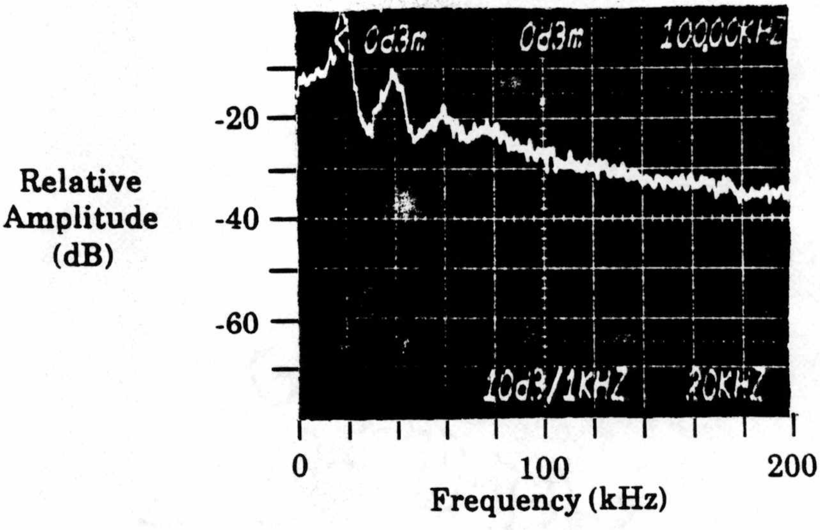

Figure IV-2. Fourier power spectrum associated with signal in Figure IV-1

3. Phase Space Portraits

As mentioned previously, the concept of phase space is very helpful when studying dynamical motion. There are two features to look for when examining a trajectory in phase space. One feature is that a chaotic signal will not produce a closed orbit, since this implies periodic motion. The other feature is the self-similarity of strange attractors. This simply means that the geometric structure on one scale is similar to that at another. This behavior is depicted in Figure IV-3. The top figure shows a complete two-dimensional view of the Rossler attractor. Each successive figure is an enlargement of the region enclosed in the small inner boxes. Even though the attractor is blown up several times, the lower three figures look very similar.

4. Poincare Sections

This method extends directly from the concept of phase space. When working with a three-dimensional phase portrait, a Poincare section is obtained simply by intersecting the trajectory with a plane of suitable orientation. Figure IV-4 illustrates this concept. On the right side of the figure is a three-dimensional phase portrait of the Lorenz attractor with a plane intersecting the lower part. The intersection of the trajectory with a plane gives a two-dimensional cross section of the attractor. This is what is shown on the left side of the figure. Figure IV-5 is a list of the possible outcomes when taking a Poincare section as well as their corresponding significance.

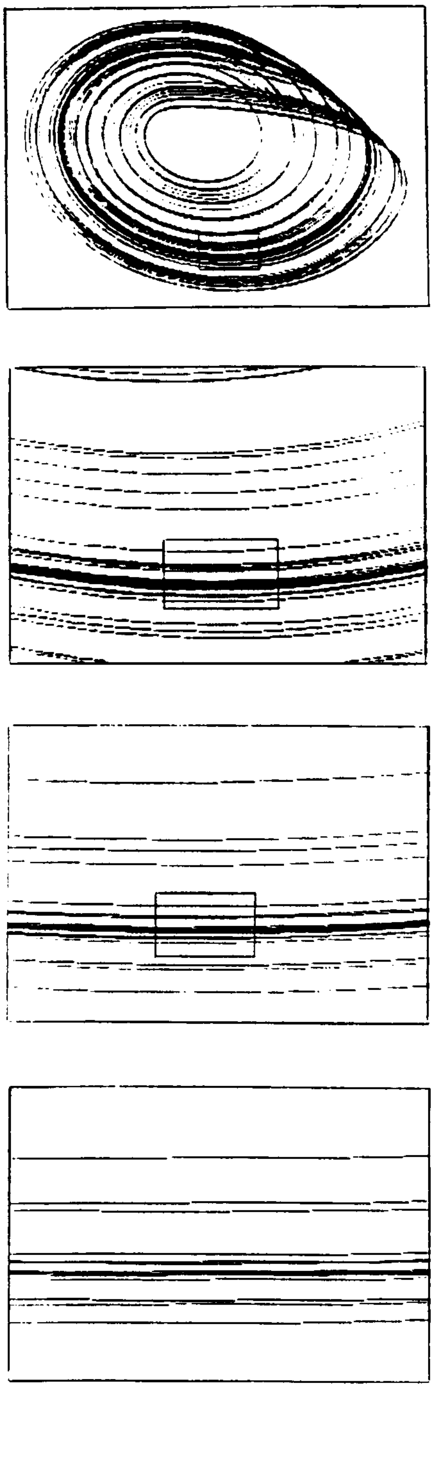

Figure IV-3. Illustration of self-similarity

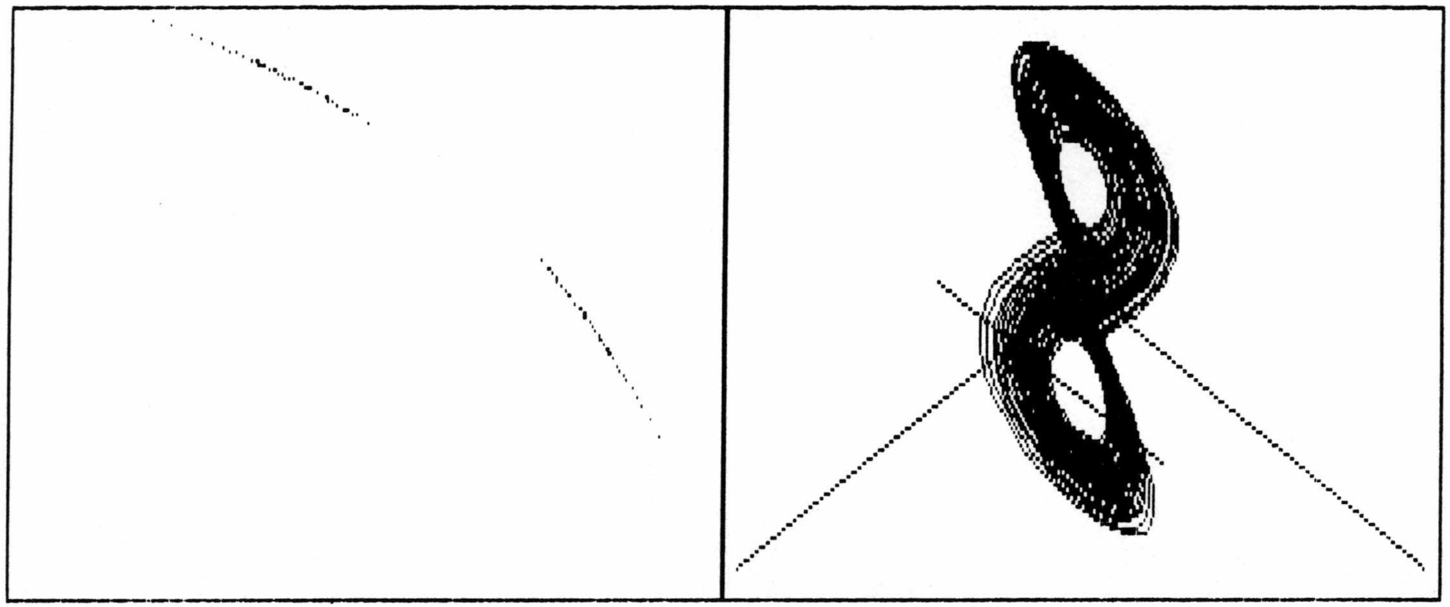

Figure IV-4. Method of obtaining Poincare section

Finite number of points: periodic or subharmonic oscillation

Closed curve: quasiperiodic, two incommensurate frequencies present

Open curve: suggest modeling as a one-dimensional map; try plotting $x(t)$ versus $x(t + T)$

Fractal collection of points: strange attractor in three phase space dimensions

Fuzzy collection of points: (i) dynamical system with too much random or noisy input; (ii) strange attractor but system has very small dissipation—use Lyapunov exponent test; (iii) strange attractor in phase space with more than three dimensions—try multiple Poincaré map; (iv) quasiperiodic motion with three or more dominant incommensurate frequencies.

Figure IV-5. Classification of Poincare sections (Source: Chaotic Vibrations, F. C. Moon)

B. Quantitative

The previous methods of identifying chaotic behavior yield only qualitative information. Therefore, these methods are not always adequate. One shortcoming is that a Fourier spectrum will not distinguish between chaos with a small number of degrees of freedom and white noise. Another disadvantage is that Poincare sections are limited to three-dimensional phase spaces. For these reasons, much effort has been put into developing means of quantifying chaos.

1. Fractal Dimension

The concept of a fractal, or non-integer, dimension can be quite difficult to comprehend. For "normal" attractors, it is easy to define a dimension. A fixed point has a dimension of zero, while a limit cycle and two-torus have dimensions of one and two, respectively. It is due to their regular structures that these classic attractors have integer-valued dimensions. The structure of a strange attractor is not regular by any means. As it turns out, most strange attractors have non-integer dimensions.

One might ask: What is the significance of a fractal dimension? In general, the dimension reveals the amount of information that is needed to specify the location of the trajectory within a given accuracy (Farmer et al., 1983). Most importantly, the dimension of a system is a lower bound on the number of variables that are necessary to model the system's dynamics. Therefore, if a system with ten degrees of freedom has a fractal dimension of 2.9, it may be possible to model its behavior using only three variables.

There are many different ways in which to measure the dimension of a set of points. Two of these will now be discussed. The first will be a geometric definition called the capacity. Next will be the widely-used correlation dimension. For a more detailed description of the different measures of dimension, see the article by Farmer et al. (1983).

a. Capacity

The first, and most basic, definition to consider is called the capacity. In this case, one is given the trajectory in p-dimensional space. It is desired to cover the set of points with small cubes of dimension ε, as shown in Figure IV-6. Letting $N(\varepsilon)$ be the minimum number of these cubes that is needed to cover the trajectory, the capacity dimension can be defined as (Farmer et al., 1983)

$$d_c = \lim_{\varepsilon \to o} \frac{\log N(\varepsilon)}{\log\left(\frac{1}{\varepsilon}\right)} . \qquad \text{(IV-1)}$$

The only requirement for this definition is that the number of points in the set be large.

In order to use this definition to get the dimension of a line of length L, one must realize that $N(\varepsilon) = L/\varepsilon$. By inserting this into the above equation and using L'Hopital's Rule, one can show that the capacity dimension of a line is one. In the same manner, it is simple enough to see that for a surface area, the dimension will be two. These results are obviously in agreement with the classic, or Euclidean, definition of dimension.

To show that the capacity can take on non-integer values, one may consider the two fractal objects introduced last chapter. It should first be pointed out that $\varepsilon \to o$ corresponds with $m \to \infty$, where m is the number of points in the set. Therefore, an alternate way of defining the capacity dimension is

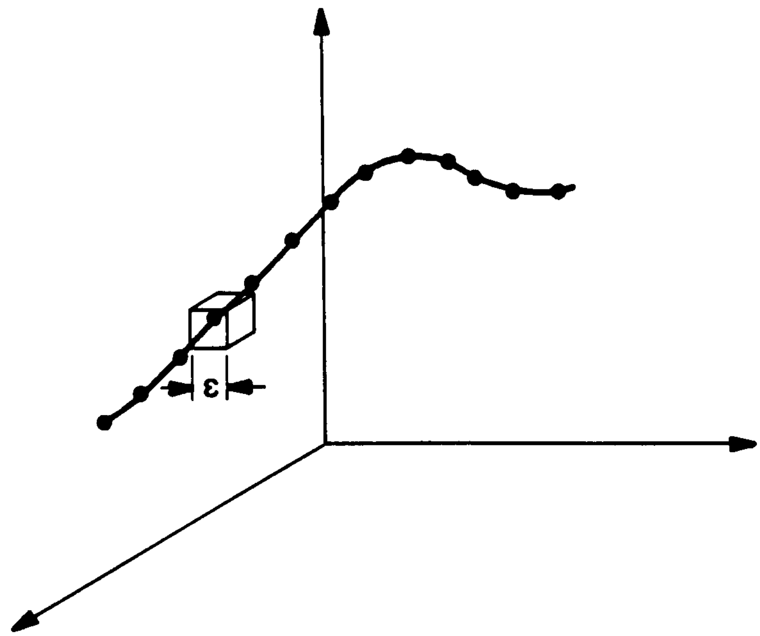

Figure IV-6. Illustration of the covering of a trajectory

$$d_c = \lim_{m \to \infty} \frac{\log N(\varepsilon)}{\log(\frac{1}{\varepsilon})} . \qquad \text{(IV-2)}$$

The dimension of the Cantor set (see section III-D) can be calculated rather easily. For $\varepsilon = 1/3$, the number of cubes needed to cover the set is two. Similarly, for $\varepsilon = 1/9$, $N(\varepsilon) = 4$. In general, for $\varepsilon = (1/3)^m$, $N(\varepsilon) = 2^m$. The above definition yields

$$d_c = \lim_{m \to \infty} \frac{\log 2^m}{\log 3^m} . \qquad \text{(IV-3)}$$

This is simply

$$d_c = \frac{\log 2}{\log 3} \approx 0.631. \qquad \text{(IV-4)}$$

Following the same procedure, one can compute the dimension of the Koch curve (see section III-D). Consider the m th iteration of the curve, where the zeroth is the original triangle. Letting the cube dimension be equal to the length of a line segment, it can be seen that $\varepsilon_m = (1/3)^m$ and $N_m(\varepsilon) = 4^m$. This results in a capacity dimension of

$$d_c = \frac{\log 4}{\log 3} \approx 1.262. \qquad \text{(IV-5)}$$

For simple fractal objects, the capacity dimension is adequate. However, when studying higher dimensional systems, the limit converges too slowly and this measure becomes computationally inefficient (Grassberger and Procaccia, 1983). For this reason the following definition was developed.

b. Correlation Dimension

The concept of the correlation dimension was established with the intention of improving upon the capacity. The concept behind it is as follows. Consider the set of points on an attractor. Due to the exponential divergence of trajectories, points far apart in time are dynamically uncorrelated. However, since the points lie on the attractor, they will be spatially correlated. This spatial correlation is measured from the correlation integral, C(r), which is defined as (Grassberger and Procaccia, 1983)

$$C(r) = \lim_{N\to\infty} \frac{1}{N(N-1)} \sum_{\substack{i=1 \\ i\neq j}}^{N} \sum_{j=1}^{N} H(r - |x_i - x_j|), \tag{IV-6}$$

where N is the total number of points, and H is the Heaviside function, which is defined as $H(x) = 1$ for positive x and $H(x) = 0$ for x less than or equal to zero. Figure IV-7, which is a representation of a simple reconstructed trajectory in three-dimensional space, illustrates this concept. The correlation integral defined above is related to the standard correlation function.

Obviously, C(r) increases from zero, for very small values of r, to one, for r very large. The main argument by Grassberger and Procaccia is that for small r

$$C(r) \sim r^{\nu} . \tag{IV-7}$$

If this is true, the correlation dimension is defined as

$$\nu = \lim_{r\to 0} \frac{\log C(r)}{\log r} . \tag{IV-8}$$

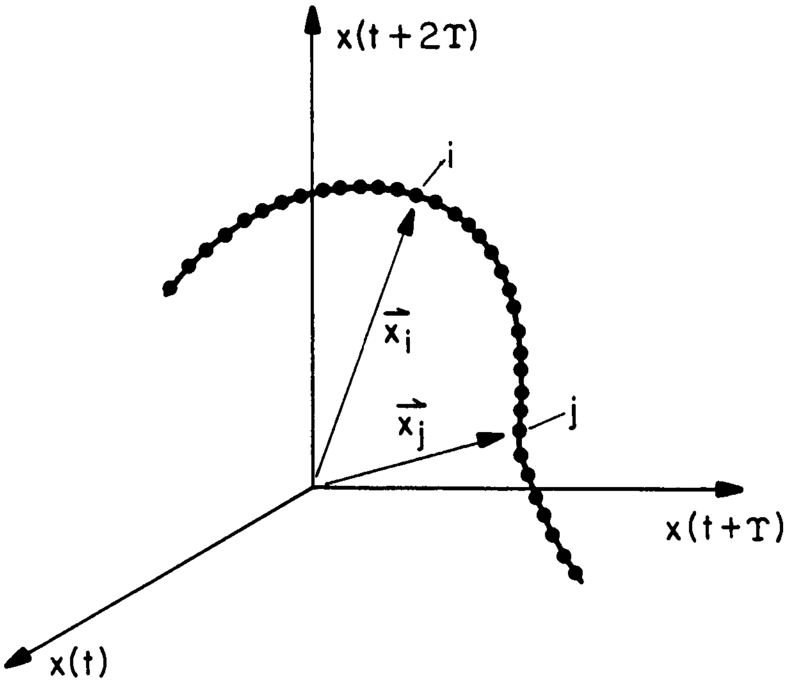

Figure IV-7. Representation of a reconstructed trajectory in three-dimensional space

In order to get a value of the correlation dimension, it is necessary to reconstruct the attractor in a p-dimensional space for increasing values of p. For each value of p, the correlation integrals are computed for the desired range of r. Also for each value of p, the logarithm of C(r) is plotted versus the logarithm of r itself. This logarithm can be either the natural or base-10 value, since it is the slope that is important. If the signal that is being examined is chaotic, the slope will become independent of the dimension. For the case of a random signal, the slope will continue to increase as the dimension is increased. These two possibilities are illustrated in Figures IV-8 and IV-9, respectively.

This measure of fractal dimension has been used extensively. It has been observed that in some cases the correlation and capacity dimensions agree but they do not do so all of the time. This occurs because the capacity is independent of the frequency with which the trajectory visits different portions of the attractor. The correlation dimension takes this into account. Regions of the attractor that are visited more often contribute more to the dimension than those regions which are visited less often. For a trajectory that uniformly covers its attractor, the two dimensions are equal. When the covering is unequal, the capacity will always be greater than the correlation dimension. Since the correlation dimension is sensitive to the dynamical properties of coverage of the attractor, Grassberger and Procaccia claim that it is a more relevant measure.

2. Lyapunov Exponents

As previously mentioned, chaotic systems exhibit a very sensitive dependence upon initial conditions. Two trajectories that are initially close

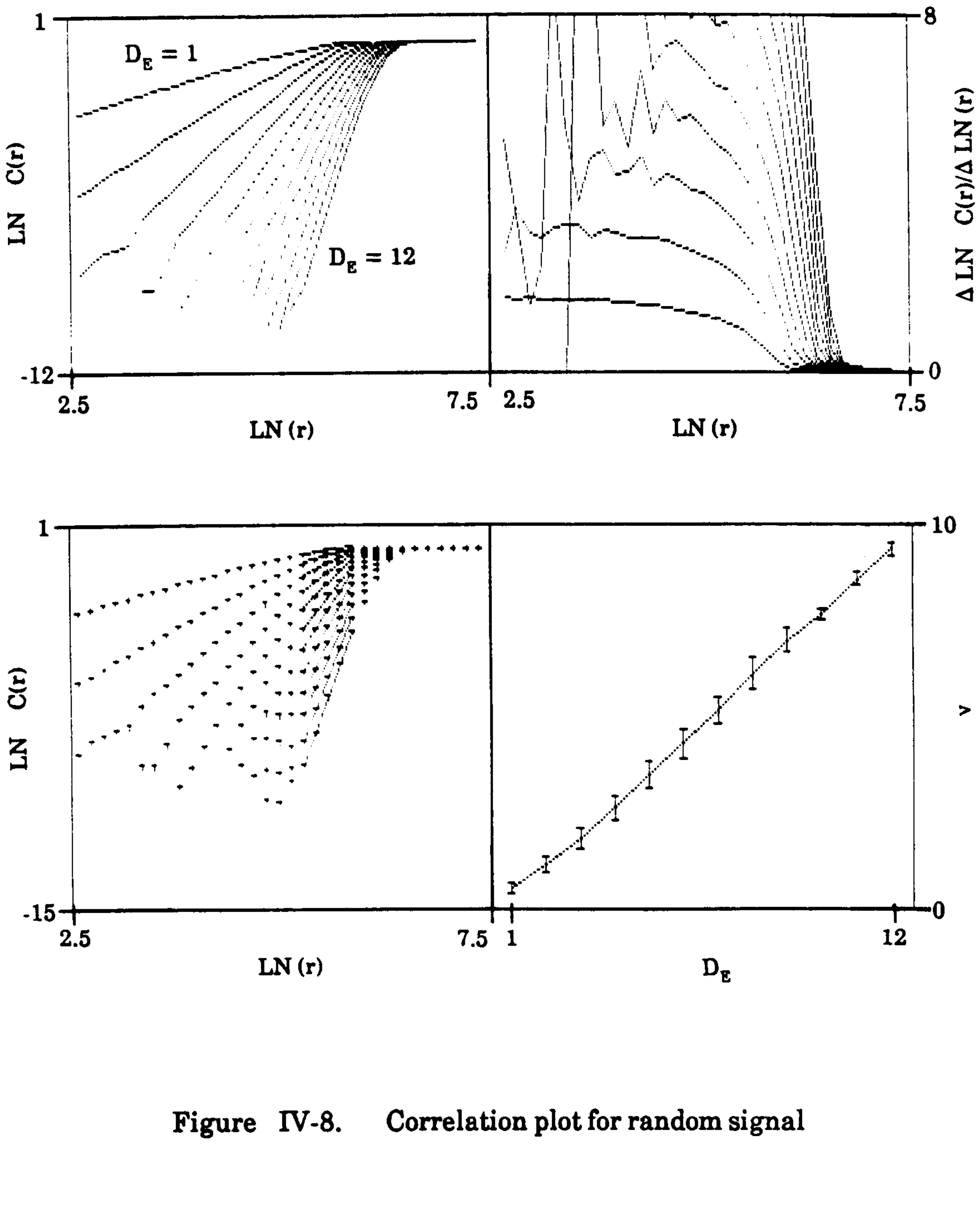

Figure IV-8. Correlation plot for random signal

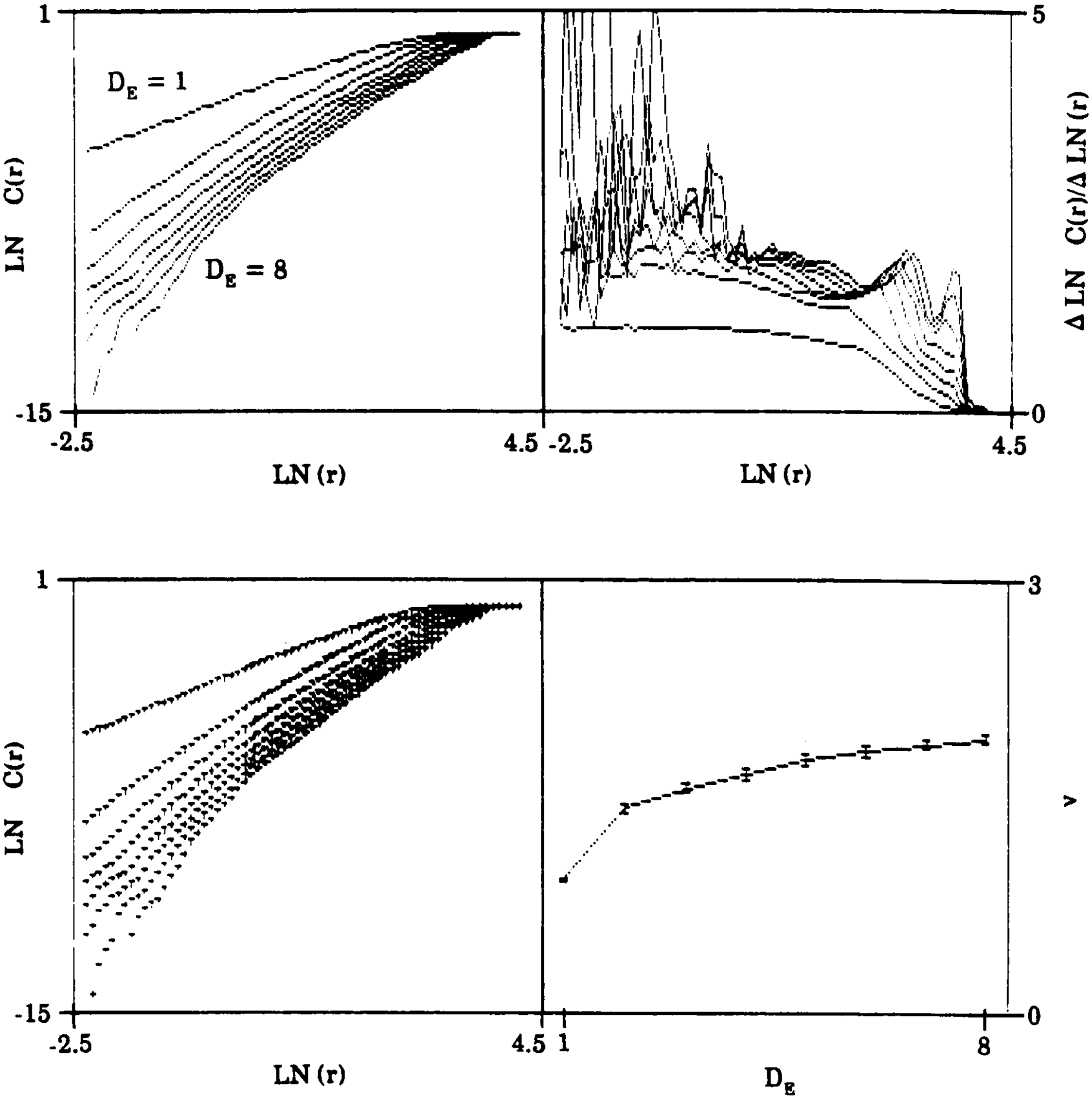

Figure IV - 9. Correlation plot for the Lorenz attractor

together move exponentially away from each other as time progresses. Lyapunov exponents are defined to be the average rates of convergence or divergence of nearby trajectories in phase space. For example, let x_0 be the distance between two starting points. A short period of time later the distance will be

$$x(t) = x_0 e^{\lambda t} , \tag{IV-9}$$

where λ is the Lyapunov exponent. Any system which has at least one positive Lyapunov exponent is considered to be chaotic, since this implies divergence. The magnitude of the exponent is related to the time it takes for the system to become unpredictable.

The divergence of orbits must be local since it is impossible for x(t) to go to infinity. Therefore, it is necessary to take a long-term average of the growth rates about the attractor. Consider the diagram in Figure IV-10. Beginning with a reference trajectory and a point on a nearby trajectory, the rate at which the two diverge is measured. When the trajectories become too far apart, another point near the reference trajectory is chosen and the procedure is repeated. This is carried out until the entire attractor has been covered and an average value is then obtained. For a more detailed discussion as well as a computer program that computes Lyapunov exponents, see Wolf et al. (1985).

Lyapunov exponents can provide another dimension-like measure of chaotic behavior called the Lyapunov dimension (Schuster, 1984). A dynamical system has a Lyapunov exponent for each degree of freedom. For a set of equations it is fairly straightforward to obtain all of the exponents. However, when studying experimental data it is usually possible to obtain

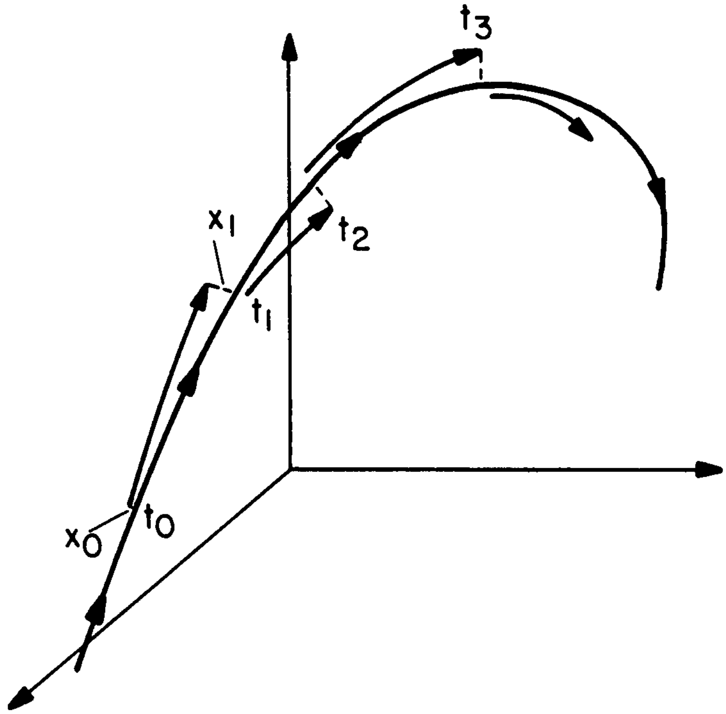

Figure IV-10. Method used to estimate the largest Lyapunov exponent from an experimental time series

only the largest exponent, or at most all of the positive ones. In any case, when it is feasible to compute the entire spectrum of exponents, one can obtain the Lyapunov dimension.

The Lyapunov dimension is defined as

$$d_L = j + \frac{\sum_{i=1}^{j} \lambda_i}{|\lambda_{j+1}|}, \tag{IV-10}$$

where the λ's are the Lyapunov exponents arranged in descending order and j is the largest integer for which

$$\sum_{i=1}^{j} \lambda_i > o. \tag{IV-11}$$

The so-called Kaplan-Yorke conjecture states that the Lyapunov dimension is equal to another measure called the information dimension (Kaplan and Yorke, 1978). This has been shown to be the case for some low-dimensional systems. Since Lyapunov exponents are relatively easy to calculate from sets of equations, this method could be quite appealing and should be studied further.

CHAPTER V

THE EFFECTS OF NOISE

When analyzing experimental data, one usually encounters some form of noise. In this context, noise could be of two kinds: measurement or dynamical. Measurement noise is due to a lack of precision, or a poor signal-to-noise ratio, while dynamical noise results from fluctuating parameters. The data obtained for this report have a considerable amount of noise that is mostly of dynamical origin. The apparatus used for the experiment does not allow independent control over all parameters. The self-consistent behavior of the system results in small fluctuations which are a result of the system's dynamics. Since noise plays a significant role when applying chaos theory to experimental data, some of its effects on computing the correlation dimension and Lyapunov exponents will now be discussed.

A. Correlation Dimension

As a result of the way in which the correlation dimension is defined, a certain amount of noise does not render this measure useless (Mizrachi et al., 1984). By comparing the two correlation integral plots in Figures V-1 and V-2, one can see the effect of adding noise to a periodic signal. Figure V-1, which is the case for a sine wave produced by a function generator, shows a fairly wide region in which the slopes are constant. It is apparent that the correlation dimension is approximately one. Figure V-2 is the result of applying this procedure to the same signal with random noise added to it. Obviously, there are two distinct regions in Figure V-2. The position of the knee is related to the noise level of the system. Below the knee the noise

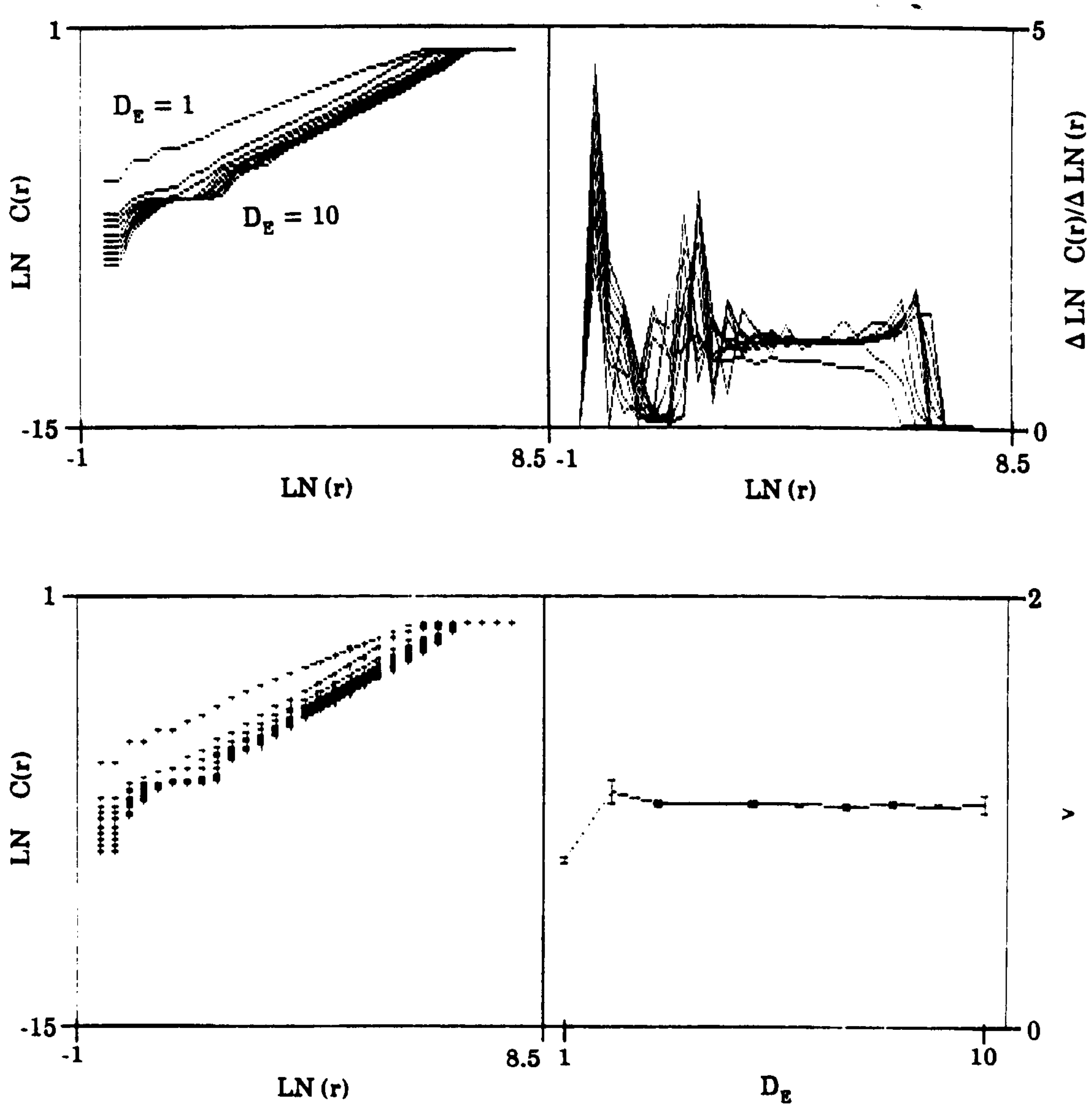

Figure V-1. Correlation plot for sine wave

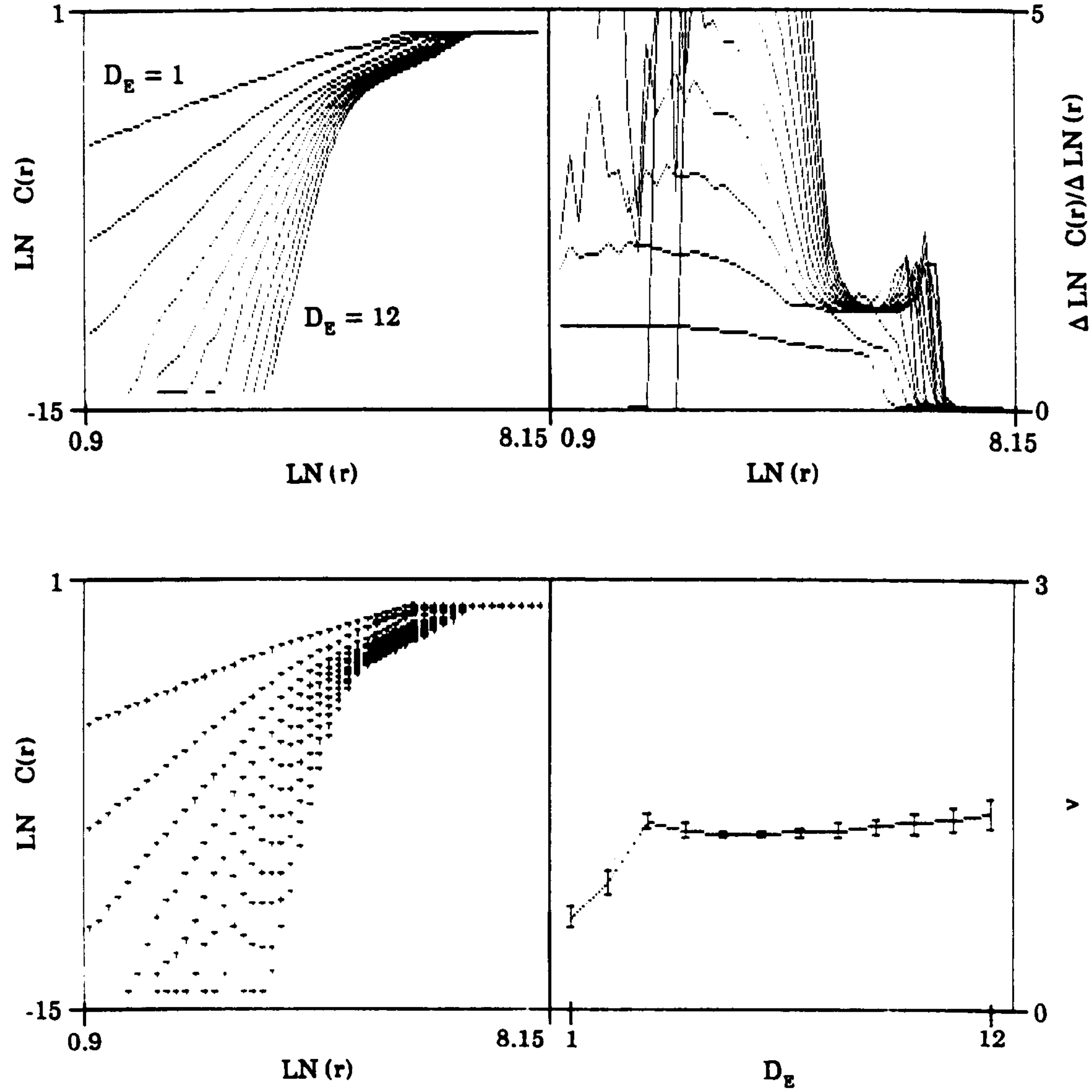

Figure V-2. Correlation plot for sine wave with noise added dominates and one can see that the slope is dependent upon the embedding dimension. However, the noise has no effect on scale sizes above the knee and the dimension can be obtained in this region. Therefore, for levels of noise that are small compared to the attractor size, the correlation dimension can still be obtained. However, as the noise level is increased the scaling region will diminish and eventually be unidentifiable.

B. Lyapunov Exponents

The effect of noise on the computation of Lyapunov exponents is not as clear-cut as with the correlation dimension. In any case, it should be obvious that the noise level of a signal will limit the scale size over which the separation of trajectories is meaningful. Though quite ambiguous, one can only state that when noise levels are too high, it is not possible to determine Lyapunov exponents very accurately.

CHAPTER VI

PREVIOUS APPLICATIONS OF CHAOS THEORY TO PLASMAS

Since the development of chaotic dynamics, the main application has been in the field of fluid dynamics, primarily fluid turbulence. Since fluid and plasma turbulence are strongly related, it was just a matter of time before the concepts of chaos theory were utilized by plasma researchers. Around 1980 publications on this subject began to appear. The first articles reported on the study of sets of differential equations. By the mid 1980's researchers began looking for experimental evidence of deterministic chaos in plasmas. Some types of plasmas that have been examined are gaseous discharges, solid-state plasmas, magnetoplasmas, and tokamak plasmas. These applications of chaos theory to plasmas are briefly discussed in this chapter.

A. Modeling Of Plasma Behavior

Considerable effort has been put into the modeling of nonlinear wave interactions in plasmas. Many of the models which have been developed have been studied using the concepts of chaotic dynamics. Some of these will be briefly introduced and referenced for those interested in reading further.

The book <u>Intrinsic Stochasticity in Plasmas</u> is comprised of papers that were presented at a workshop held in Orsay, France. Several of these papers dealt with modeling and chaos. Adam et al. (1979) were studying the nonlinear decay of linearly unstable waves into linearly damped waves. Another paper by Treve et al. (1979) discussed an MHD analog of Rayleigh-Benard convection. Their model was shown to reduce to Lorenz's model for certain conditions; thereby indicating that MHD flow could produce a strange attractor. A third paper by Lashinsky (1979) was concerned with modeling a plasma with a limited number of discrete modes of the collisionless drift instability.

A model of Langmuir turbulence has been investigated by Wang (1980). He began with Zakharov's equations. These model Langmuir turbulence in a plasma which is immersed in an external homogeneous electric field oscillating at the electron plasma frequency. After simplifying Zakharov's model to a set of single-mode equations, Wang was able to observe chaotic behavior.

Instability saturation by nonlinear three-wave mode coupling was studied by Wersinger et al. (1980). Their simple model consists of the resonant three-wave coupling equations, with the highest frequency wave being linearly unstable, and the two lower frequency waves being damped. It was shown that as the amount of damping was varied, the system underwent a succession of bifurcations. The behavior ranged from simple periodic motion to what appeared to be chaotic motion.

Another study, which was performed by Weiland and Mondt (1985), was concerned with a nonlinear three-wave system which contains a linear instability. This instability is an electromagnetic, high-frequency analog of the current convective instability (Kadomtsev and Pogutse, 1970). This system was shown to exhibit evidence of chaotic behavior.

More recently, chaos has been observed in two other models. Jingqing and Liulai (1988) developed a model of a plasma sheath under the excitation of a periodic external force. By varying the control parameters, they were able to see each of the three main routes to chaos. A group of Europeans developed a model to describe an electrostatically turbulent plasma (Pettini et al., 1988).

Their interest was in studying the diffusion of charged particles across magnetic field lines due to a known spectrum of turbulence. It was found that for high enough electric field amplitudes, chaos appeared and diffusion across the magnetic field lines began.

B. Solid-State Plasma

Held and Jeffries (1986) produced some interesting results with their experiment on electron-hole plasmas generated in steady-state electric and magnetic fields in germanium crystals. For this type of arrangement, an unstable helical density wave forms and creates current oscillations in the plasma. By varying the electric field, the instability can be either damped or enhanced. When the electric field was increased to sufficiently high values, they were able to observe the transition to chaos. Two types of behavior were found to exist. In one case, a strange attractor with a dimension of approximately three was found; while for other conditions the fractal dimension was indeterminately large.

A second experiment performed on a solid-state plasma was conducted by Martin et al. (1984). They studied the electrical conduction characteristics of barium sodium niobate ($Ba_2NaNb_5O_{15}$) crystals. Depending upon the control parameters, stationary, periodic or chaotic behavior could be observed. The correlation dimension was estimated to be approximately 5.3 for these data.

C. Electron Beam Plasmas

Another plasma-related experiment was performed by Boswell (1985). This experiment involved the natural oscillation of an electron beam. The arrangement had the beam propagating parallel to a magnetic field and through a low pressure gas. For relatively low beam currents, the electrons appeared to be neutralized by the ions created from collisions with the background gas. As the current was increased, the oscillation's frequency and amplitude increased. When the beam current reached a critical value, a sequence of period-doubling bifurcations began. Eventually, the oscillations became chaotic.

D. Gaseous Discharges

Braun et al. (1987) conducted experiments on a variety of electrical discharge tubes. They found that for proper conditions the discharge current would exhibit either stationary, periodic or chaotic behavior. Once again, the period-doubling route to chaos was observed. An unusual route was also found to exist. In this case, the period-doubling cascade was interrupted by the appearance of a bifurcation with a period multiplied by integers other than one.

E. RF-Generated Plasmas

A paper by Lin I and Wu (1987) discussed the computation of the correlation dimension for density fluctuations of an RF-generated plasma. Their results show a noticeable dependence upon the background pressure. A pressure of 5 mtorr yielded a dimension of approximately fourteen. Increasing the pressure to 20 mtorr resulted in a dimension of about ten. The results of this study are somewhat suspect for two reasons. When computing the correlation dimension, the embedding dimensions were multiples of ten up to a value of one hundred. These extremely high embedding dimensions introduce significant errors. Secondly, in order to obtain such large correlation dimensions one needs considerably more data points than were used (Simm et al., 1987 and Smith, 1988).

F. Pulsed Plasma Discharges

Chaotic behavior has been observed in a pulsed plasma discharge by Cheung and Wong (1987). Their experiment was performed on a large, unmagnetized plasma device. The discharge was formed by ionizing the background neutral gas with electrons emitted from hot tungsten filaments. The discharge voltage was pulsed periodically in order to extract the primary electrons into the chamber. The time history of the discharge current pulses was measured for different values of voltage. For small voltages, the current pulses were regular. As the voltage was increased, regions of chaos were seen, as well as periodic regions. Under proper operating conditions, the period-doubling route to chaos was observed.

G. Steady-State Plasma Discharges

Cheung et al. (1988) also reported an experiment performed on a steady-state plasma discharge. The device consisted of an electron-emitting cathode and a current-collecting anode. By applying a sinusoidal signal as well as a dc component to the anode, chaos could be induced. They were able to observe a transition from laminar current oscillations to chaotic oscillations by increasing the amplitude of the sinusoidal voltage. This arrangement exhibited the intermittent route to chaos.

H. Tokamak Fluctuations

In the past several years researchers have applied the concept of correlation dimension to some of the major tokamak experiments. A few of these appear to produce low-dimensional chaos, while others do not. There exists a principal distinction among these experiments. While some groups were concerned with low frequency, coherent oscillations, others were studying broadband fluctuations.

A tokamak is a toroidal plasma containment device. The plasma is confined by a toroidal magnetic field and heated by a large toroidal current. A tokamak plasma exhibits fluctuating number densities, magnetic fields and potentials. At frequencies below several kilohertz, relatively coherent fluctuations can be observed. These are known as Mirnov oscillations. As long as their amplitudes are small, Mirnov oscillations have no effect on containment. It is the higher frequency fluctuations that are thought to be the underlying cause of the anomalous transport that is observed in tokamak plasmas. These published reports will now be briefly discussed.

1. DITE

Arter and Edwards (1986) performed a study on the Divertor and Injection Tokamak Experiment's (DITE) Mirnov oscillations. In this experiment, magnetic field fluctuations were observed with eight Mirnov coils. These were equally spaced in poloidal angle about the tokamak. Their data resulted in a correlation dimension of approximately 2.1. This appears reasonable, since Mirnov oscillations are fairly coherent. In the article, the authors attempted to identify the processes involved.

2. TOSCA

Low frequency magnetic field fluctuations were measured on the TOSCA device by Cote et al. (1985). This study yielded a correlation dimension of approximately 2.4. However, density fluctuation measurements were also obtained using a CO_2 scattering method. These CO_2 data appeared to be random.

3. JET

Cote et al. (1982) also examined the Joint European Torus's (JET) MHD activity. These data were acquired with pick up coils located inside the vacuum vessel. For coherent modes, the correlation dimension fell between 2.4 and 2.9. When conditions were such that there was no coherent activity, the correlation integral failed to converge.

4. TCA

Sawley et al. (1987) studied the broadband magnetic and density fluctuations of Tokamak Chauffage Alven (TCA) plasmas. Data were obtained with magnetic probes and a CO_2 laser phase contrast diagnostic. Many discharges were analyzed, but no saturation in slope was observed. This experiment yielded two possible interpretations. One was that the dimension was greater than ten, or that the fluctuations result from time-varying plasma conditions. For the latter case, the concept of correlation dimension is not appropriate in its usual form.

5. TFTR

Zweben et al. (1987) examined edge turbulence in the Tokamak Fusion Test Reactor (TFTR). As part of their study, they attempted to compute the correlation dimension from floating potential fluctuations. Their results were unclear. Upon close examination of the derivative of the correlation integral, a sufficiently large scaling region could not be found to establish a correlation dimension.

6. TFR

A CO_2 laser scattering technique was employed by Barkley et al. (1988) to measure density fluctuations on Torus Fontenay-aux-Roses (TFR) plasmas. This experiment produced some very interesting results. The correlation dimension could be obtained, but it was shown to depend upon the wavenumber of the measured signal. The dimension was 2.6 and 3.2 for wavenumbers of 6 cm^{-1} and 18 cm^{-1}, respectively. The authors point out that convergence could only be obtained for sufficiently high sampling frequencies. Convergence was observed when sampling at 100 MHz, but not at 5 MHz.

CHAPTER VII

EXPERIMENTAL APPARATUS

The experimental data for this study were obtained on a Penning discharge plasma. The operation of this device will now be discussed. Also covered in this chapter will be the modifications that were made on the apparatus, the characteristic operating conditions, and the data handling system.

A. Classical Penning Discharge

The conventional Penning discharge was originally developed by F. M. Penning (Penning and Neinhuis, 1949) in the late 1930's. It was originally used as a vacuum gauge. By measuring the current flowing through the tube, one could determine the gas pressure. This device was shown to work down to about 0.5 microtorr. The Penning discharge tube could also be used for leak detection.

Roth (1966) modified the original, "classical" design in such a way that a Penning discharge could be used to generate large volume, steady-state plasma in a magnetic mirror field. This configuration is called a "modified Penning discharge", and has been used in plasma physics research to produce highly turbulent, hot-ion plasma.

The vacuum vessel of the Penning discharge used in this experiment is a cylindrical section of six inch diameter pyrex pipe. As seen in Figure VII-1, the vessel is surrounded by confining magnetic field coils. The sixteen water-cooled coils are energized by a power supply which furnishes up to 1000 Amperes at 40 Volts. The coils are arranged to produce a magnetic mirror.

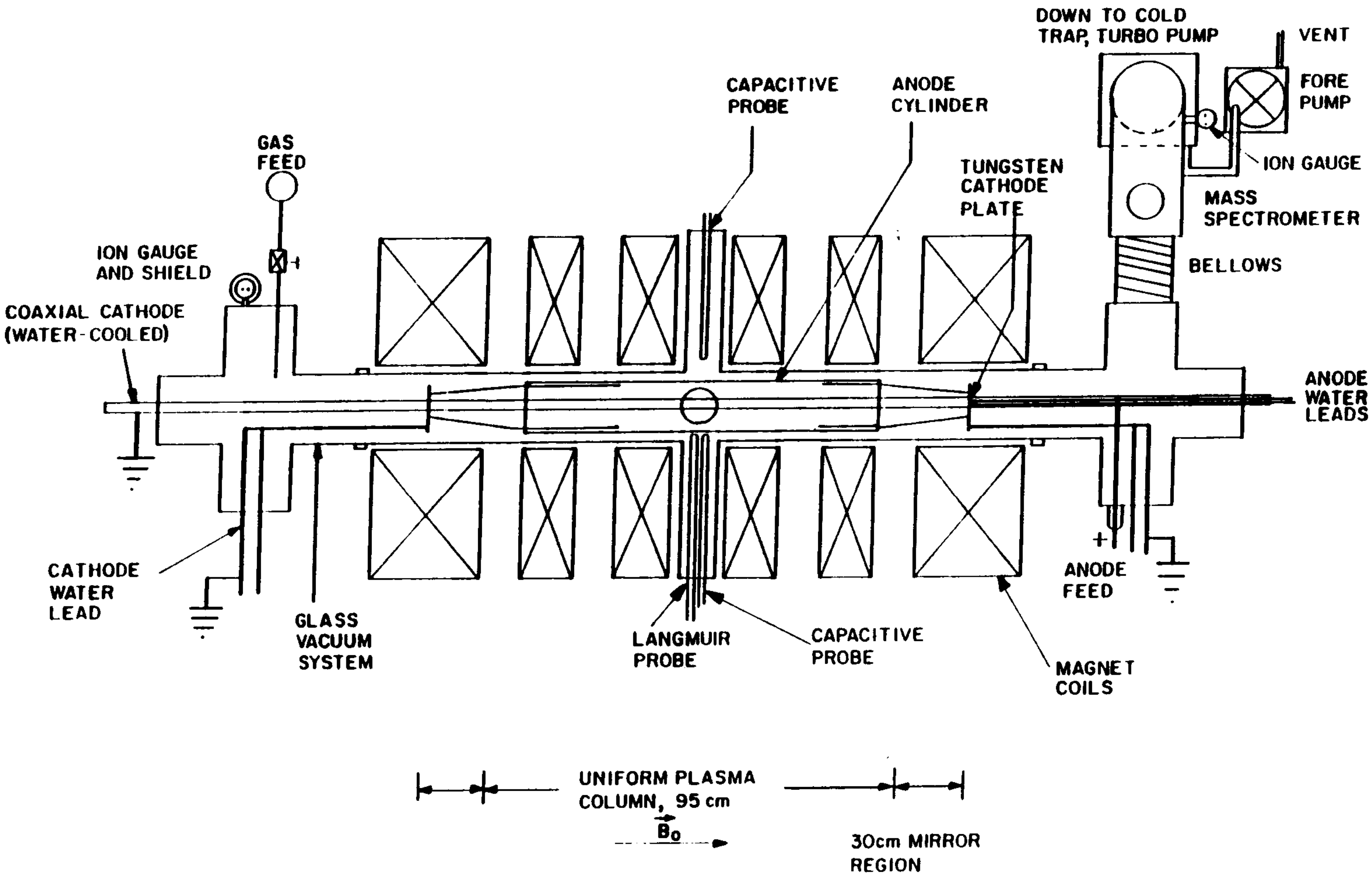

Figure VII-1. Experimental apparatus

The normalized axial magnetic field is shown in Figure VII-2. The region of constant field strength is approximately 95 cm in axial length. The mirror ratio, B_{min}/B_{max}, is about 0.77. Figure VII-3 shows the variation of the magnetic field strength with coil current. The maximum field at the midplane is approximately 0.2 Tesla.

The gas to be ionized is fed into the system through a leak valve located at one end of the vacuum vessel. For this experiment, helium was used for all data runs. The pumping system is at the other end of the vessel. This consists of a mechanical pump in series with a turbomolecular pump. Pressure is monitored by two ion gauges, one at each end. The base pressure of the system is approximately 5 microtorr. Also installed in the system is a mass spectrometer, which is used to monitor the composition of the gas inside the vacuum vessel.

A classical Penning discharge employs an anode ring and two cathodes. The anode is situated at the midplane with the cathodes placed at each end. The anode consists of a ring of copper tubing which is water-cooled. The cathodes are grounded, water-cooled circular tungsten discs. The background gas is ionized by applying a DC voltage to the anode. This applied voltage is generally a few kilovolts, with the current being several tens to several hundreds of milliamperes. The anode supply can provide up to 40 kilovolts and 1 Ampere.

The arrangement of the Penning discharge allows easy access to the plasma for diagnostics. Diagnostics that have been installed on this system are capacitive probes, Langmuir probes, retarding potential energy analyzers, a microwave scattering device, a microwave interferometer and equipment

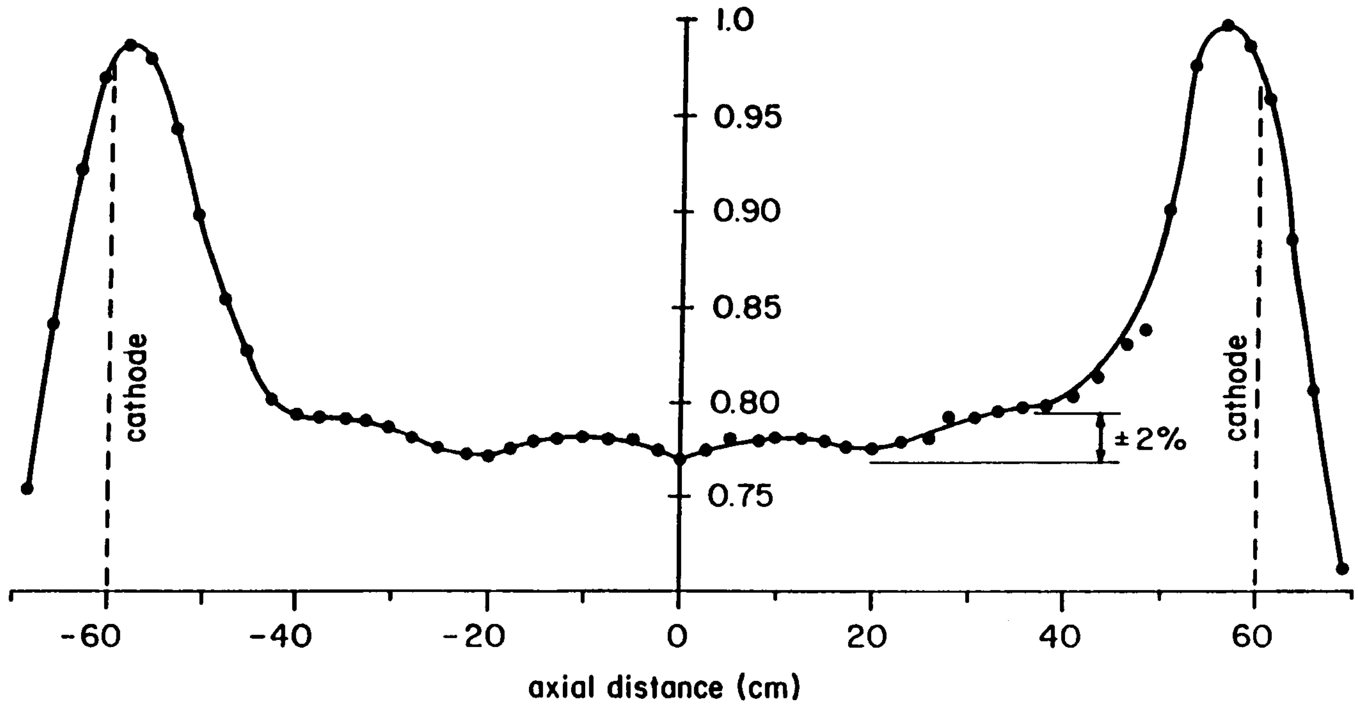

Figure VII-2. Normalized axial magnetic field

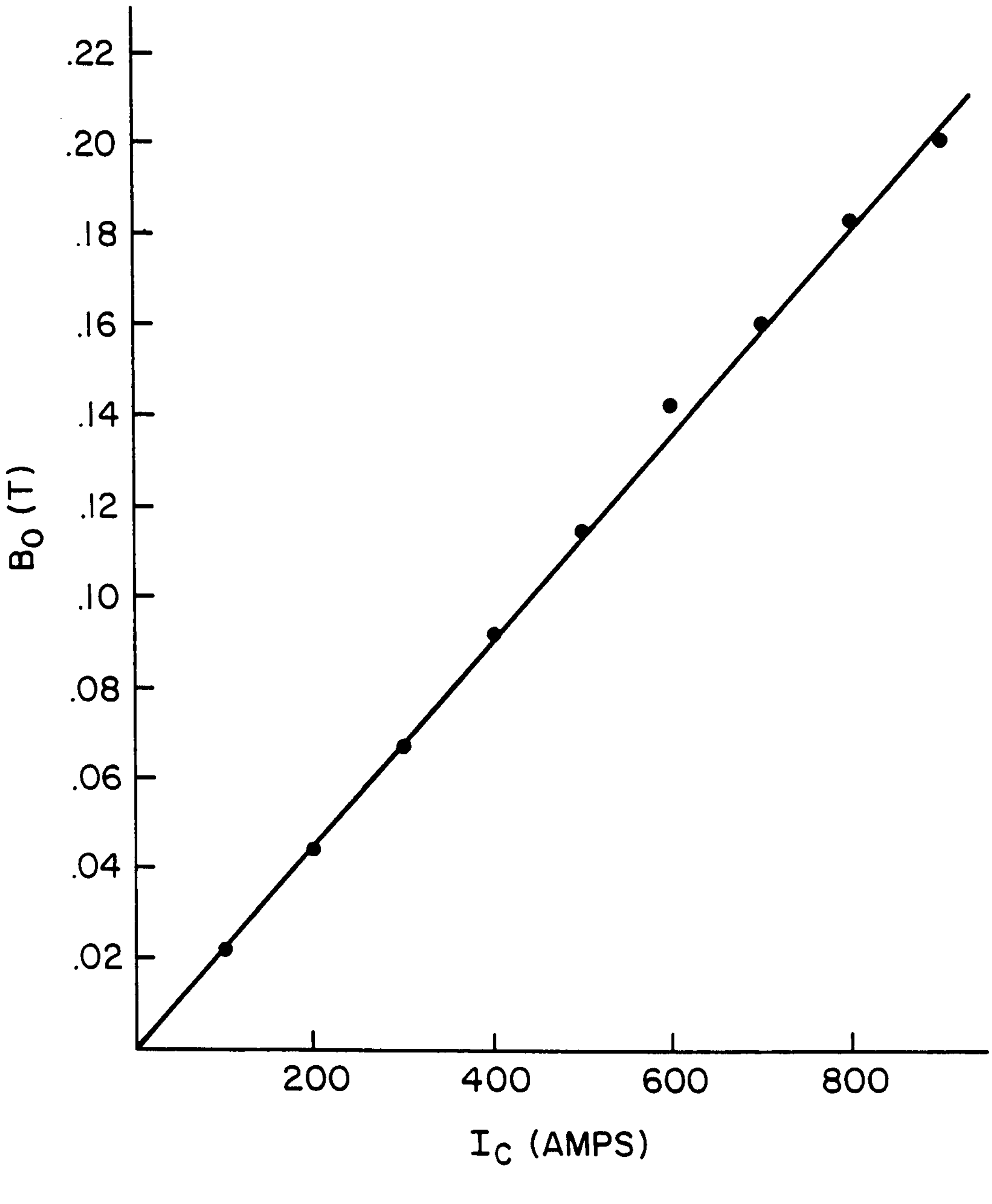

Figure VII-3. Variation of the magnetic field at the mid-plane with coil current

used to study microwave resonance absorption. Those used in this investigation include a radial capacitive probe and a radial Langmuir probe.

B. Characteristic Operating Conditions

A classical Penning discharge produces a steady-state, weakly-ionized plasma. The electron number density measured with a Langmuir probe is characteristically 2.5×10^{9} cm^{-3}. The electron kinetic temperature tends to range between 40 and 100 eV. Langmuir probe measurements suggest an ion kinetic temperature an order of magnitude or more higher. By using a retarding potential energy analyzer to observe the ion energy distribution function, it has been shown that for certain operating conditions at high neutral gas pressures the ion and electron temperatures are approximately equal (Spence et al., 1988).

C. Modifications

A Penning discharge plasma tends to be quite turbulent. This is because a variety of instabilities are active. These instabilities are excited by density and temperature gradients. E x B drift waves have also been observed by Baylor et al. (1984) and Laroussi et al. (1985).

For this experiment, it was desired to drive a coherent E x B drift mode in the plasma. This was accomplished with two modifications to the classical Penning discharge arrangement. As can be seen in Figure VII-1, a long cylindrical anode is used in place of an anode ring. A coaxial cathode is used along with the two cathode plates. Using this arrangement produces a constant radial electric field along the axis of the anode region. This, in turn, creates what appears to be a strong E x B drift wave at the outer edge of the plasma.

Figure VII-4 exhibits a radial profile of the potential fluctuations while the parameters were held constant. In this case the plasma edge was located at R = 6 cm. This shows that the mode that is being observed exists in the edge region, which is characteristic of E x B drift waves. Figures VII-5 and VII-6 show the potential fluctuations at the edge when the magnetic field and anode voltage, respectively, were varied. The peak frequencies are then plotted against the proper variable in Figures VII-7 and VII-8. These two graphs show that the frequency is inversely proportional to the magnetic field, and directly proportional to the anode voltage. This evidence indicates that the instability observed is due to E x B drift.

D. Data Handling System

The block diagram of the data acquisition and handling system is shown in Figure VII-9. The first element of the system is the capacitive probe, which is shown in Figure VII-10. The probe is constructed of semi-rigid coaxial cable. The outer conductor and insulation has been removed at the tip to allow the center conductor to pick up the potential fluctuations. For proper boundary conditions, a small sphere has been soldered to the tip.

The signal detected by the capacitive probe is fed into a Tektronix 1121 amplifier. The signal is then band-pass filtered through the use of two Krohn-Hite 3200 filters. The high pass filter is set at 1000 Hertz in order to get rid of any line or vibration noise. The low pass filter is set at 1 Megahertz to avoid aliasing effects.

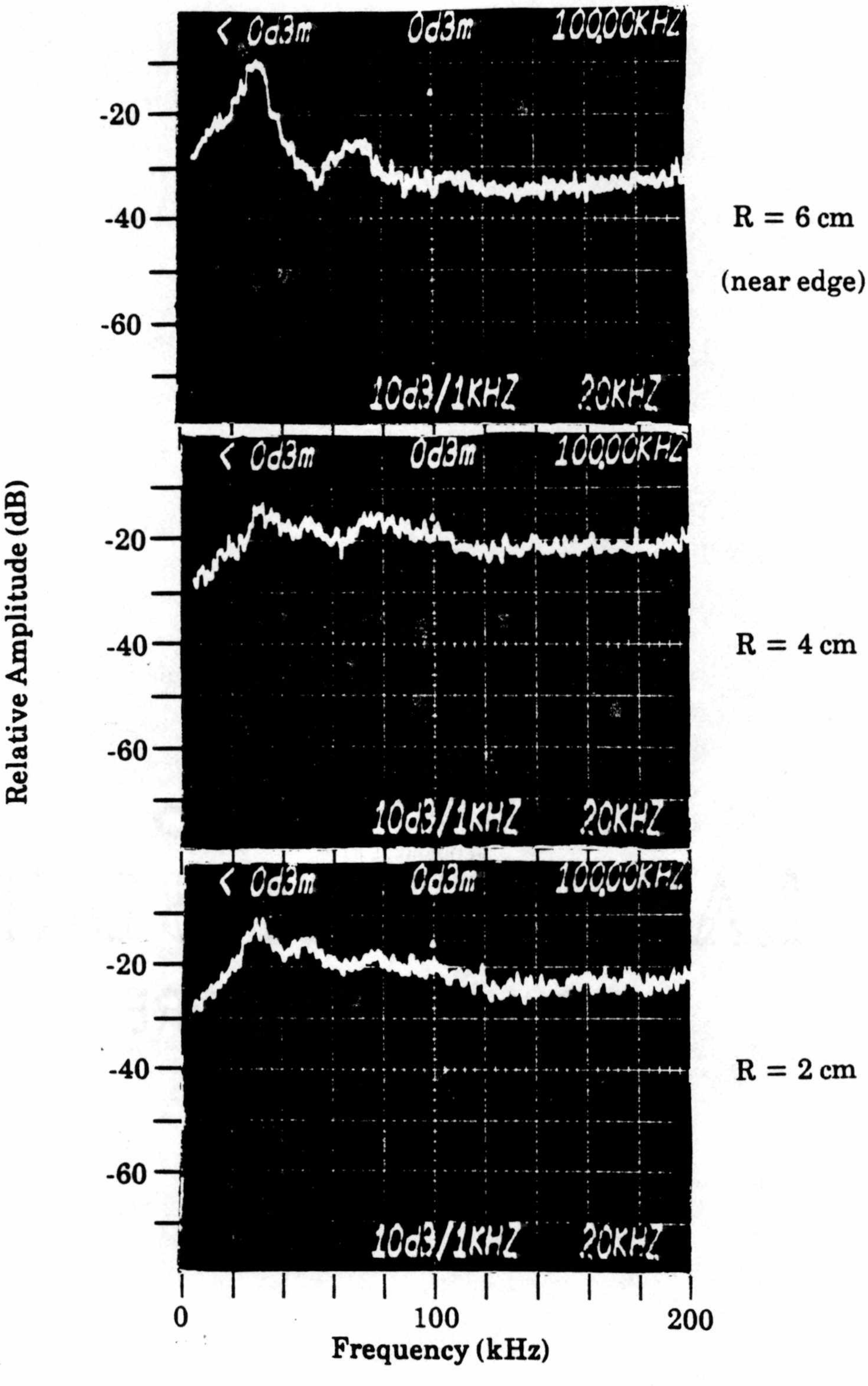

Figure VII-4. Radial profile of potential fluctuations

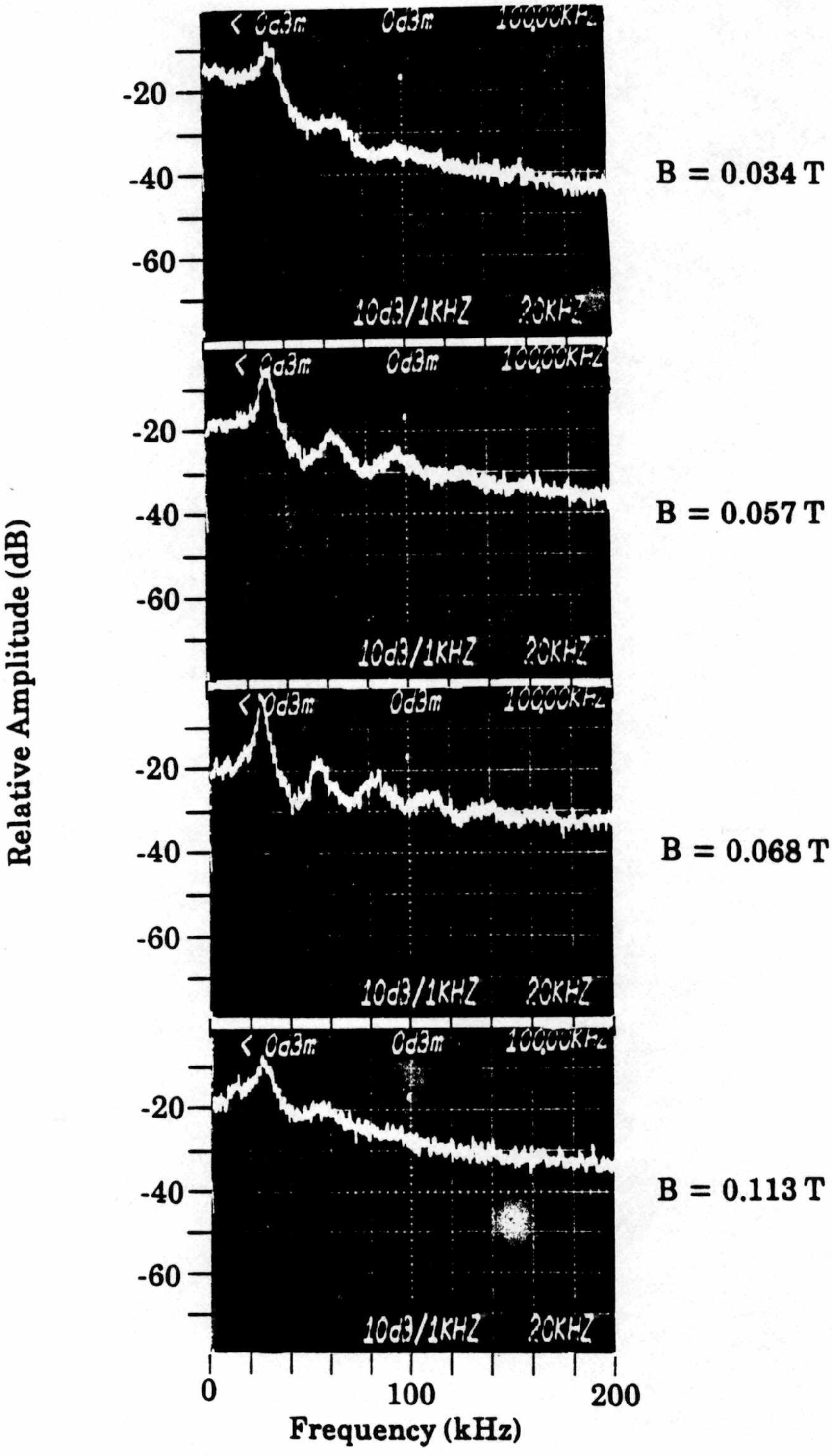

Figure VII-5. Power spectra showing variation of frequency with magnetic field strength

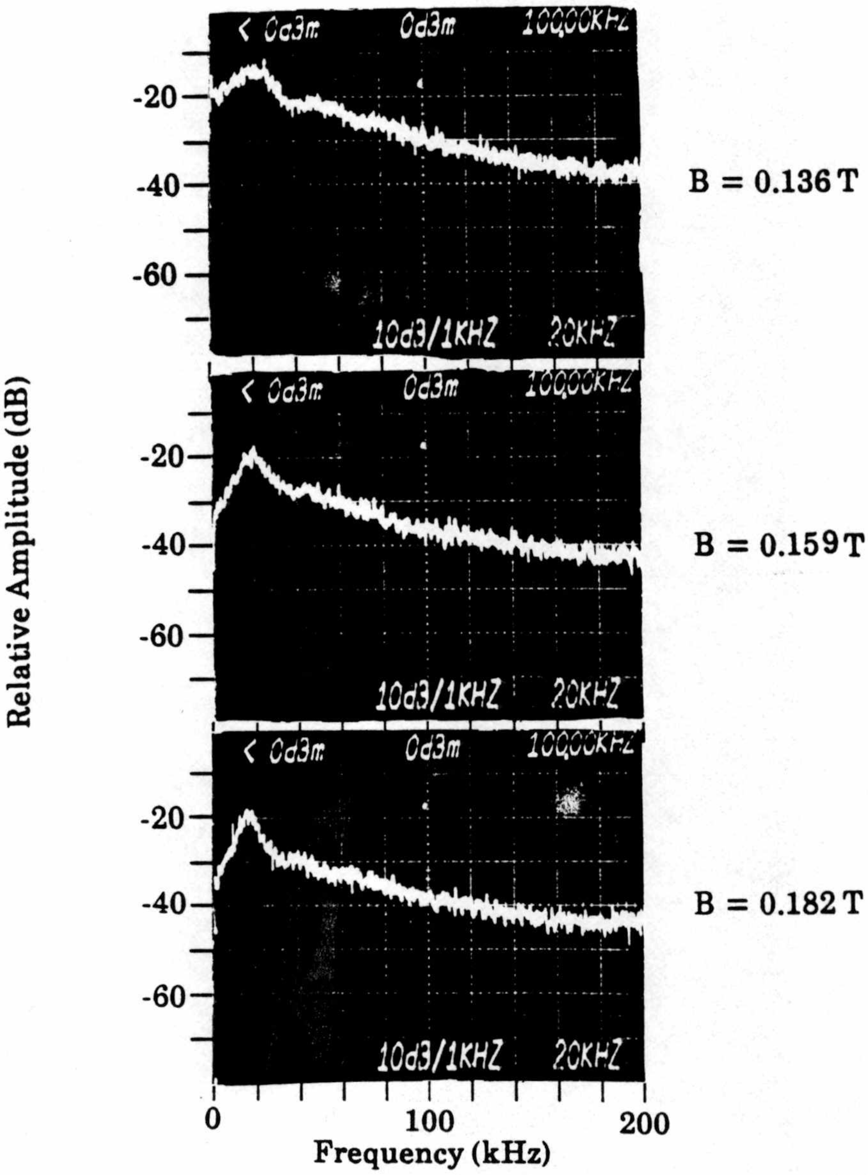

Figure VII-5. (Continued)

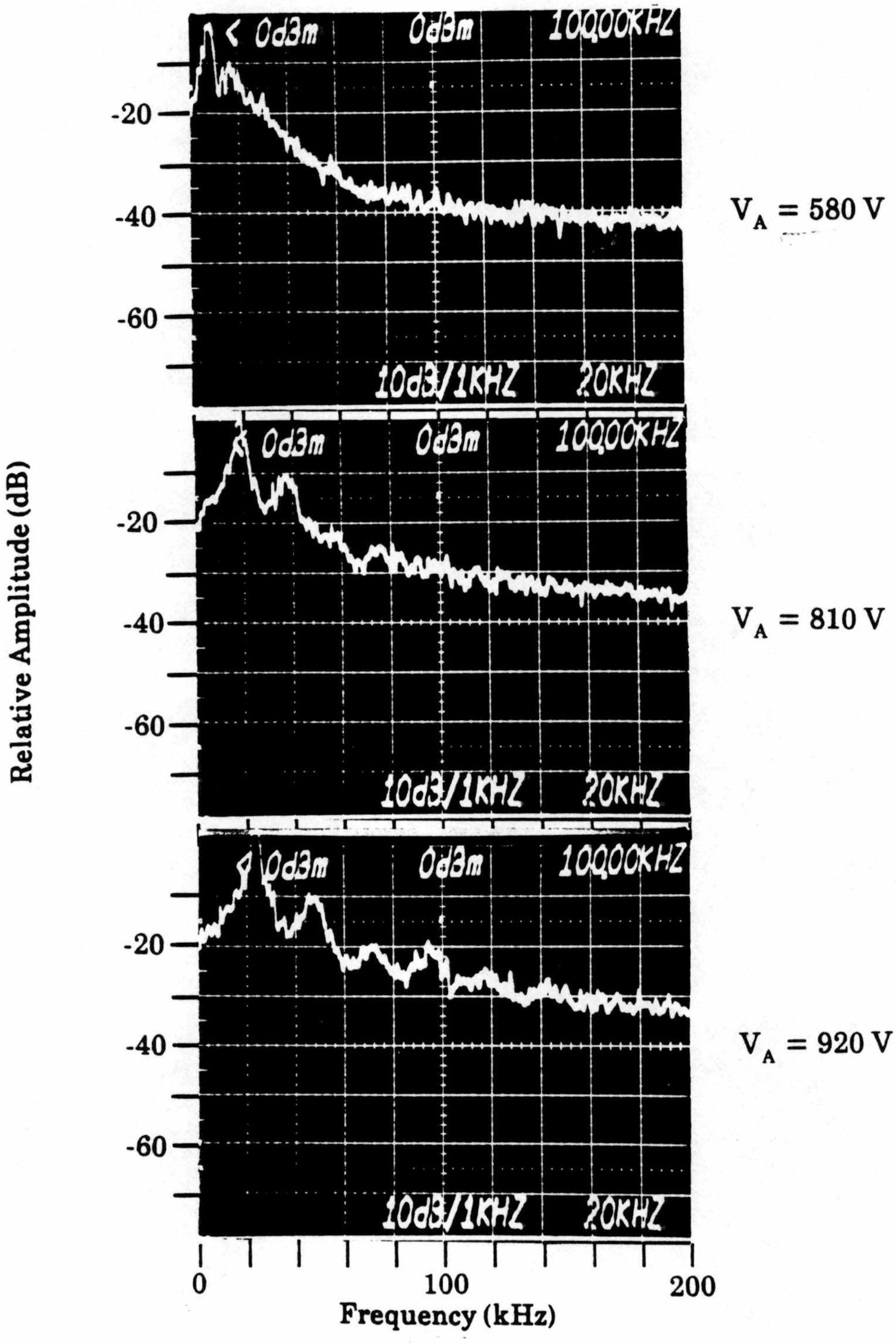

Figure VII-6. Power spectra showing variation of frequency with anode voltage

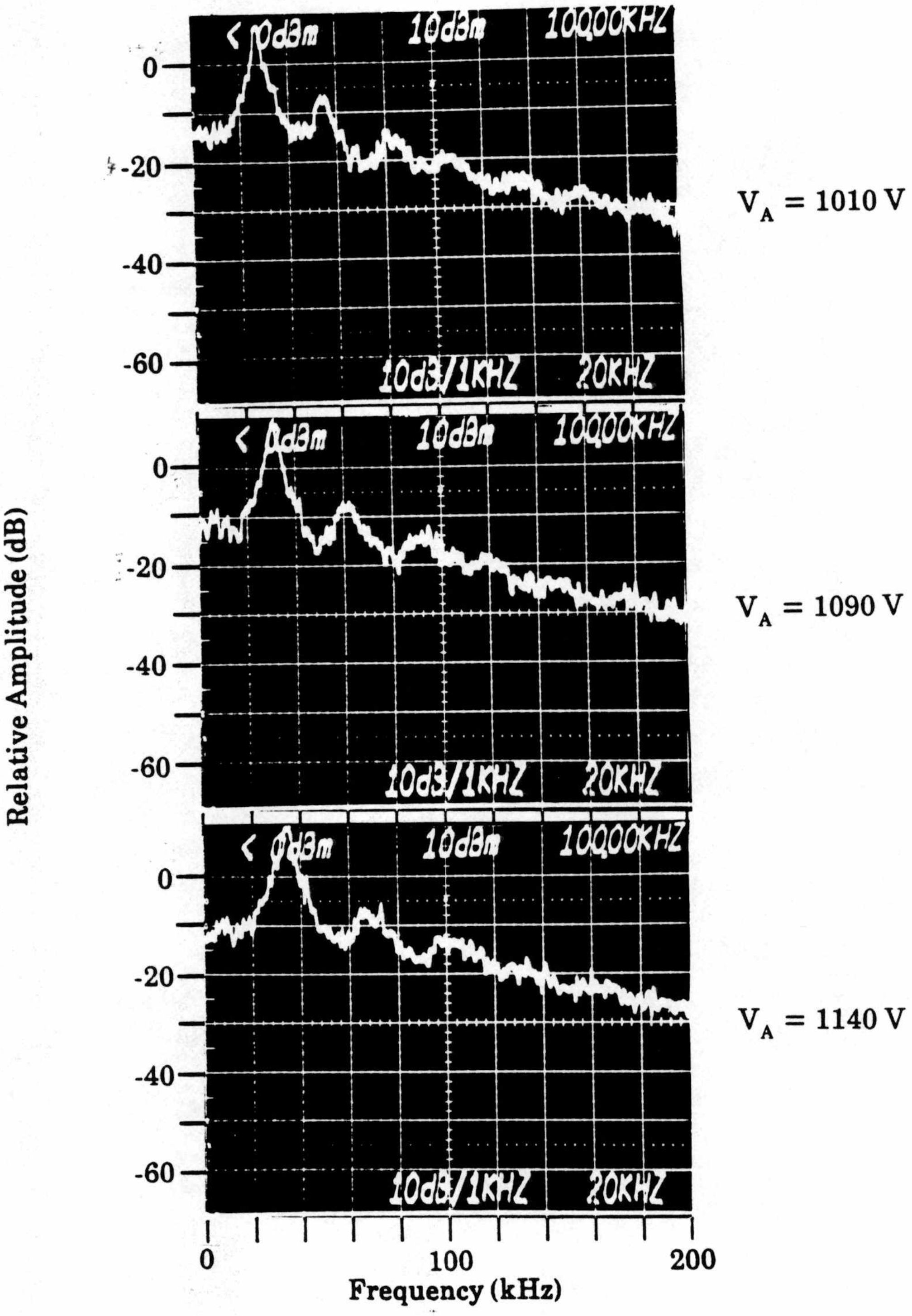

Figure VII-6. (Continued)

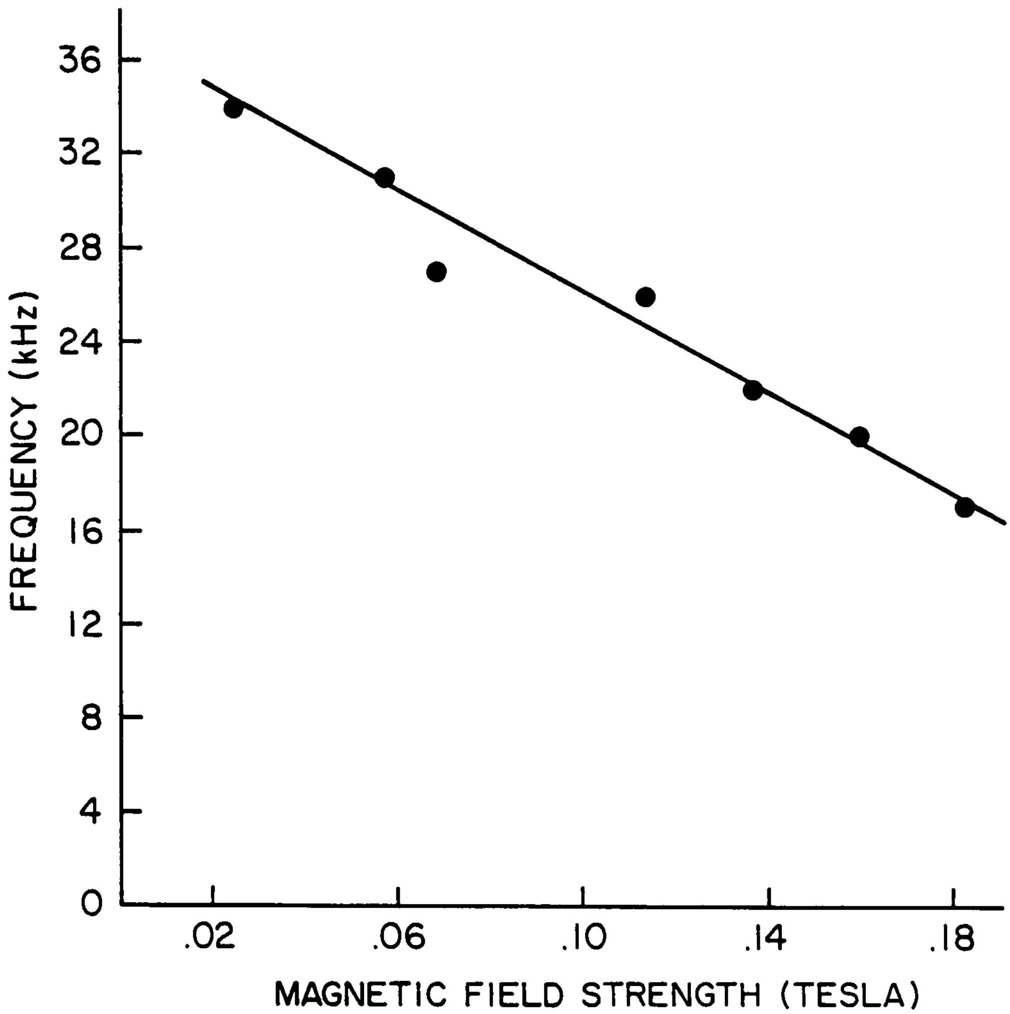

Figure VII-7. **Variation of frequency with magnetic field**

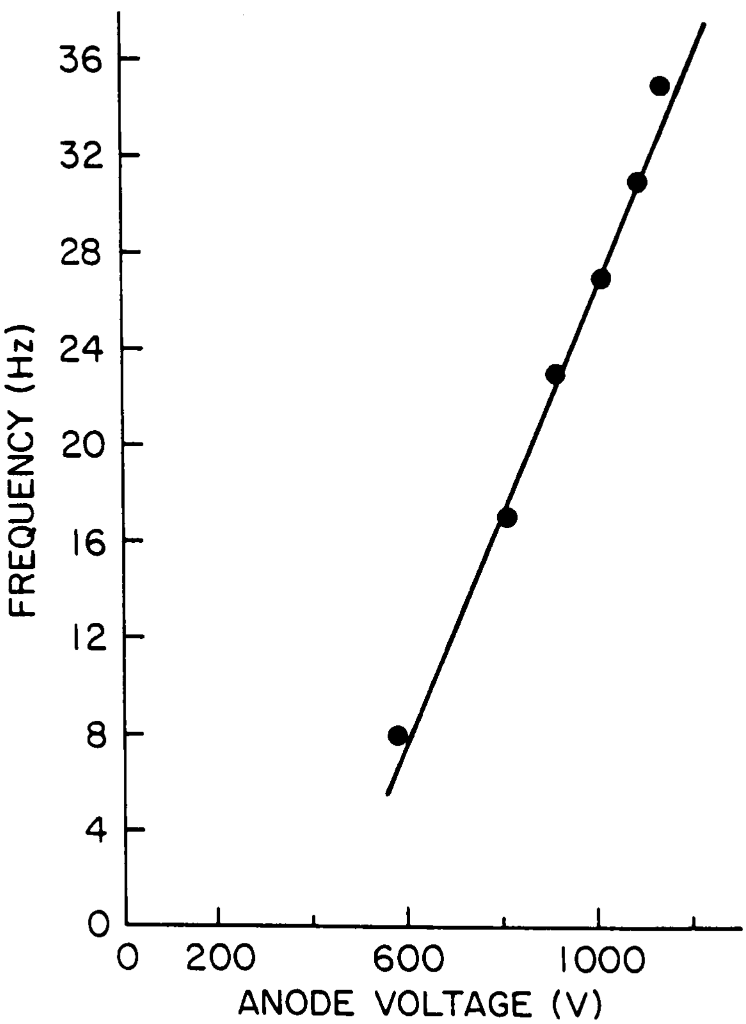

Figure VII-8. **Variation of frequency with anode voltage**

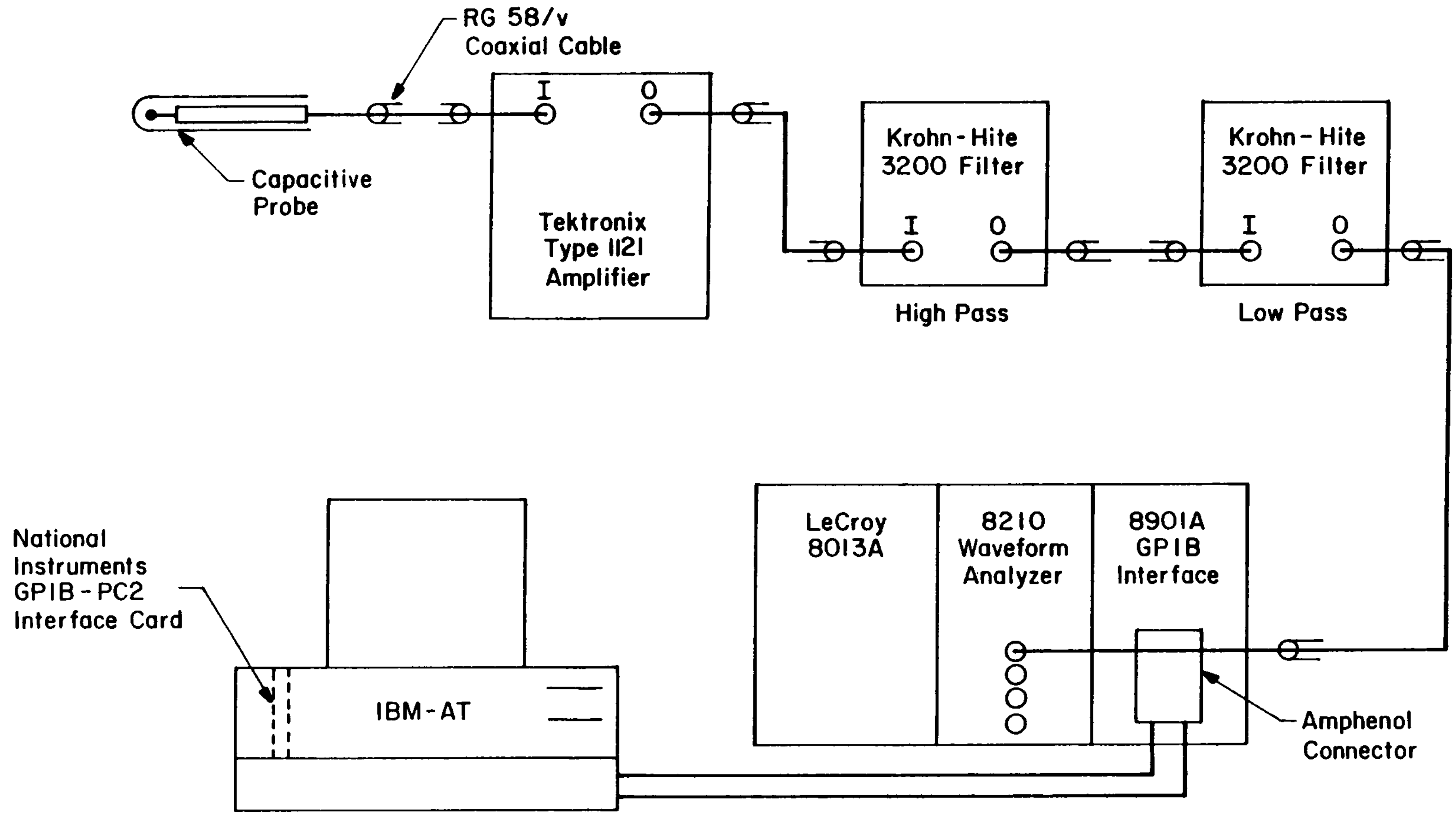

Figure VII-9. Block diagram of data acquisition system

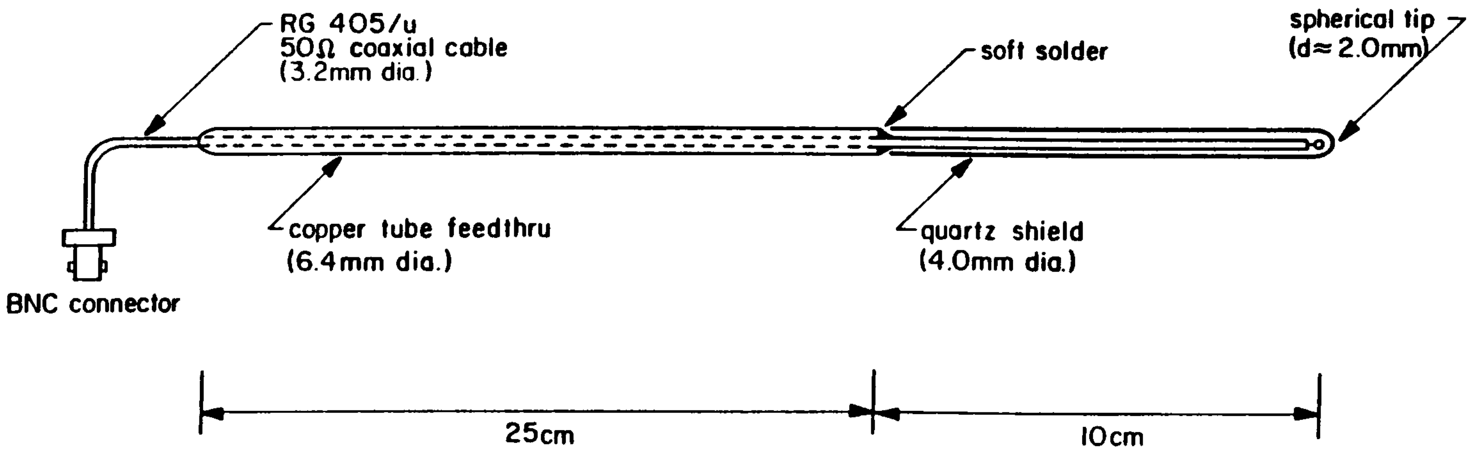

Figure VII-10. Capacitive probe design

The filtered signal is digitized by a LeCroy 8210 Waveform Analyzer. This model of analog-to-digital converter can process up to four signals simultaneously. The maximum sampling rate is 1 Megahertz for each channel and the data have ten bits of resolution.

The data are stored in an external 32K word memory module. The 8800A module is a dynamic memory designed for sequential storage of data at speeds up to 5 Megahertz. The memory is divided equally among the input channels and can be expanded.

The transient recorder is housed in a LeCroy 8013A CAMAC benchtop mainframe. This crate will accomodate eleven single-width modules and the dual-width controller. The purpose of CAMAC, which is an international standard, is to provide a means by which a wide range of modular instruments can be powered and interfaced to a computer. Three items are necessary in order to operate the recorder with the computer. These are the CAMAC module, the GPIB interface and the software. In our system, a LeCroy 8901A is installed in the LeCroy instrument mainframe. This CAMAC module provides GPIB access to the crate. The GPIB card that is installed on the IBM-AT is a National Instruments GPIB-PC2A. The acronym GPIB stands for General Purpose Interface Bus. The GPIB card is an interface system through which interconnected electronic devices communicate. In our case, the GPIB card allows the computer to communicate with the CAMAC module, which in turn controls the recorders.

In order for the system to work, two software packages are required. Software is necessary for operation of both the GPIB card and the instrument mainframe. The software supplied with the GPIB card allows one to customize their system depending upon the type and number of devices being controlled. The package also provides numerous functions for advanced communication purposes. The software supplied with the LeCroy crate is entitled Waveform-Catalyst. It is used to program the instruments, acquire data, display the data, process it and store it. Waveform-Catalyst also provides functions for advanced data handling and processing.

The operation of this system is fairly straightforward. Initially there was a conflict between the GPIB card and the extended memory card installed on the AT. After many attempts to get the cards to work together and many discussions with the manufacturers, it was finally determined that they were totally incompatible. Upon installation of a new memory card, the system worked very smoothly. The only additional requirement was a short program to reformat the data which is stored in unformatted sequential file.

CHAPTER VIII

DYNAMICAL SOFTWARE

The software that was used to study the nonlinear behavior of plasma fluctuations is entitled Dynamical Software. This package is commercially available from Dynamical Systems, Inc. This company is run by William Schaffer and is located in Tucson, Arizona. Dr. Schaffer is a faculty member of the University of Arizona and has studied the nonlinear behavior of ecological and other systems.

This software was written for use on an IBM-PC, XT or AT. It will run on IBM compatibles as well as a Tandy 2000. 640 kilobytes of memory are required as well as a graphics card. When studying sets of differential equations, a Fortran compiler is needed. Either a Microsoft or Ryan-McFarland compiler will work. A hard disk and a Microsoft-compatible mouse are helpful, but not necessary.

Dynamical software is sold in two separate packages, with the first performing the more basic operations. This first package consists of: data smoothing and interpolation routines, a two-dimensional plotter with sequential magnification, a three-dimensional plotter which will also take Poincare sections, a three-dimensional plotter with color coding by velocity, a routine for embedding time series, routines for one-dimensional and circle maps, an Adams type integrator for ordinary differential equations and a driver to iterate discrete maps. The second package has extended graphics and data transformation capabilities as well as routines for computing eigenvalues and eigenvectors, routines for spectral analysis, routines for computing fractal dimensions and Lyapunov exponents, a routine for generating bifurcation diagrams for discrete maps, a Runge-Kutta type integrator for ordinary differential equations and a delay-differential equation integrator. Dynamical Software also contains an on-line manual. This is limited to commands and syntax only. A written manual is available as well. This is quite thorough and even gives a good introduction to the subject of chaotic dynamics. The only drawback of this software package has to do with labeling of plots. Axes are not labeled, and tick marks or scales are not provided. When preparing data for presentation, this can be quite a problem.

CHAPTER IX

COMPARISON OF PLASMA DATA TO REFERENCE CASES

In order to gain a better understanding of the results obtained from the plasma data, it is helpful to first study several reference cases. In most instances the plasma fluctuations appear to consist of two components; one random and the other coherent. Thus, we will compare a set of plasma data to known coherent signals which have random noise added to them. The two reference cases will be a noisy limit cycle and a noisy torus.

The noisy limit cycle was briefly discussed in Chapter V. The sine wave was produced with a signal generator and the uniform noise from a random number generator routine. Figure IX-1 shows the power spectrum of the signal, while Figure IX-2 shows the reconstructed phase portrait and Poincare section. A noisy torus was produced in a similar manner. Two sine waves of different frequency and amplitude were produced and added together. Uniform noise was then superimposed upon this signal. The power spectrum of the resulting signal is shown in Figure IX-3, while Figure IX-4 shows the reconstructed phase portrait and Poincare section.

Naturally, the power spectra of these two signals are different, but it is difficult to distinguish between the Poincare sections. The toroidal nature of the second signal would become more evident if the relative amplitude of the noise component was decreased. However, the noisy torus was constructed in this manner so that it would resemble the particular set of plasma data to be discussed shortly.

It is also of interest to compare the correlation dimension computations for the two reference cases. According to the material in Chapter V, random

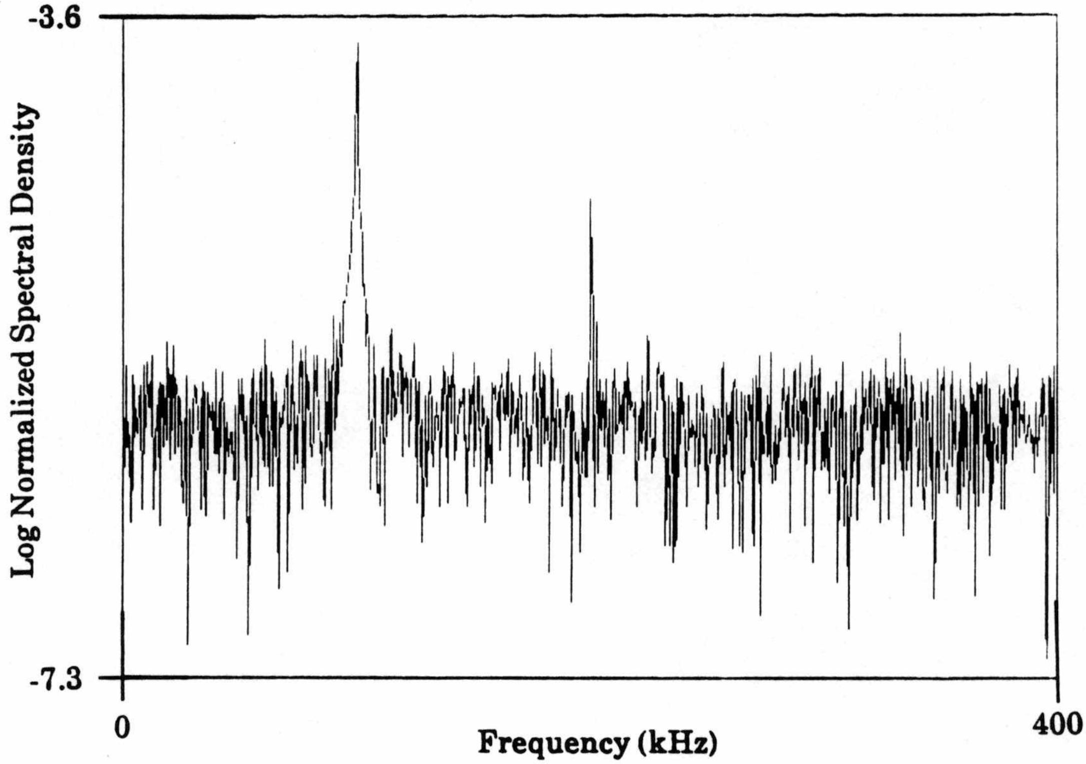

Figure IX-1. Power spectrum of a noisy sine wave

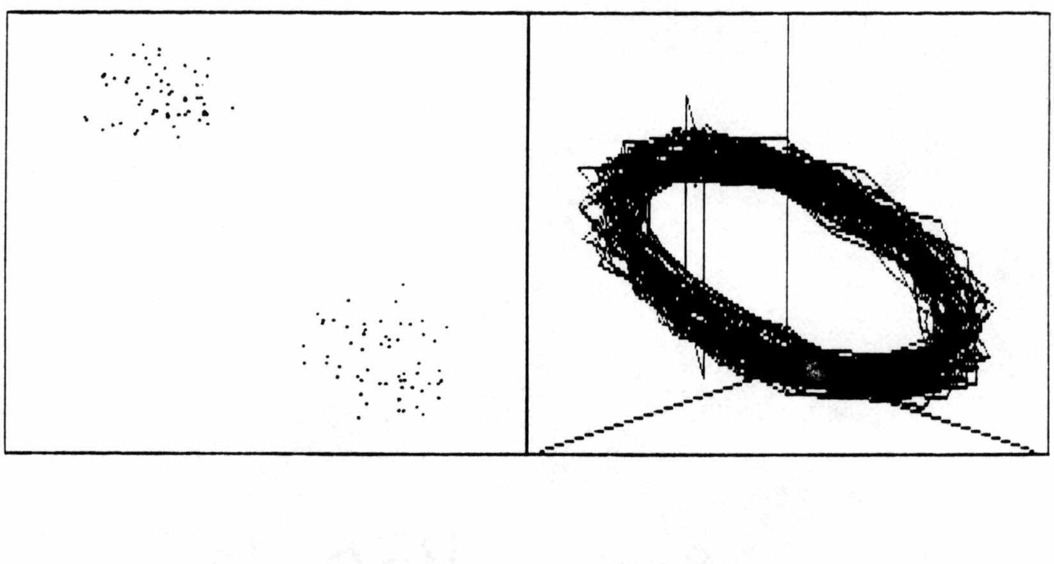

Figure IX-2. Reconstructed phase portrait and Poincare section of a noisy sine wave

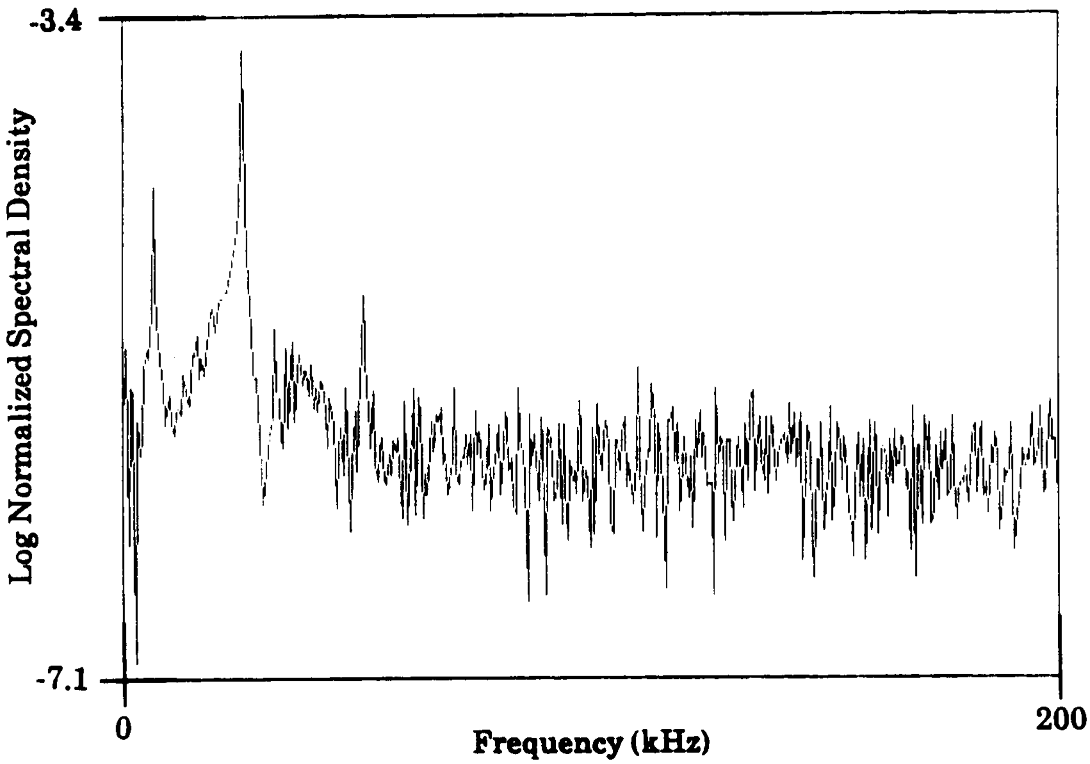

Figure IX-3. Power spectrum of a two-frequency signal with noise added

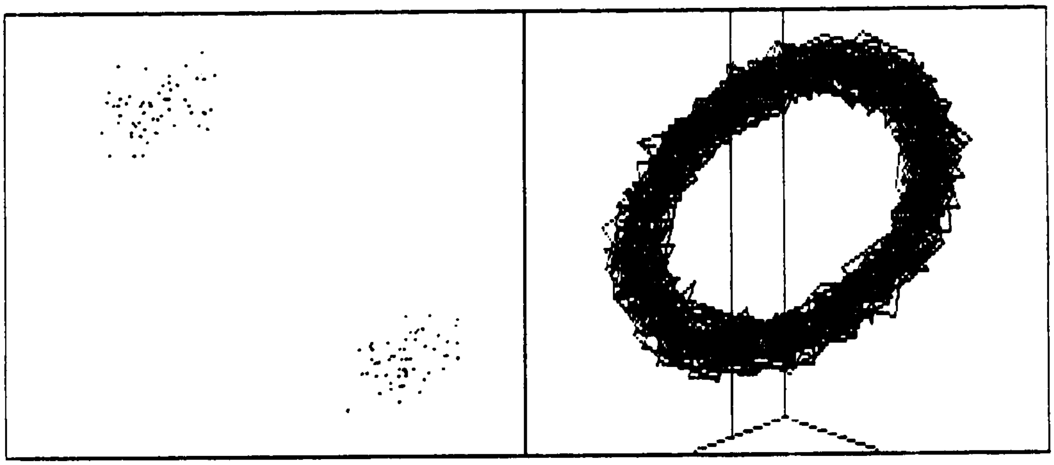

Figure IX-4. Reconstructed phase portrait and Poincare section of a two-frequency signal with noise added behavior should dominate at the smaller scale sizes, and low dimensional behavior should be observed at scale sizes above the noise level. The correlation plots for the noisy limit cycle and noisy torus are shown in Figures IX-5 and IX-6, respectively. As expected, two distinct regions are observed in both plots. Unfortunately, for the noisy torus, the scaling region is too small to designate a single region for all embedding dimensions. It was therefore necessary to define a scaling region for each embedding dimension. These scaling regions are depicted in the lower left graph, while the lower right figure is a plot of the correlation dimension as a function of embedding dimension. Interestingly enough, the correlation dimensions obtained for each signal are approximately 1.2. Apparently, this dimension routine cannot distinguish the signals either.

It is now desired to compare these two reference cases to a set of actual plasma data. The time series is shown in Figure IX-7. One can easily see that the signal contains a dominant frequency. There also appears to be evidence of a beat frequency. Though the lower frequency contains very little power, both can be observed in the signal's power spectrum, which is shown in Figure IX-8. The reconstructed phase portrait is shown in Figure IX-9. Upon first observation, the attractor appears to possibly be chaotic; but after taking a Poincare section, this does not appear to be the case. As can be seen from the Poincare section in Figure IX-10, there is no evidence of a fractal structure.

The next step would be to estimate the correlation dimension of the signal. Figure IX-11 shows the correlation plots. Once again, there are two distinct regions of the correlation integral plot. Even though the signal seems to be fairly coherent, the noise appears to dominate on most scale sizes. However, there does appear to be a very narrow scaling region. Since the

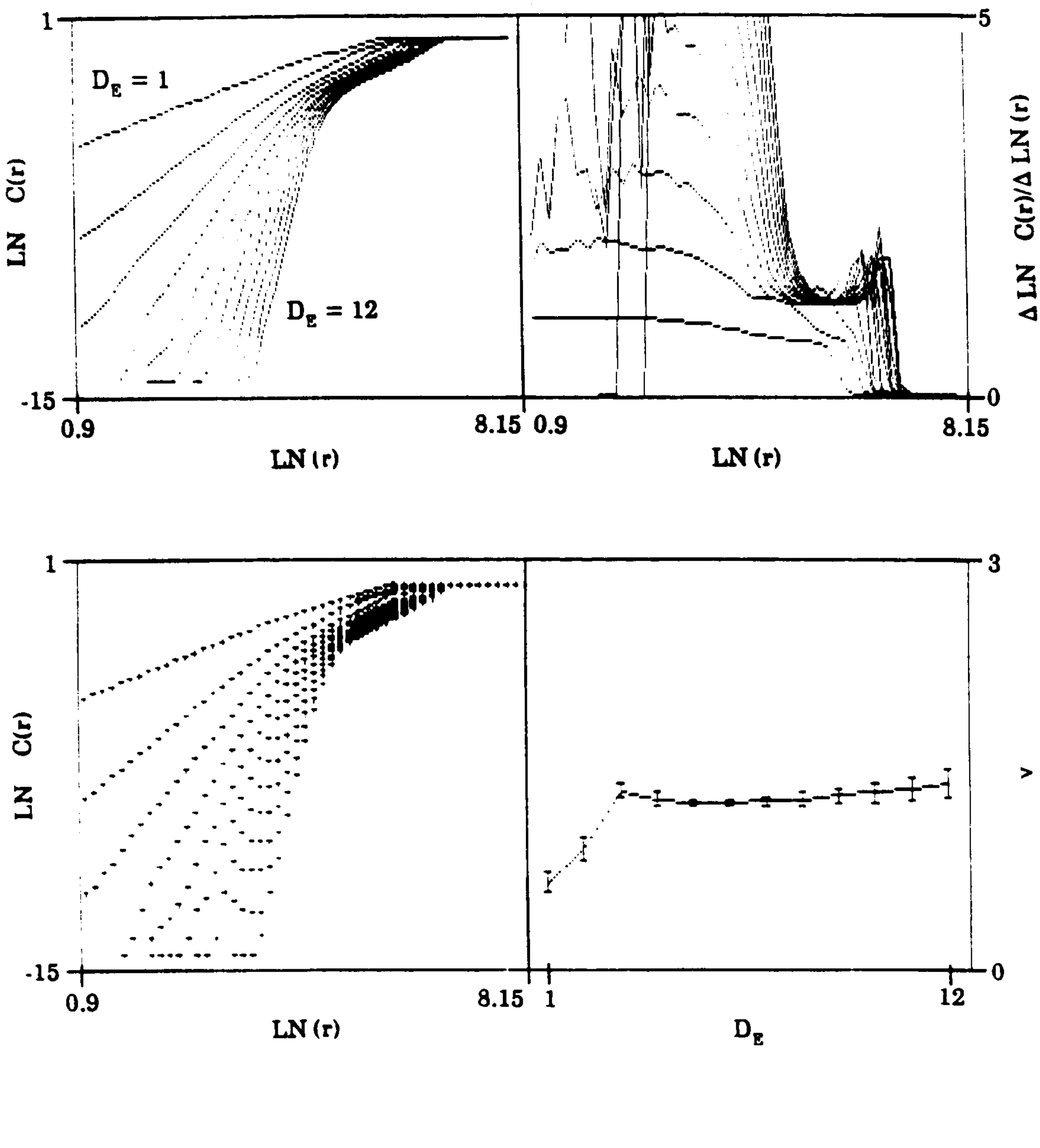

Figure IX-5. Correlation plots for the noisy sine wave

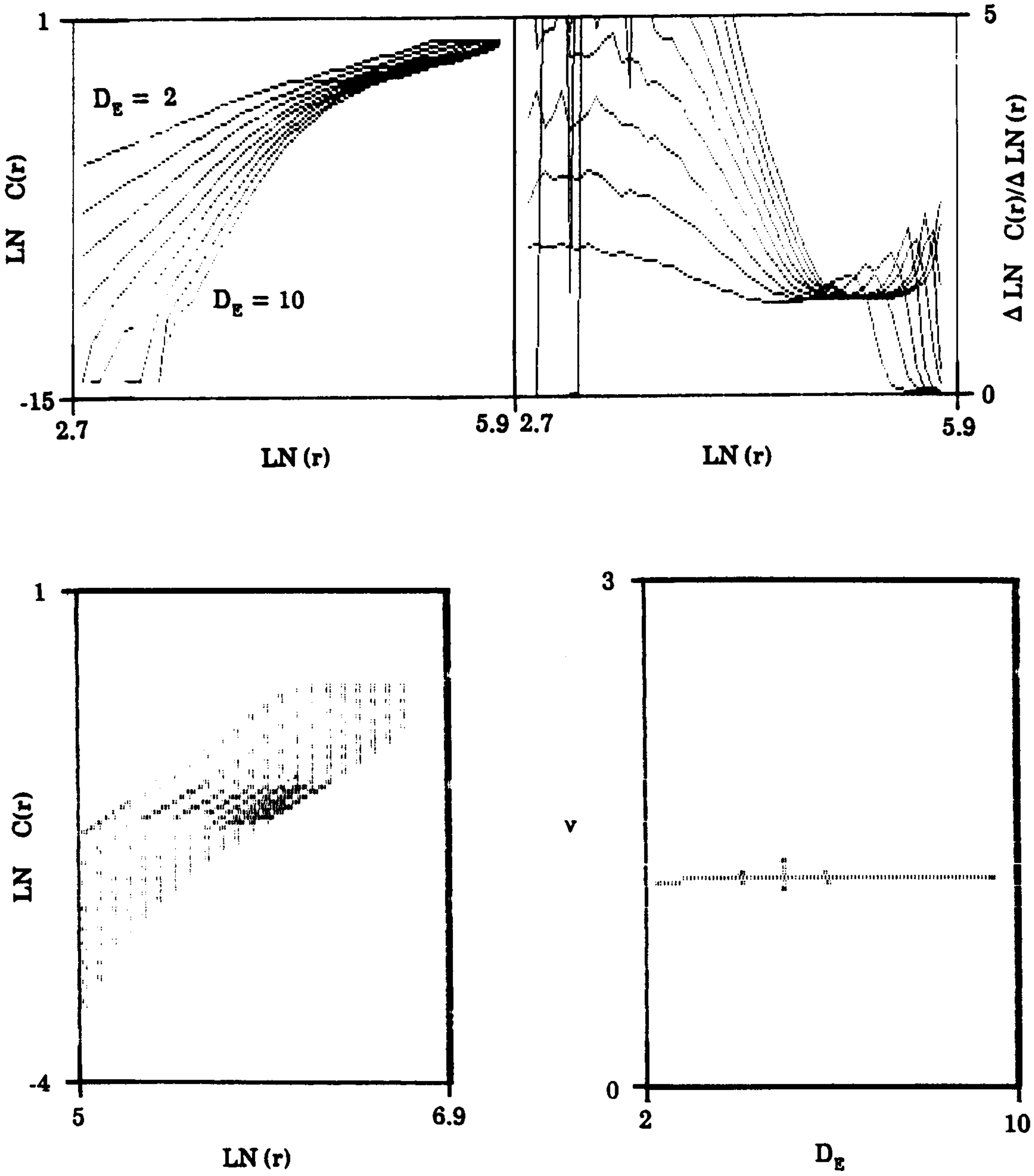

Figure IX-6. Correlation plots for the noisy torus

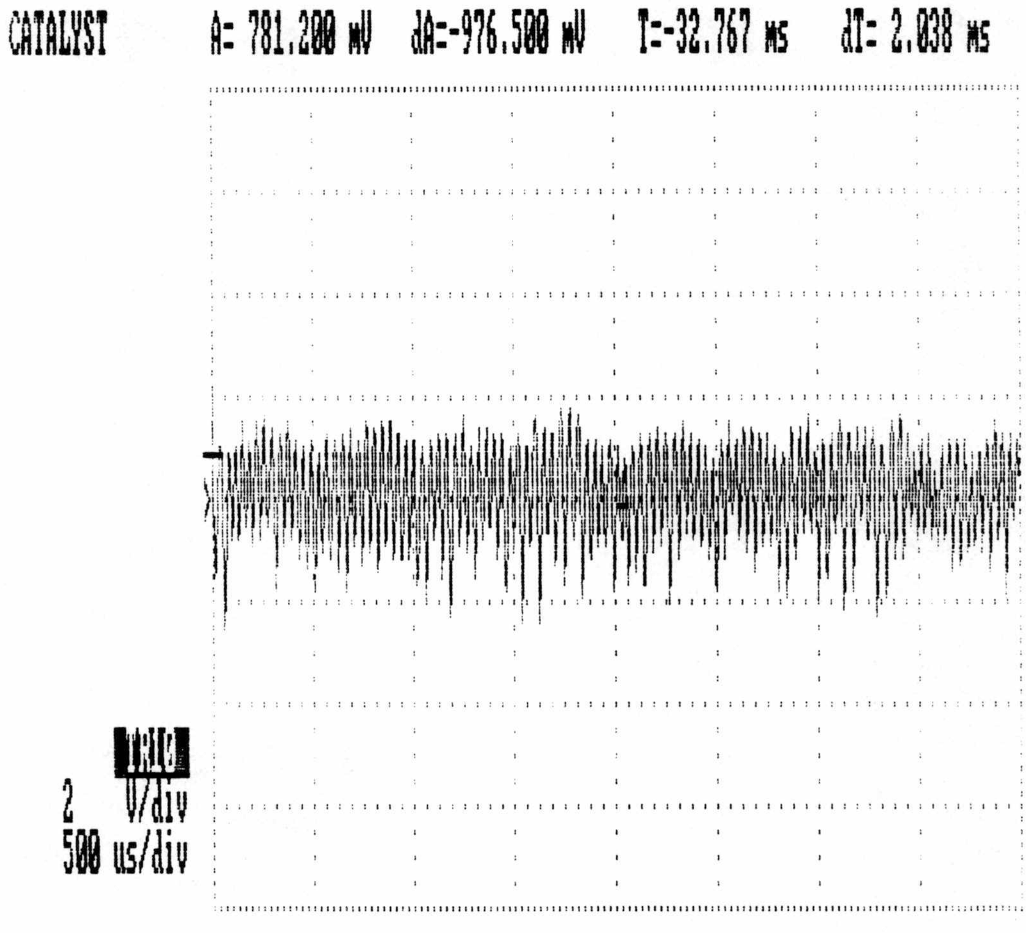

Figure IX-7. Time history of plasma fluctuation signal

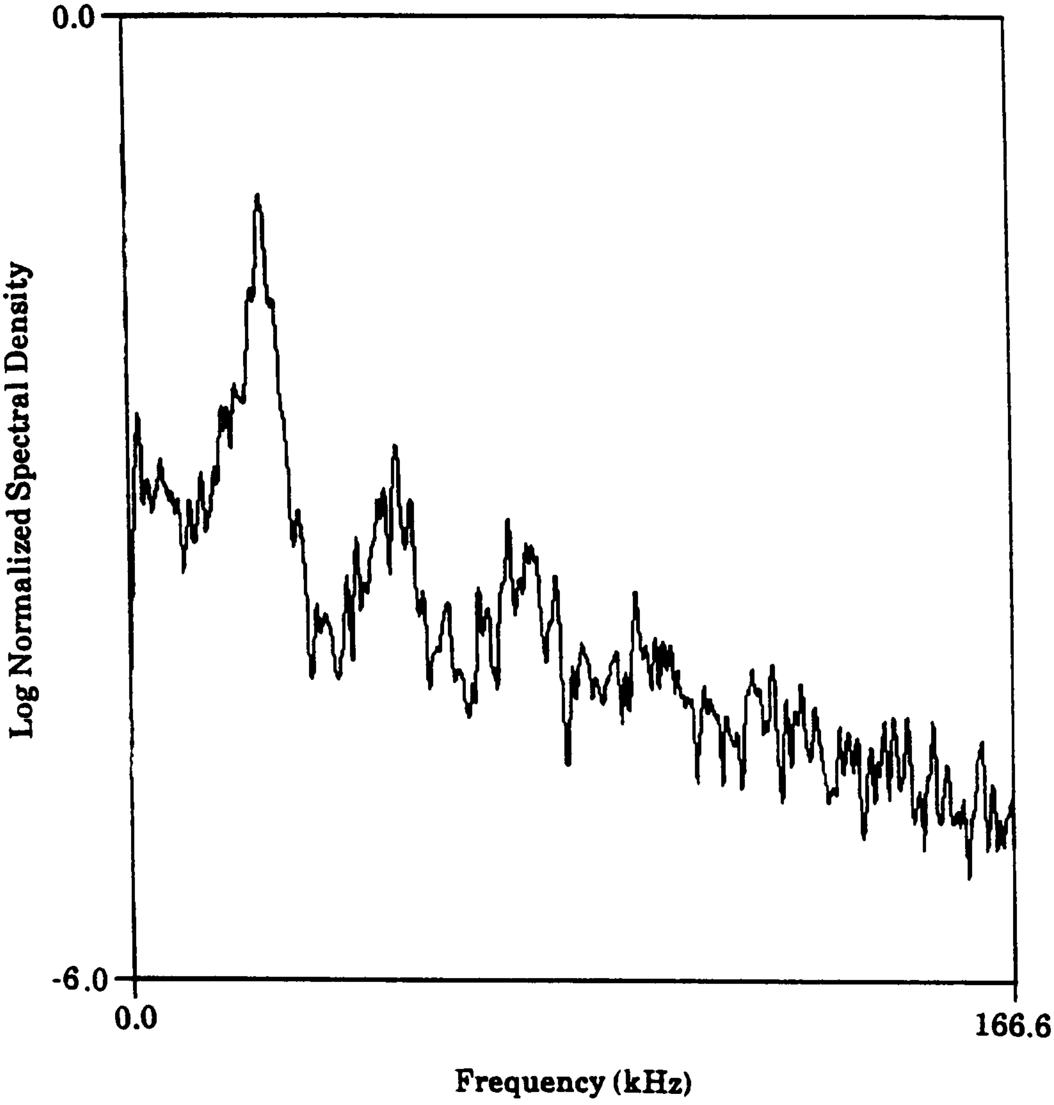

Figure IX-8. Fourier power spectrum associated with the signal in Figure IX-7

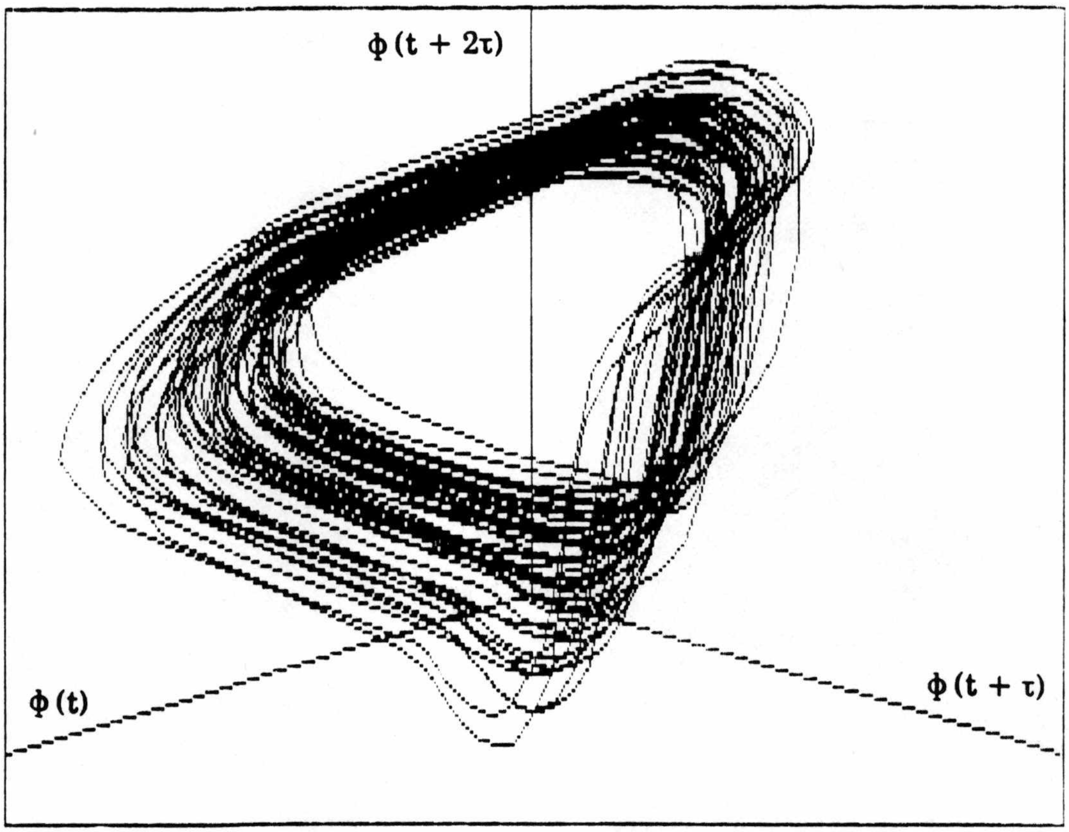

Figure IX-9. Reconstructed phase portrait of the plasma signal

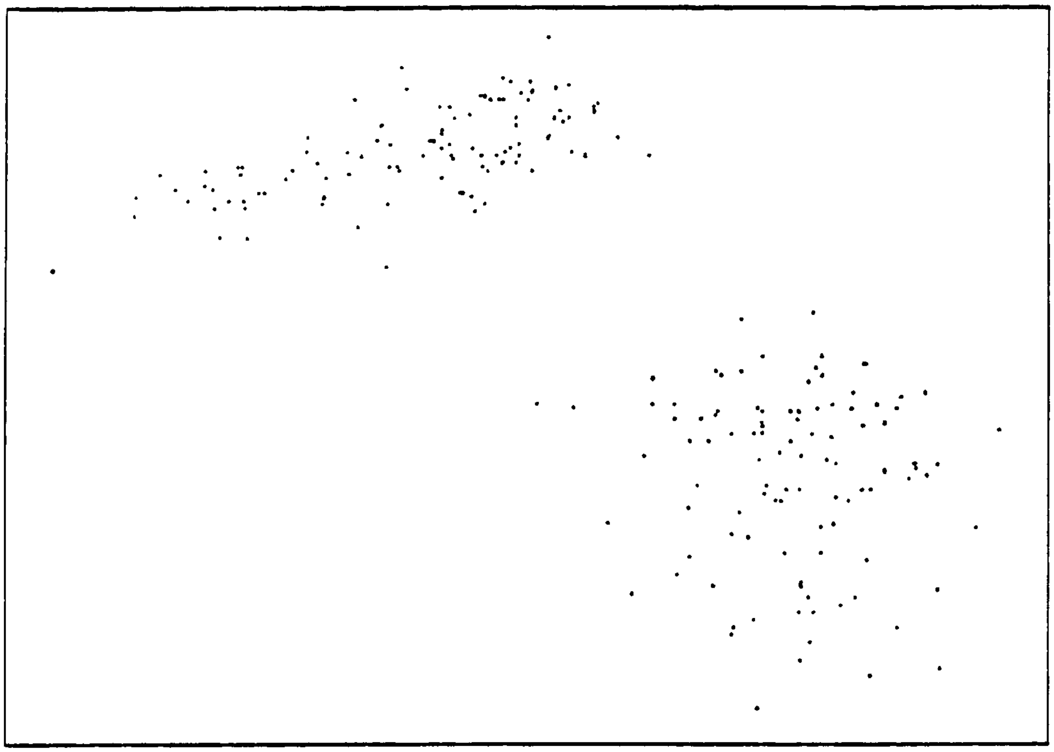

Figure IX-10. Poincare section taken from attractor in Figure IX-9

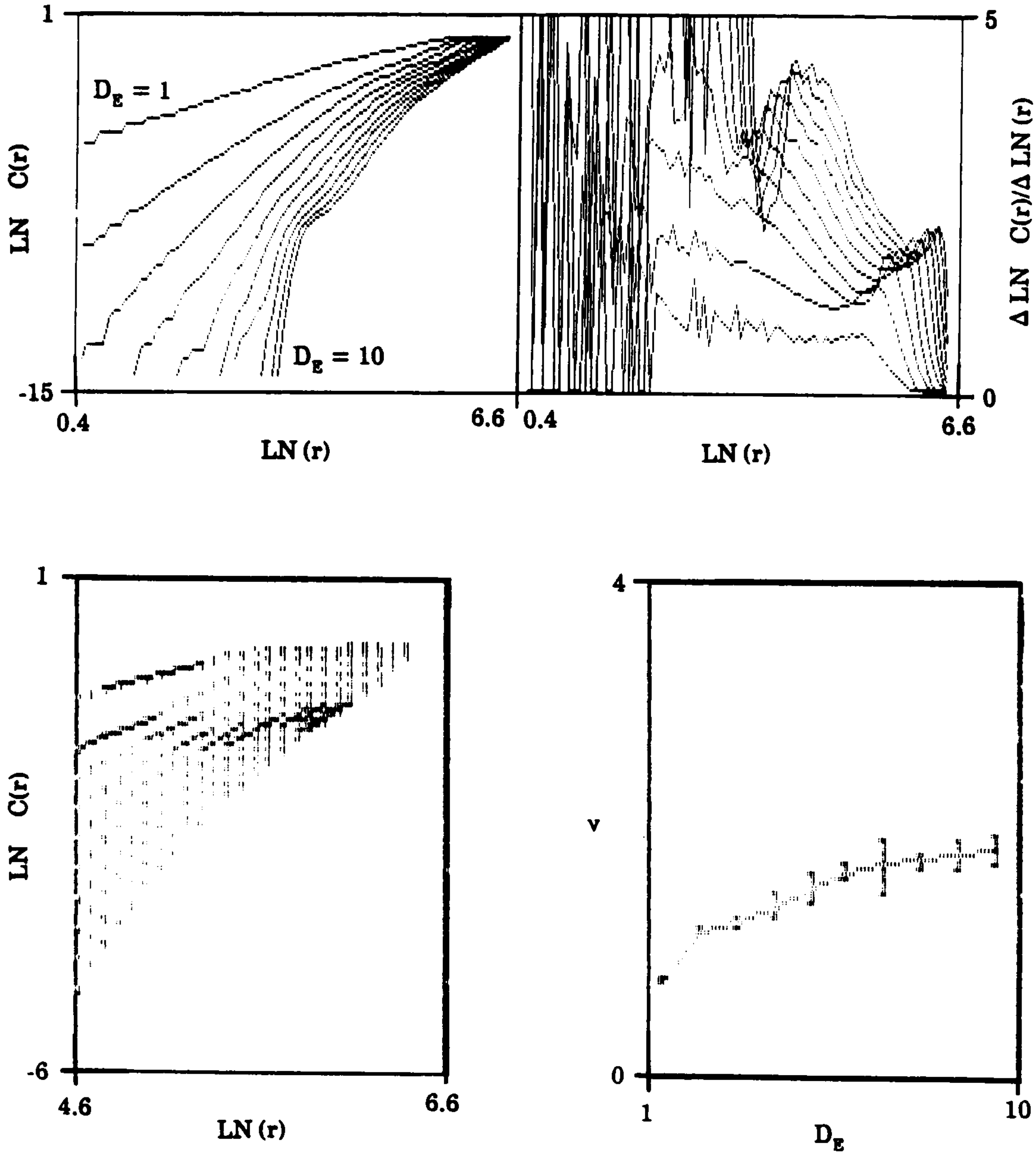

Figure IX-11. Correlation plots for plasma signal slope is relatively constant only at the larger scale sizes, the usable scaling region is limited on each side. The noise diminishes the scaling region from the left, while the bounds of the attractor take their toll on the right. For this case, the only possible scaling region leads to a value of approximately 1.9. Since the attractor does not appear to be chaotic, this value suggests that the signal is due to a noisy superposition of two incommensurate frequencies. Unfortunately, there is a significant difference between the value of correlation dimension obtained for this data and the value estimated for the noisy torus data.

One detail that should be mentioned is the knee that is present in the correlation integral plot of Figure IX-11. This is where the slope appears to saturate at low r values and then increases again for higher r values. This has been shown to result from so-called spurious correlations and sometimes occurs when studying experimental data. This effect will be discussed in more detail in Appendix B.

CHAPTER X

EFFECTS OF VARYING PLASMA PARAMETERS

This chapter consists of data for which plasma conditions were changed in order to study the effects on the state of turbulence. Three sets of data were examined, each having a different variable. The three control parameters were the gas pressure, anode voltage and magnetic field strength.

A. Variation of Gas Pressure

For this set of data, the Helium Gas pressure was varied from 260 microtorr to 1670 microtorr in five increments. The variation of the electron number density, electron kinetic temperature, and plasma floating potential measured with a Langmuir probe for the different runs is shown in Figure X-1. The effects of the pressure on the power spectra of the fluctuations can be seen in Figure X-2. For the first four runs, the signal is quite coherent and the peak frequency is 25 to 30 dbm above the noise floor. Once the pressure reaches 1200 microtorr, the signal strength drops considerably.

The reconstructed phase portraits are shown in Figure X-3. These tend to agree well with the power spectra. The signal starts out fairly coherent and remains that way until the fifth run. The drop in amplitude of the power spectrum corresponds to the decrease in size of the attractor. By the time the pressure reaches its highest value, the motion has become considerably less coherent. Figure X-4 shows the correlation dimension plots for each run. The first four runs show evidence of a narrow scaling region where a dimension may be inferred, as well as a region where the noise dominates. By Run 5, the scaling region has begun to disappear and by Run 6 the slope is steadily

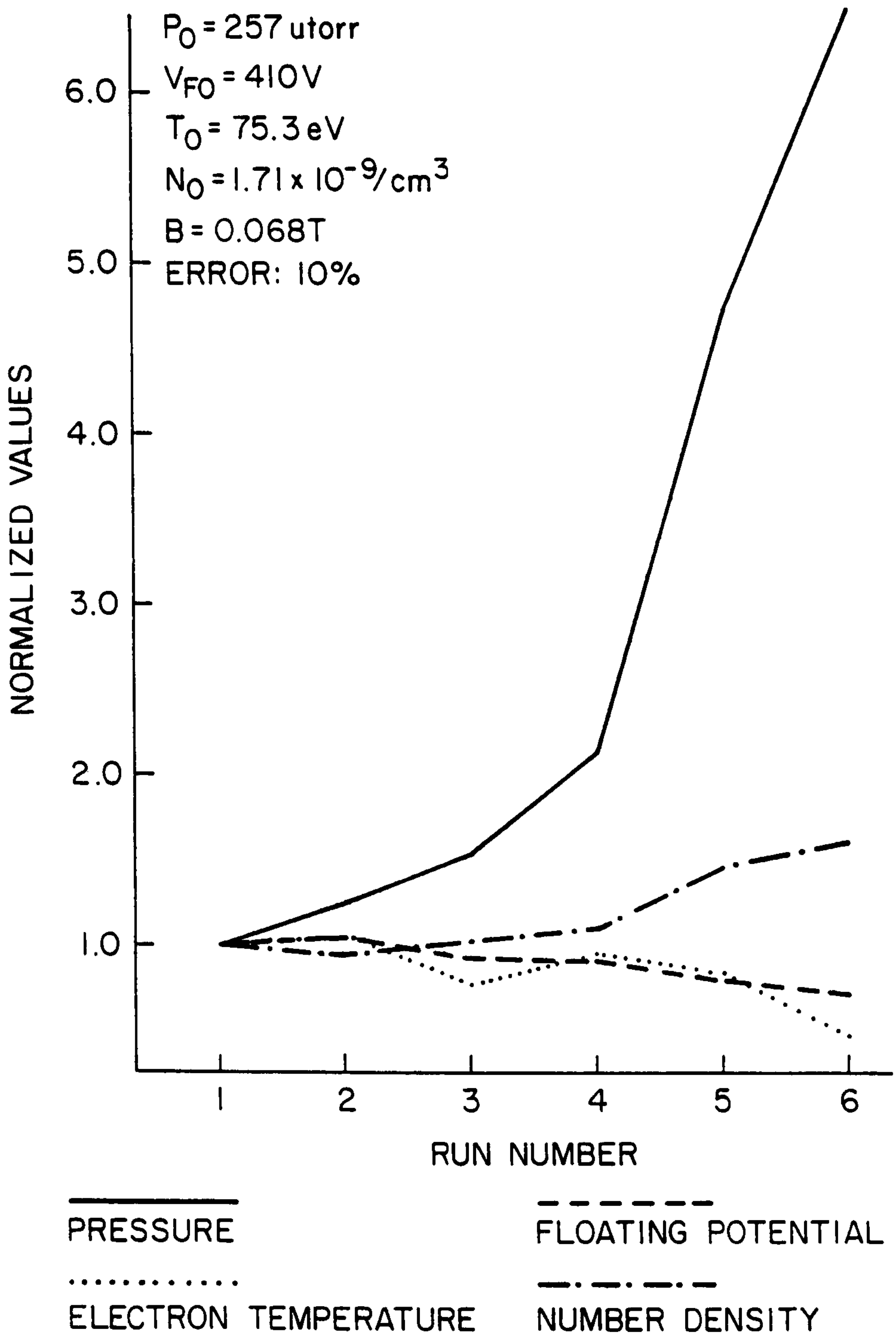

Figure X-1. **Variation of plasma parameters for different helium gas pressures**

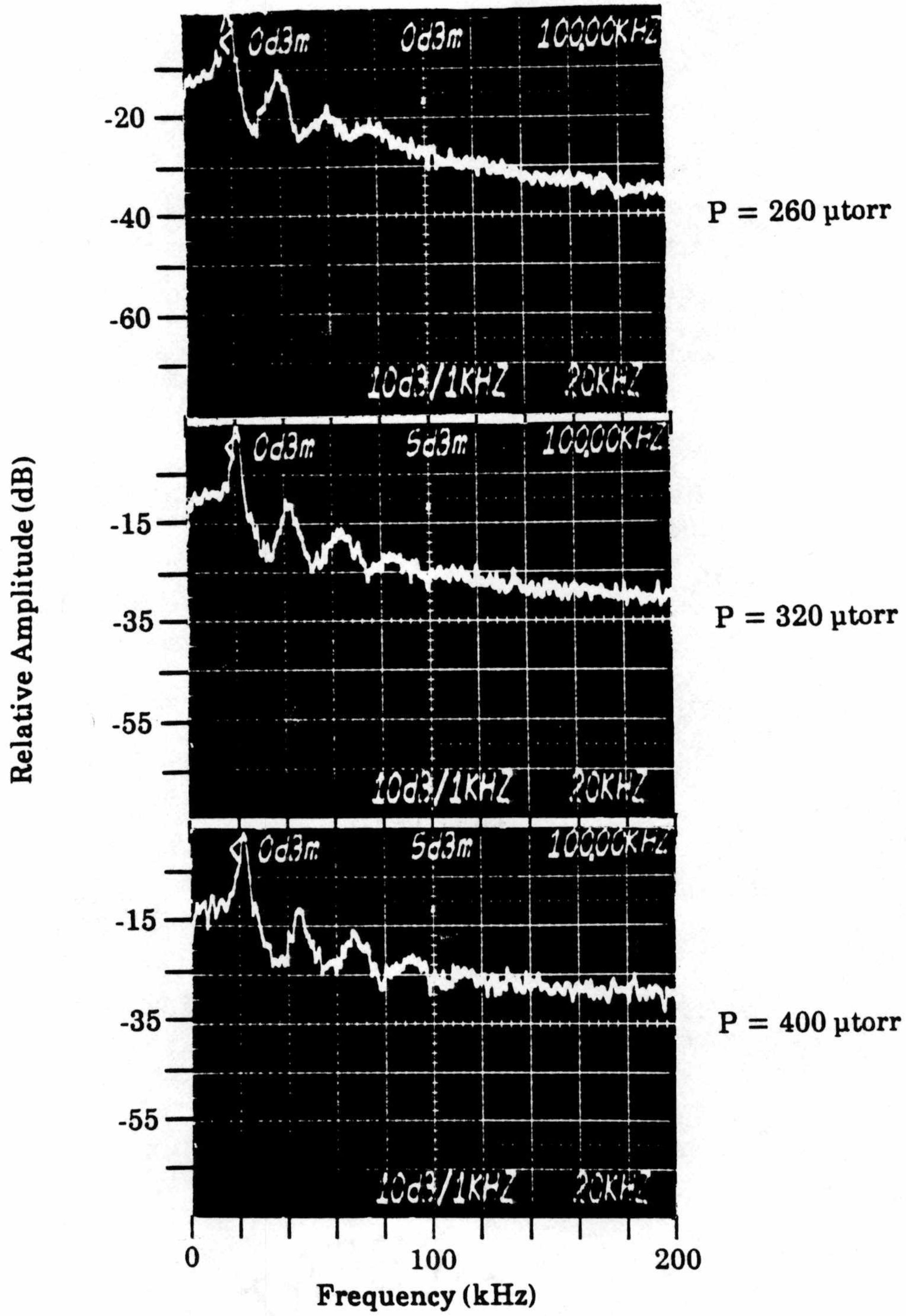

Figure X-2. Potential fluctuations for varying helium gas pressure

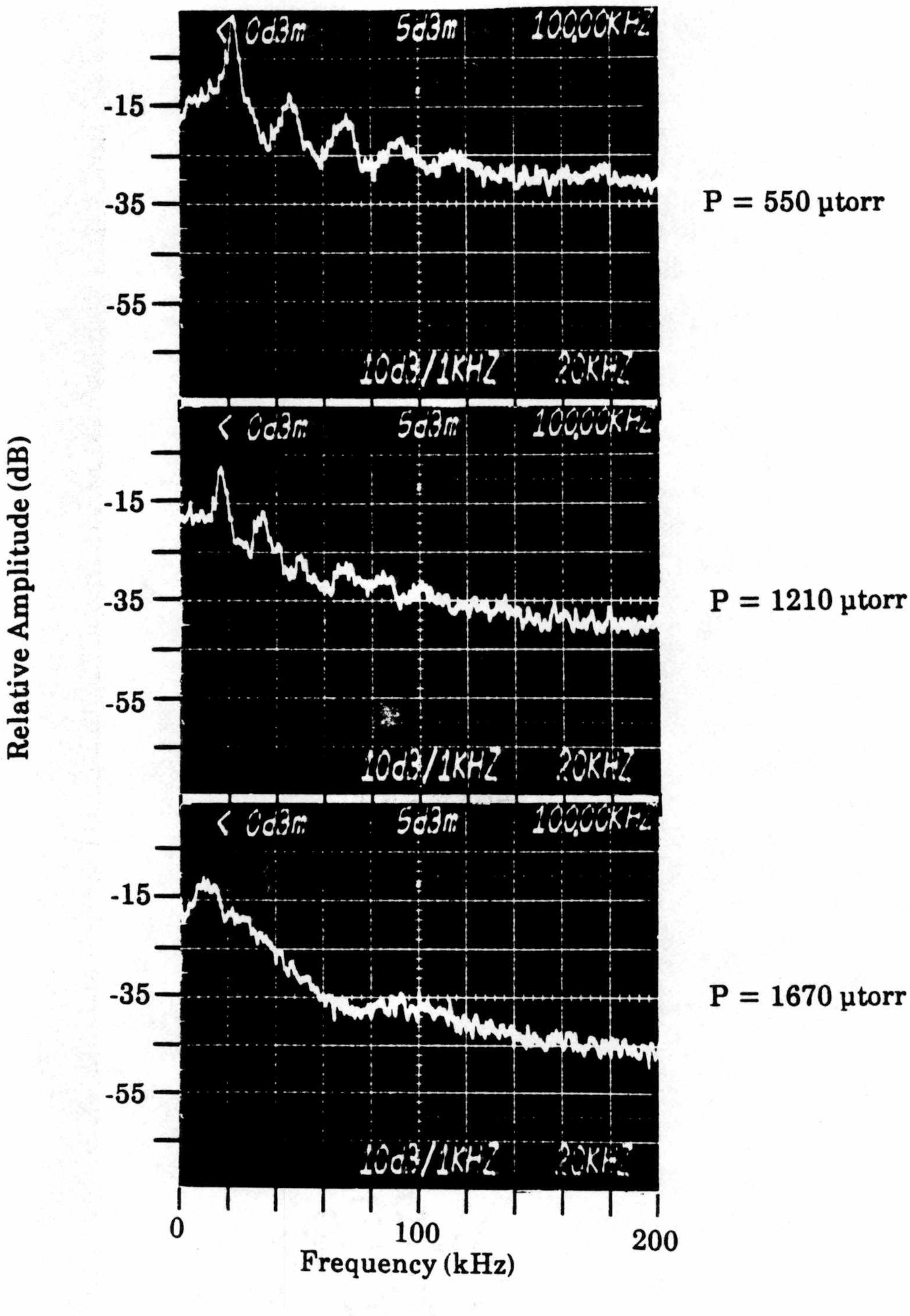

Figure X-2. (Continued)

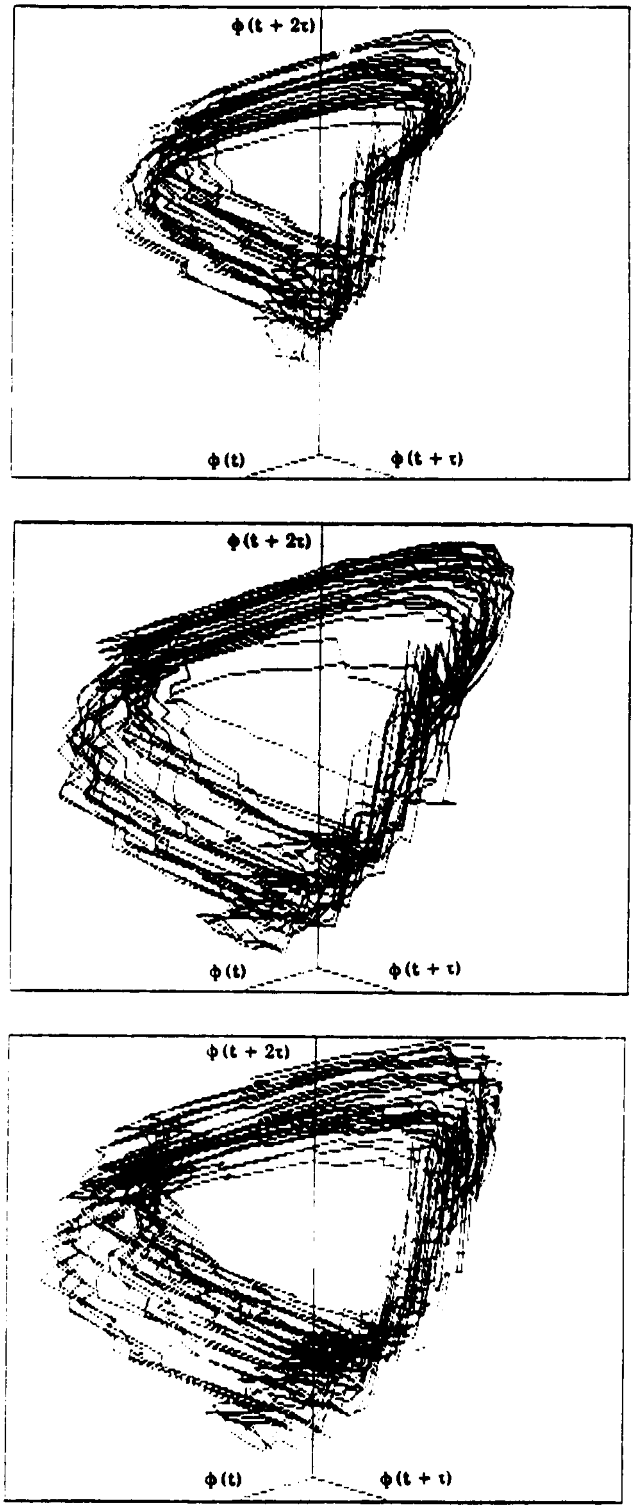

Figure X-3. Reconstructed phase portraits for varying gas pressure

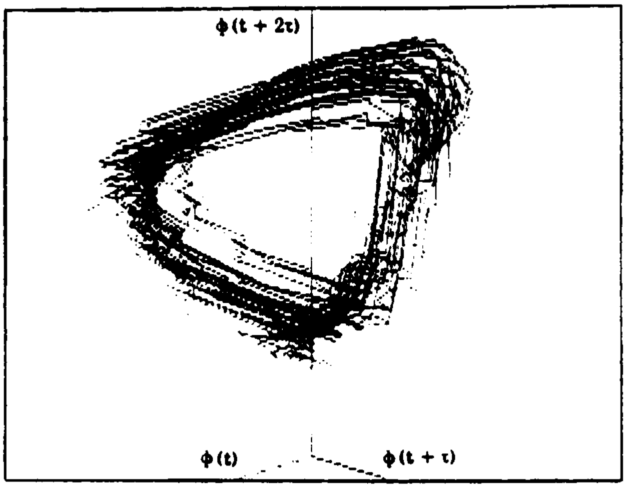

P = 550 μtorr

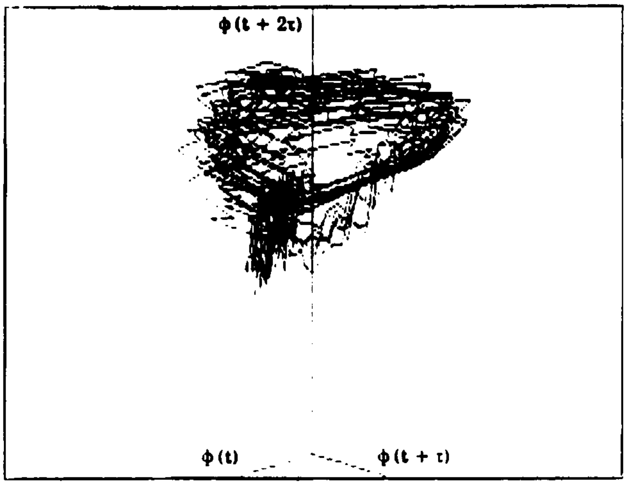

P = 1210 μtorr

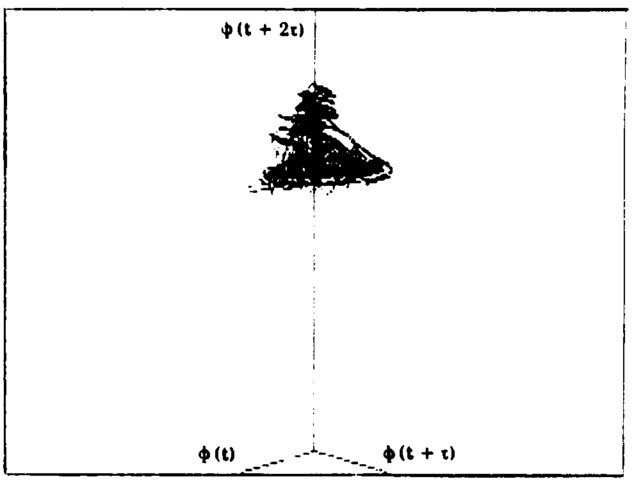

P = 1670 μtorr

Figure X-3. (Continued)

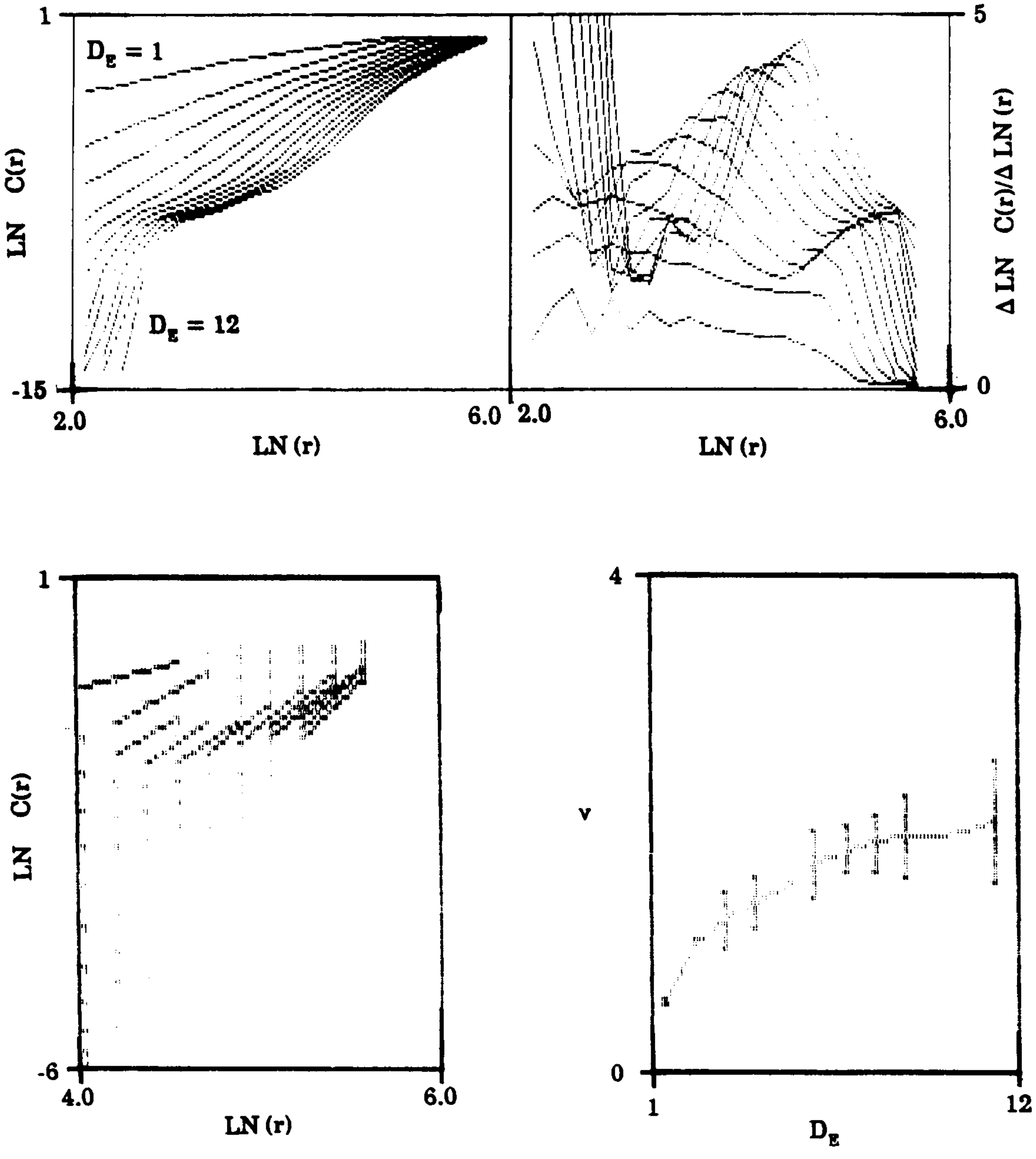

(A) P = 260 μtorr

Figure X-4. Correlation plots for varying gas pressure

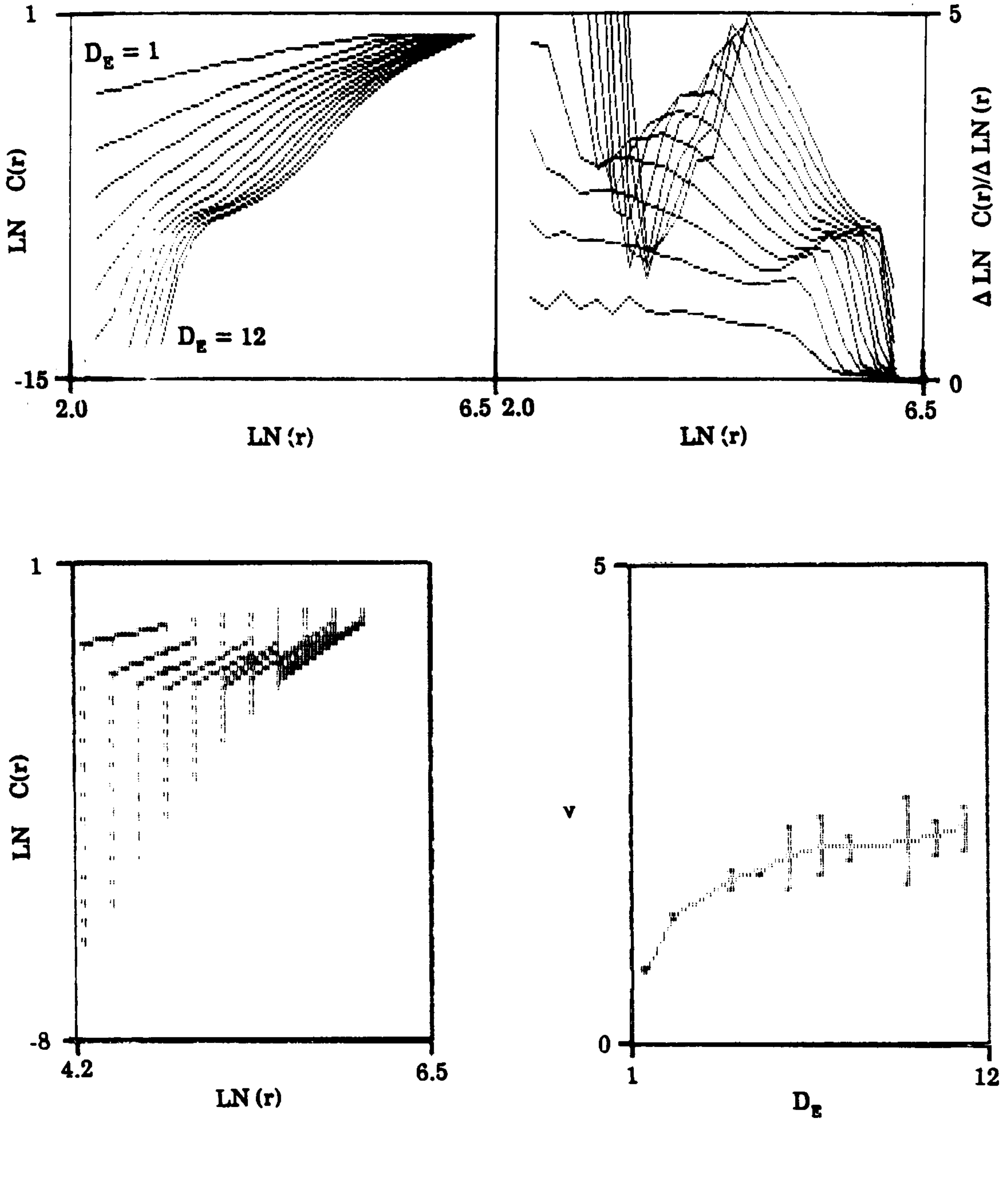

(B) P = 320 μtorr

Figure X-4. (Continued)

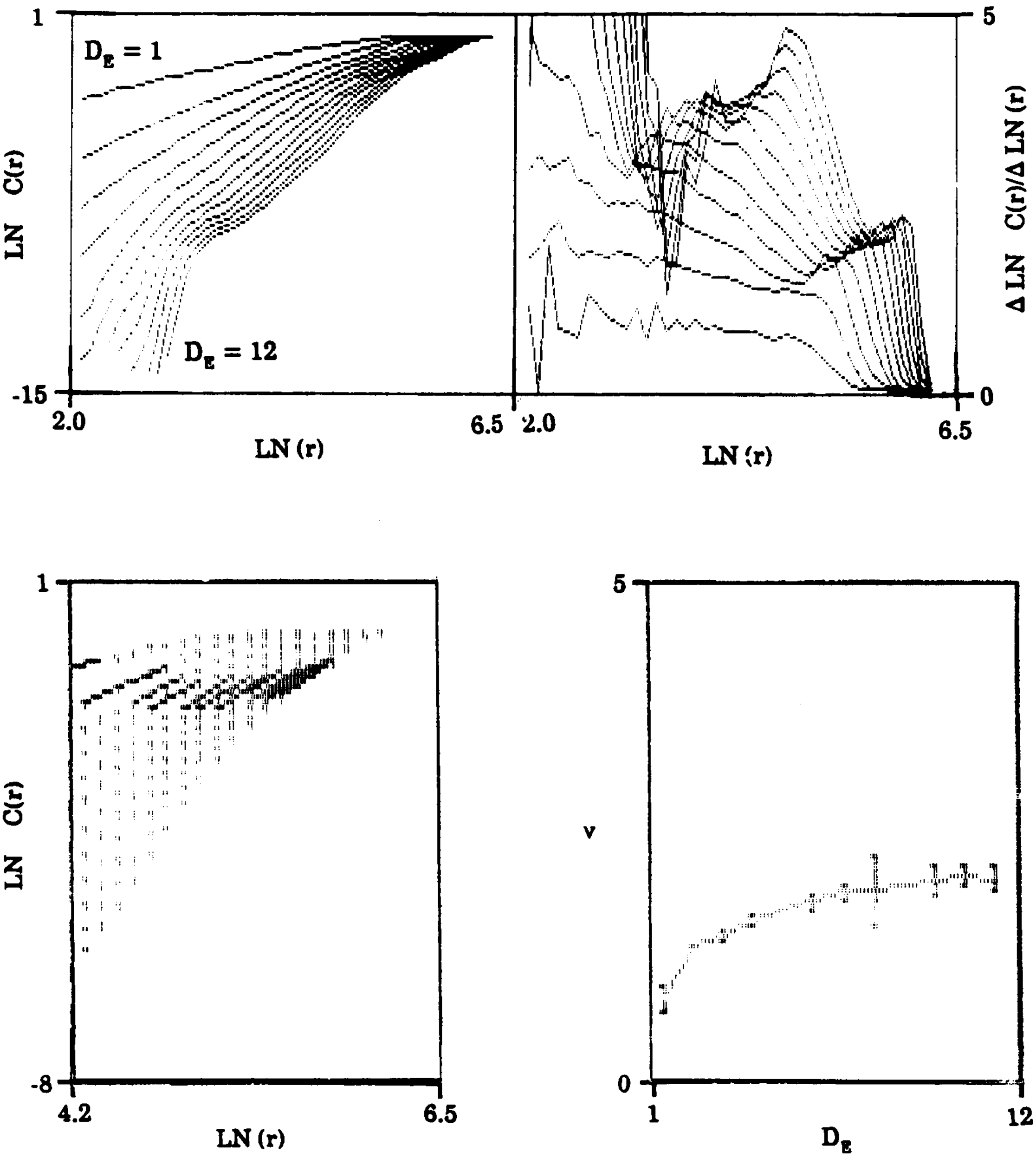

(C) P = 400 μtorr

Figure X-4. (Continued)

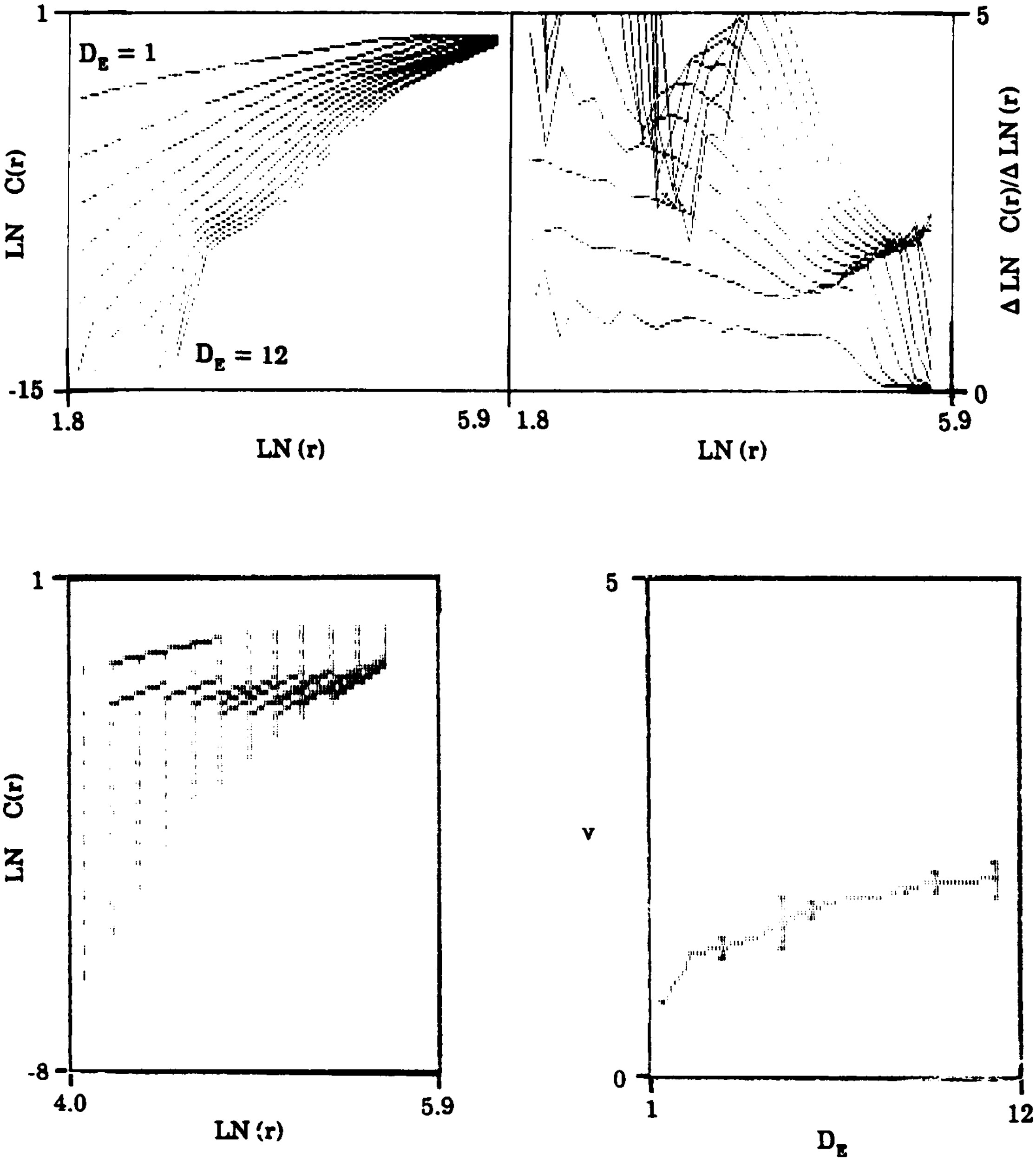

(D) P = 550 μtorr

Figure X-4. (Continued)

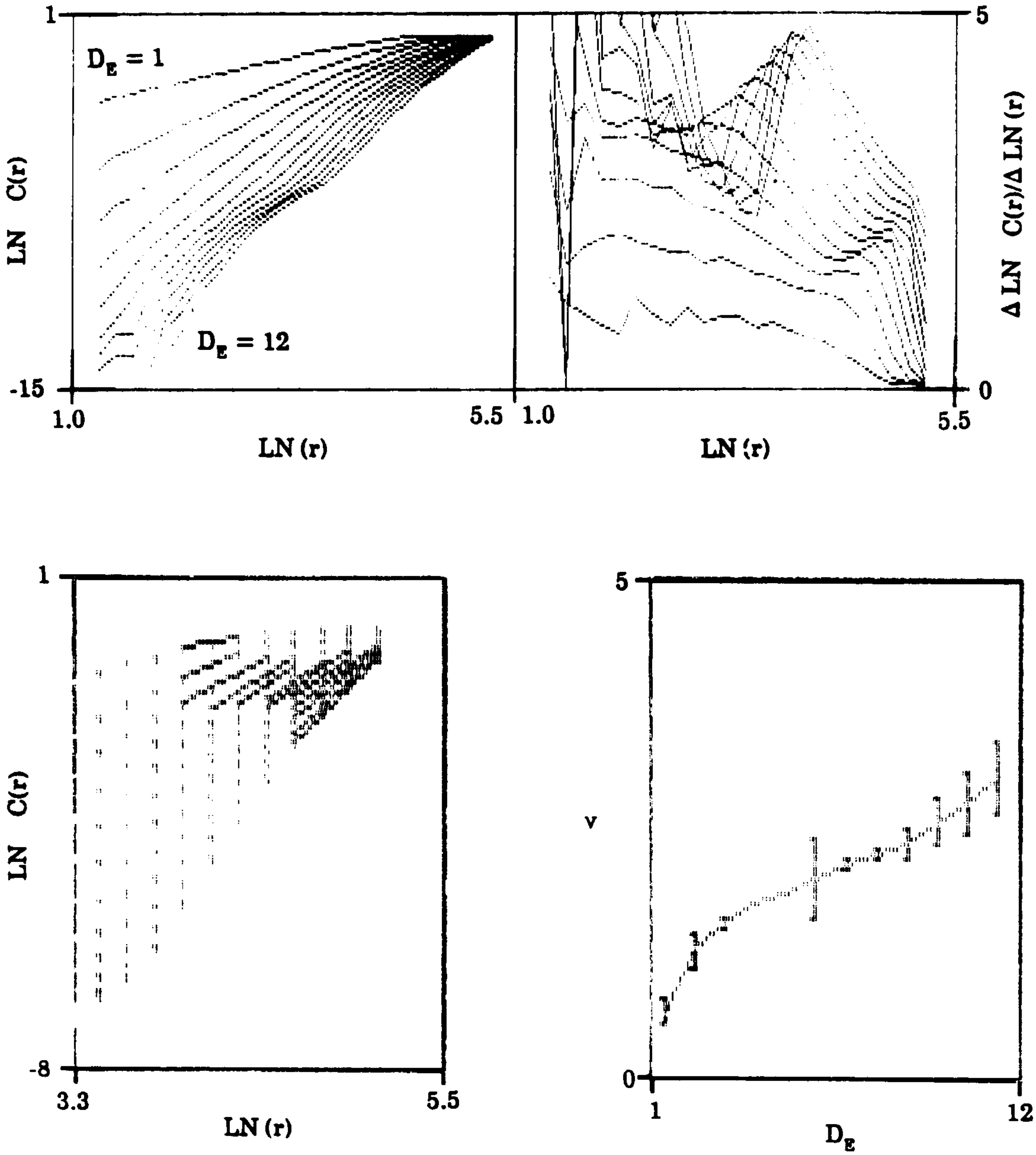

(E) P = 1210 µtorr

Figure X-4. (Continued)

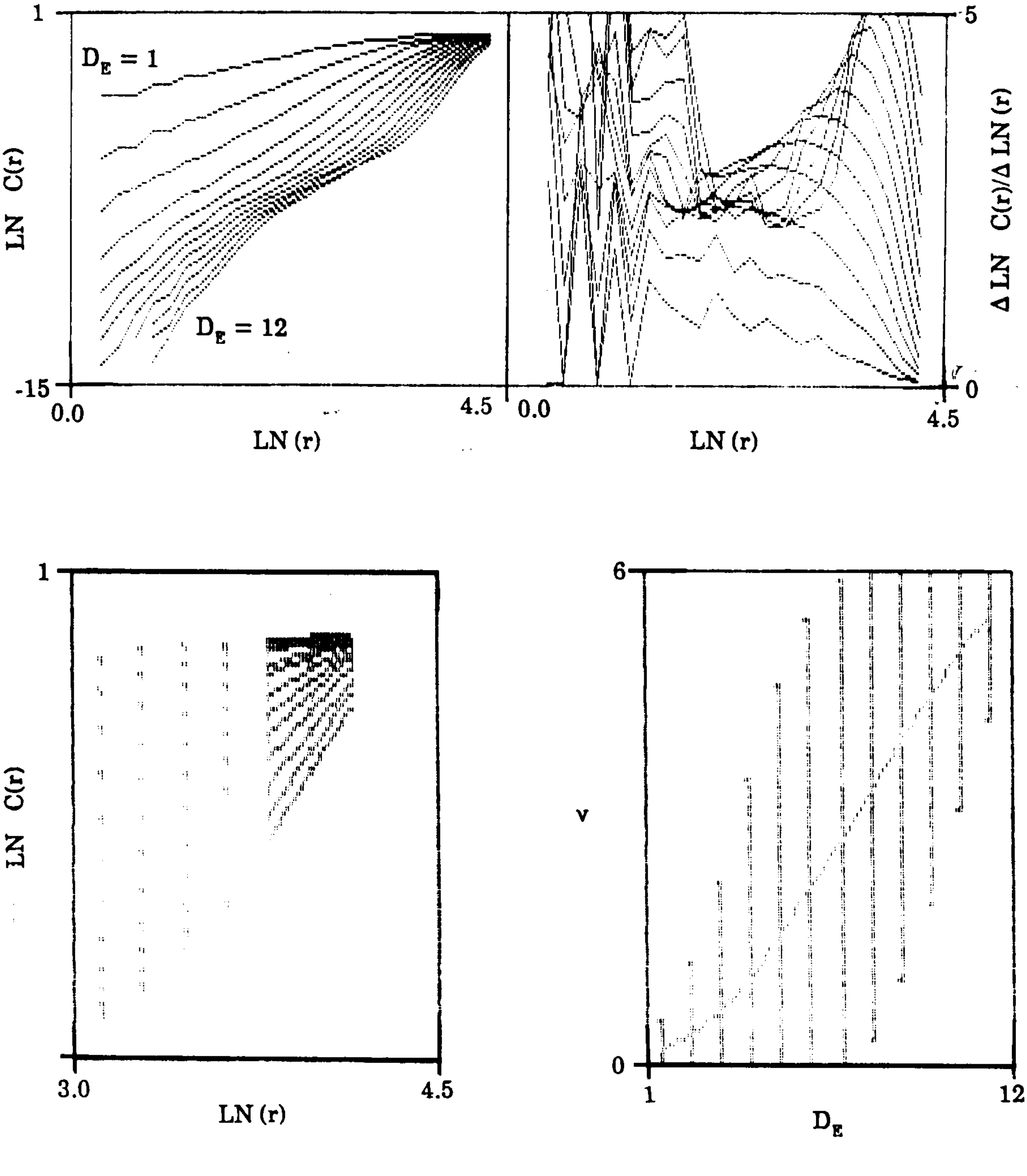

(F) P = 1670 μtorr

Figure X-4. (Continued)

increasing with embedding dimension, which implies that the fluctuations have become totally random.

Table X-1 is a list of the correlation dimensions that were obtained for each run. While these values cannot be taken as definitive, for reasons to be discussed later, the trend appears to be consistent with that observed with other means. These values are plotted as a function of pressure in Figure X-5.

B. Variation of Anode Voltage

For the second set of data, the voltage applied to the anode was varied. This voltage controls the induced electric field in the plasma. The variation of the plasma parameters measured with a Langmuir probe are plotted for the different run conditions in Figure X-6. Figure X-7 shows the effect of the anode voltage on the Fourier power spectra. The peak frequency is originally about 15 dbm above the noise floor. After increasing the applied voltage by a factor of two, the peak frequency is approximately 25 dbm above the noise. The power spectra show a steady increase in frequency and amplitude as the anode voltage is increased.

Figure X-8 displays the reconstructed phase portrait for each run, with all of them drawn with the same axis scales. The principal difference in these is that the size of the attractor increases with the anode voltage. This is explained by the increasing amplitude of the fluctuations with voltage. Also, the phase portraits become slightly more coherent as the voltage is increased.

Figure X-9 contains the correlation plots for each run. By closely observing the correlation integral and derivative graphs, one can see that the plots for each run exhibit the two distinct regions. Similar to the previous

Table X-1

Correlation Dimension for Varying Pressure

Run Number	Pressure (µtorr)	Dimension
1	257	2.5
2	321	2.2
3	395	2.0
4	548	1.95
5	1214	N.C.
6	1667	N.C.

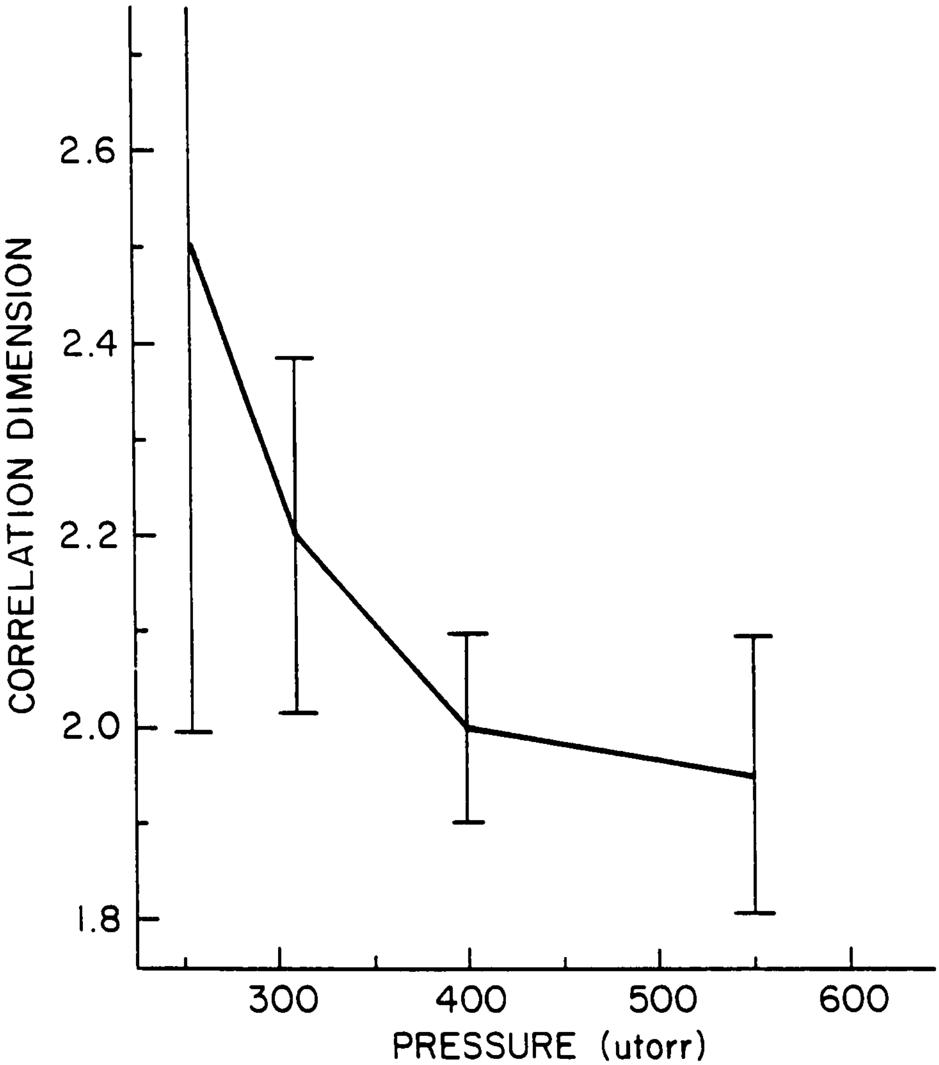

Figure X-5. **Plot of correlation dimensions as a function of pressure**

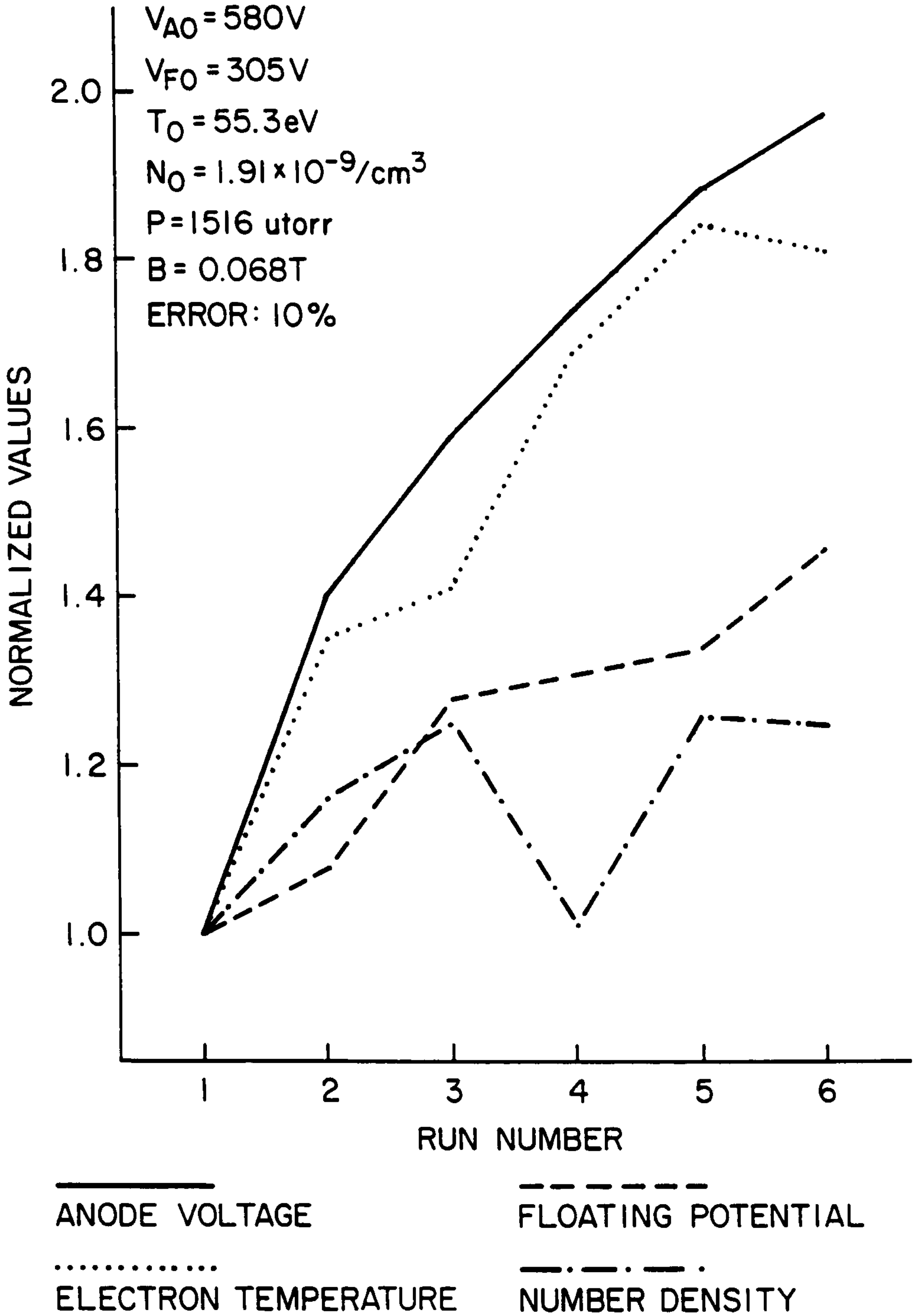

Figure X-6. Variation of plasma parameters for different anode voltages

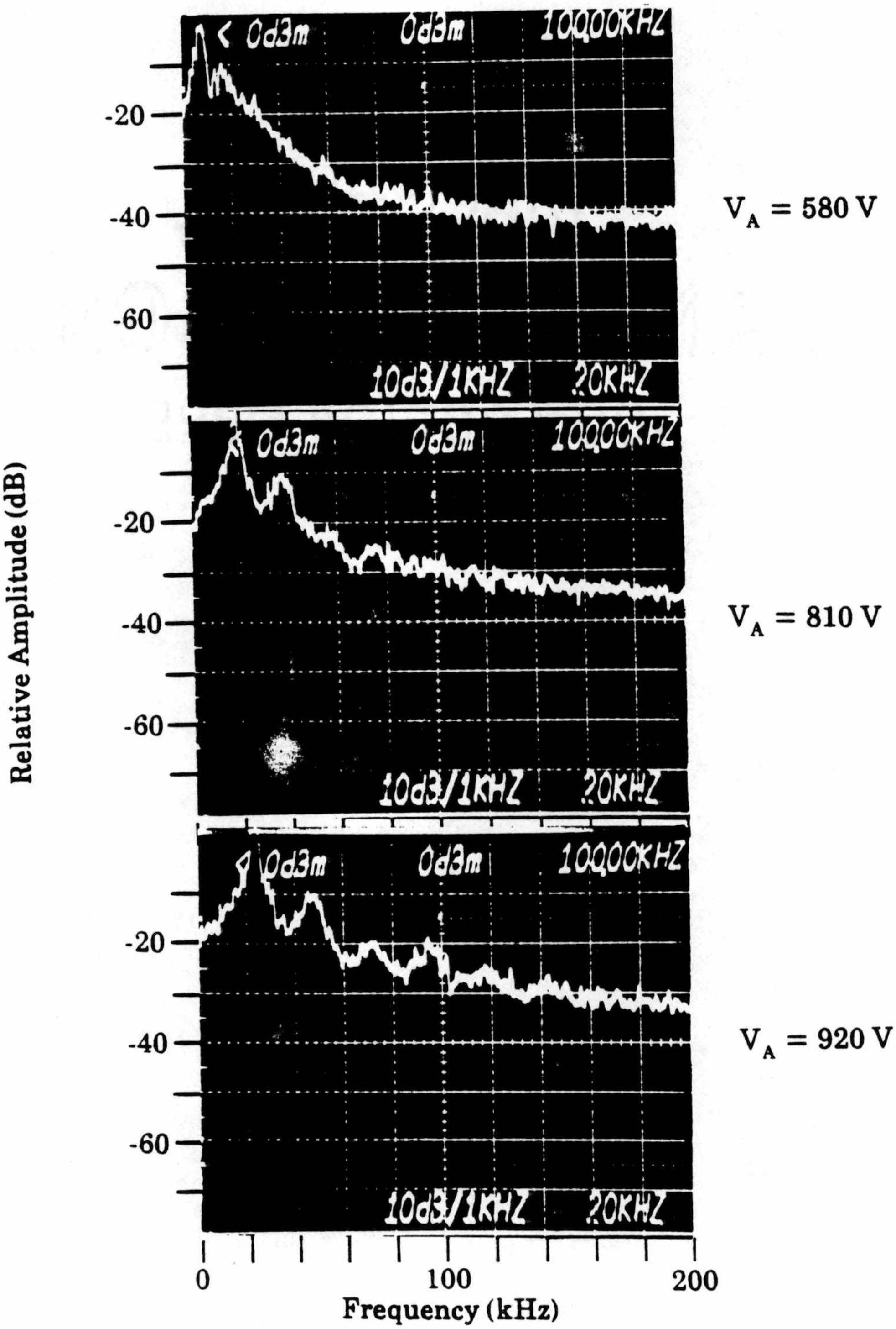

Figure X-7. Potential fluctuations for varying anode voltage

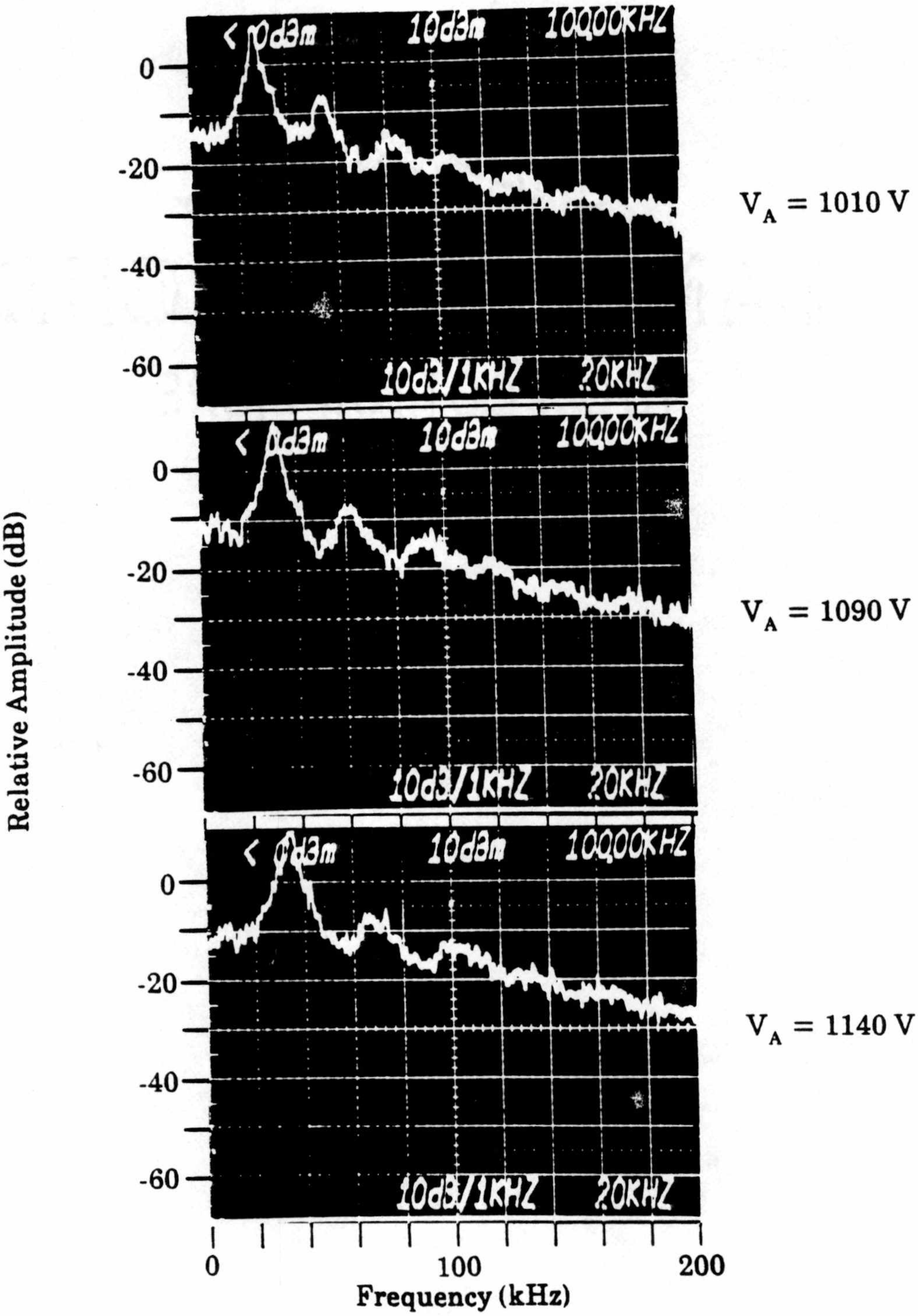

Figure X-7. (Continued)

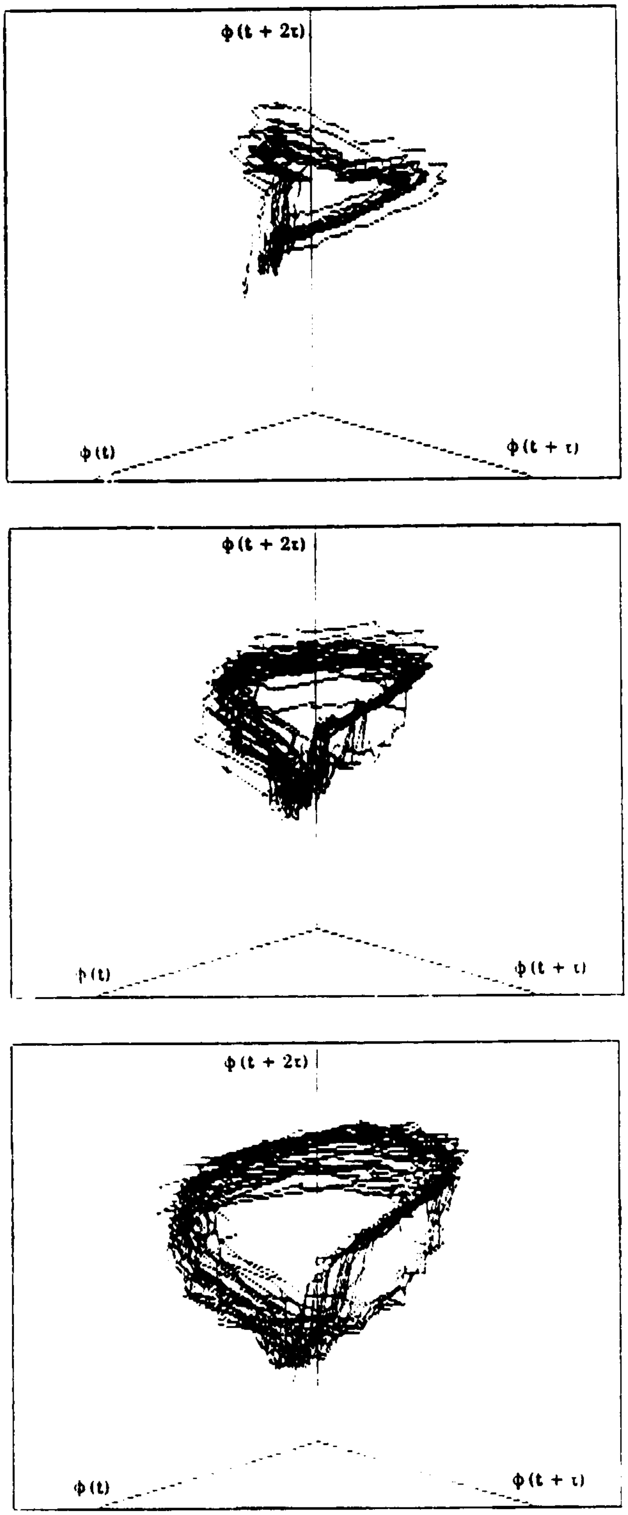

$V_A = 580$ V

$V_A = 810$ V

$V_A = 920$ V

Figure X-8. Reconstructed phase portraits for varying anode voltage

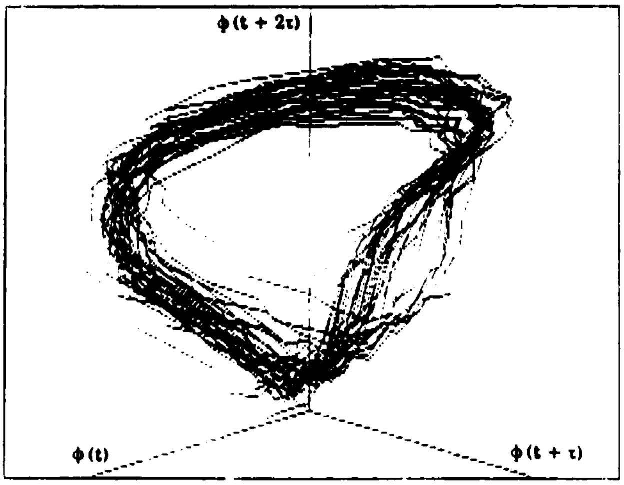

$V_A = 1010\ V$

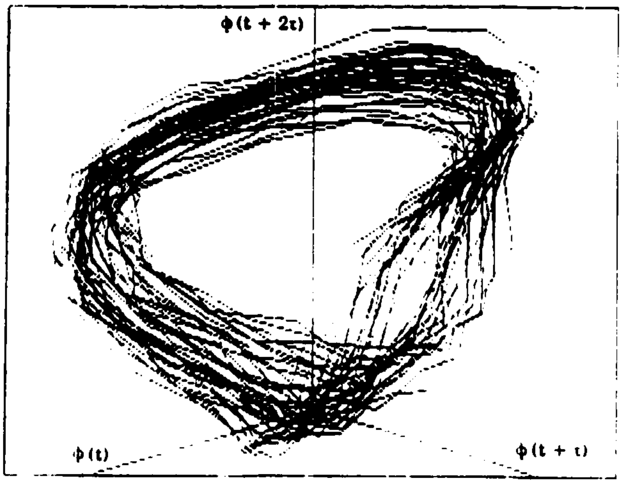

$V_A = 1090\ V$

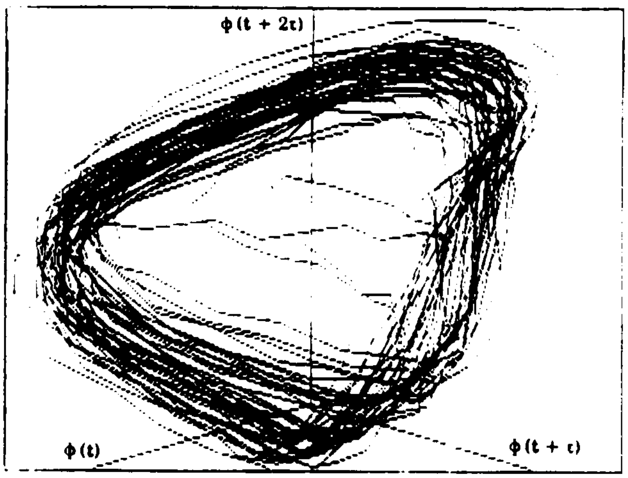

$V_A = 1140\ V$

Figure X-8. (Continued)

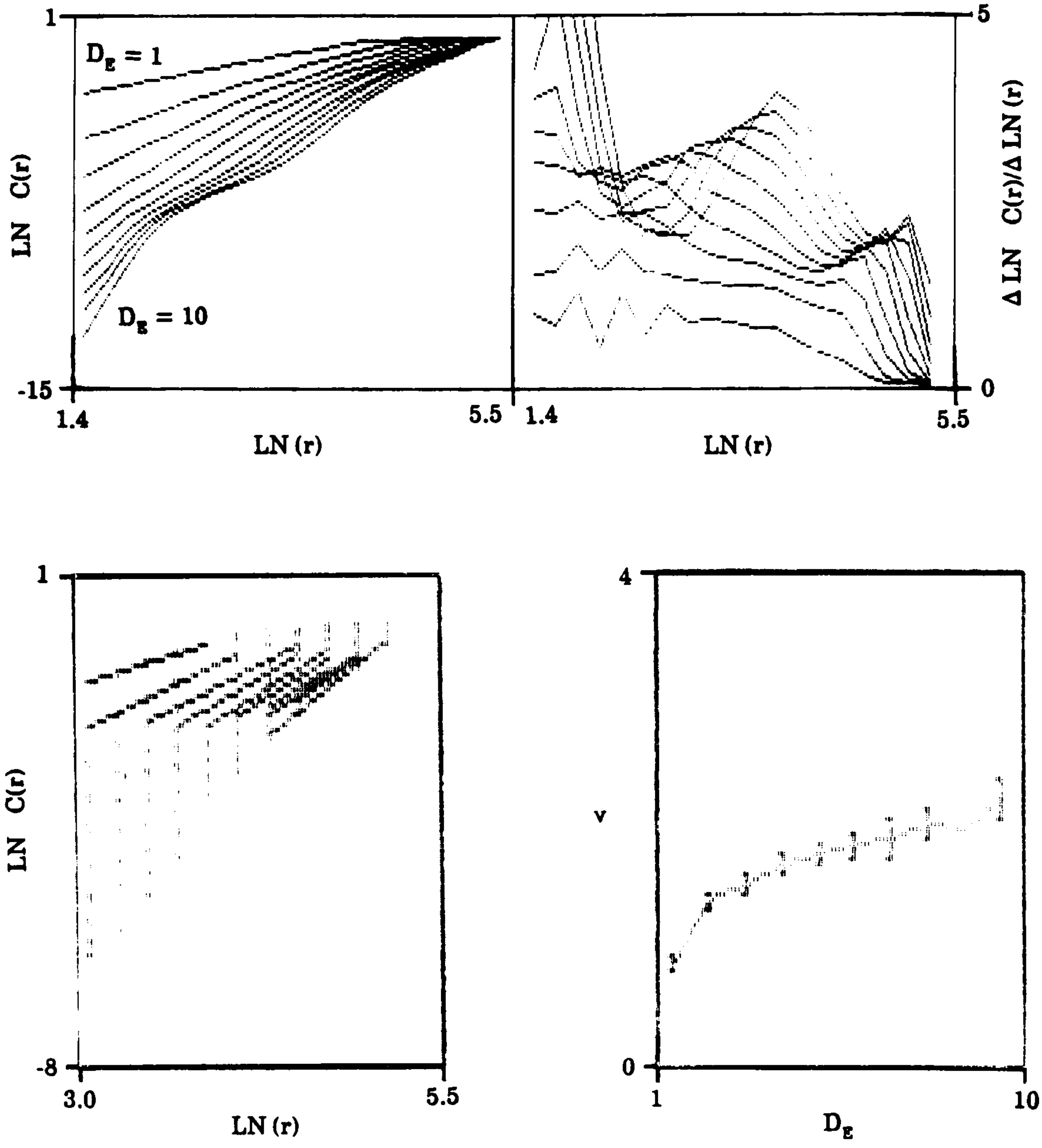

(A) $V_A = 580$

Figure X-9. Correlation plots for varying anode voltage

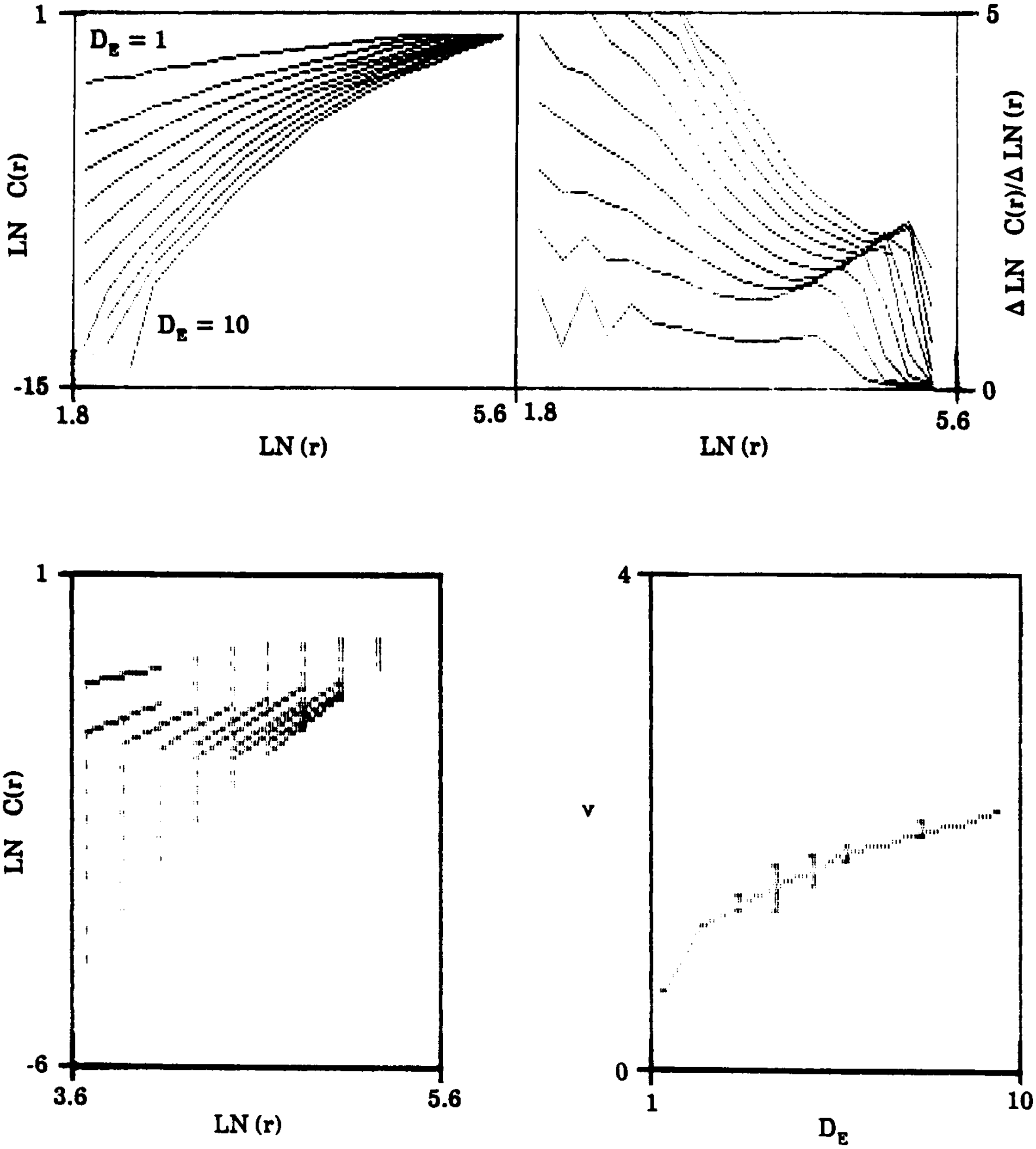

(B) $V_A = 810$ V

Figure X-9. (Continued)

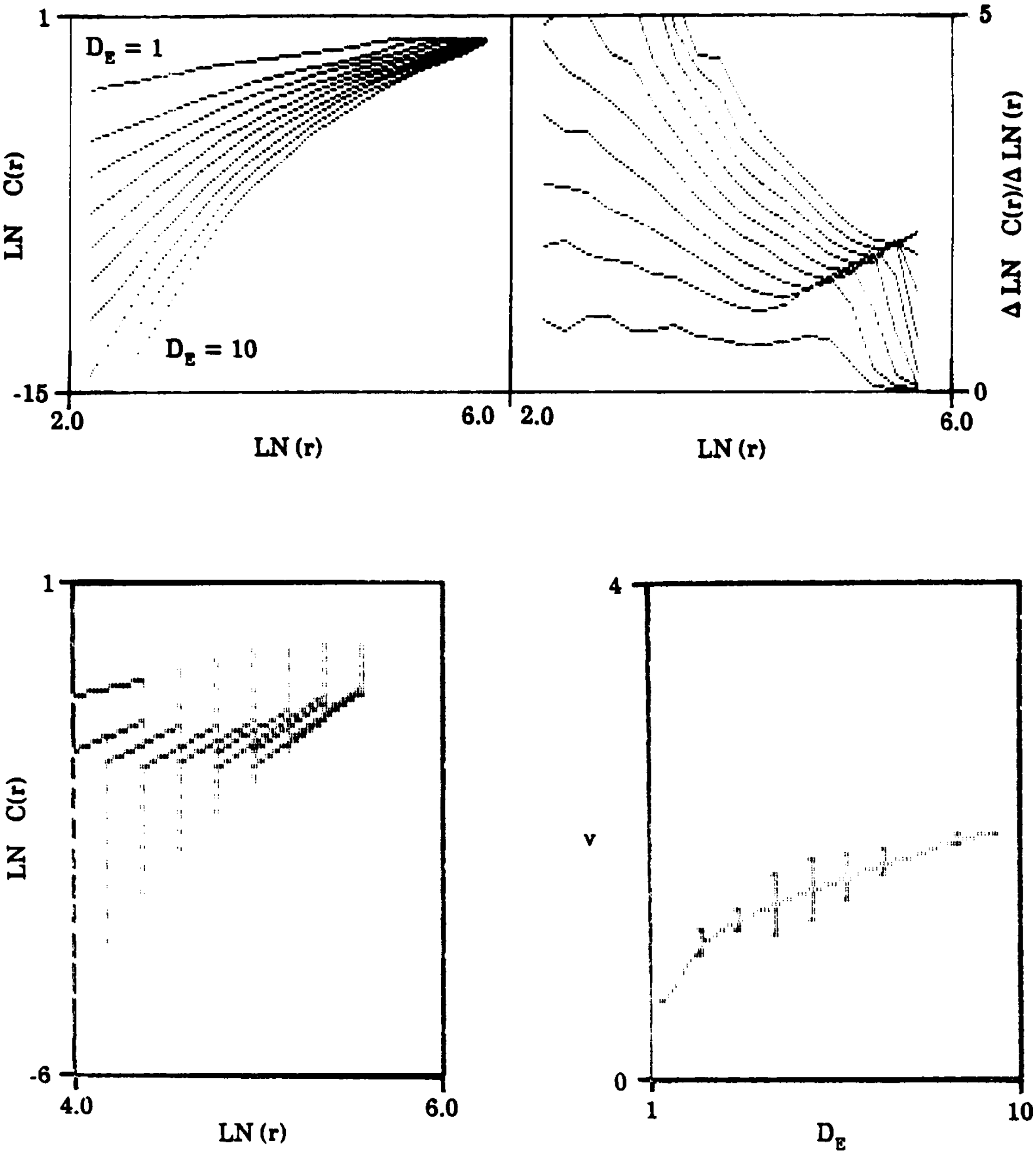

(C) $V_A = 920$ V

Figure X-9. (Continued)

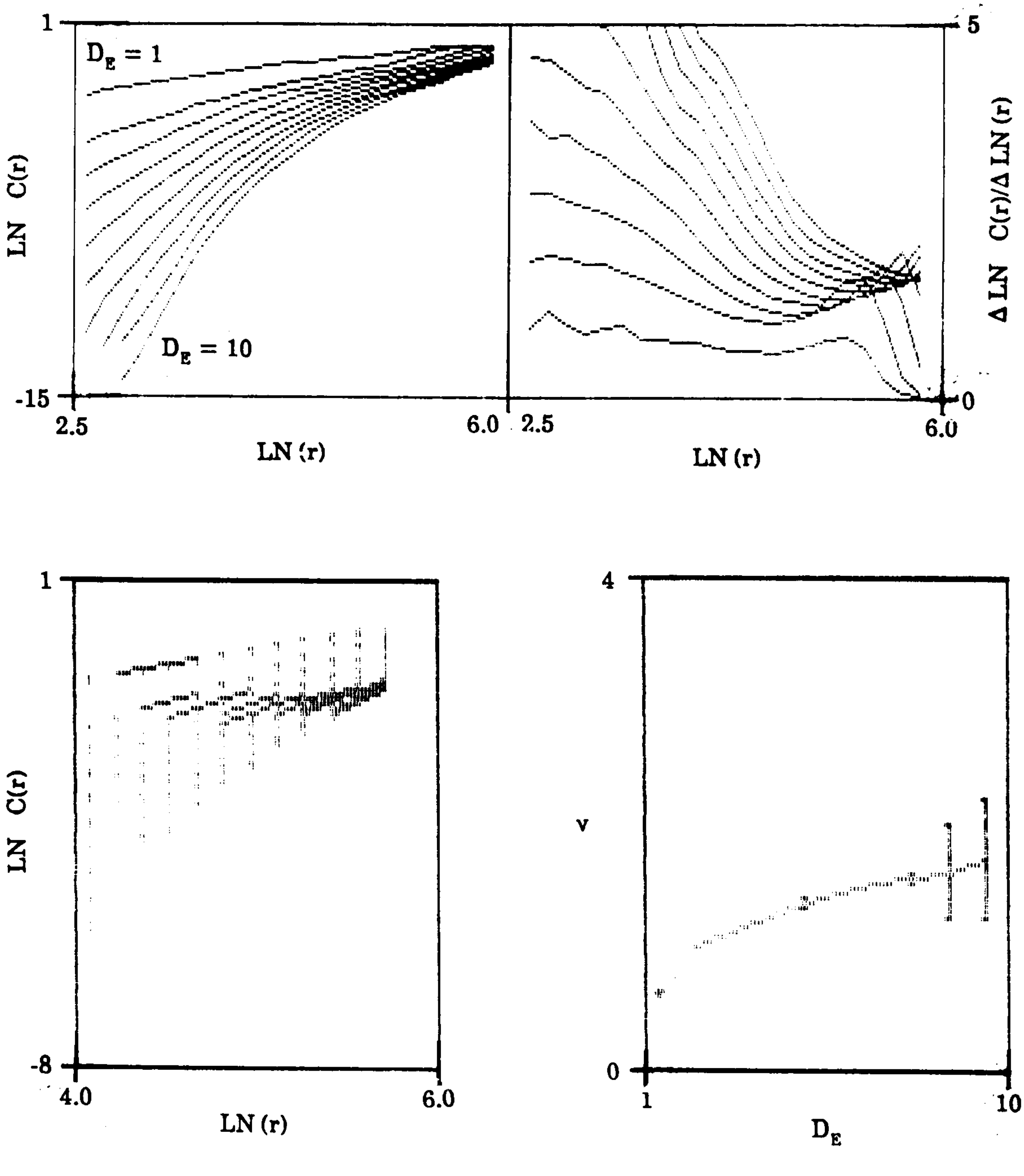

(D) $V_A = 1010$ V

Figure X-9. (Continued)

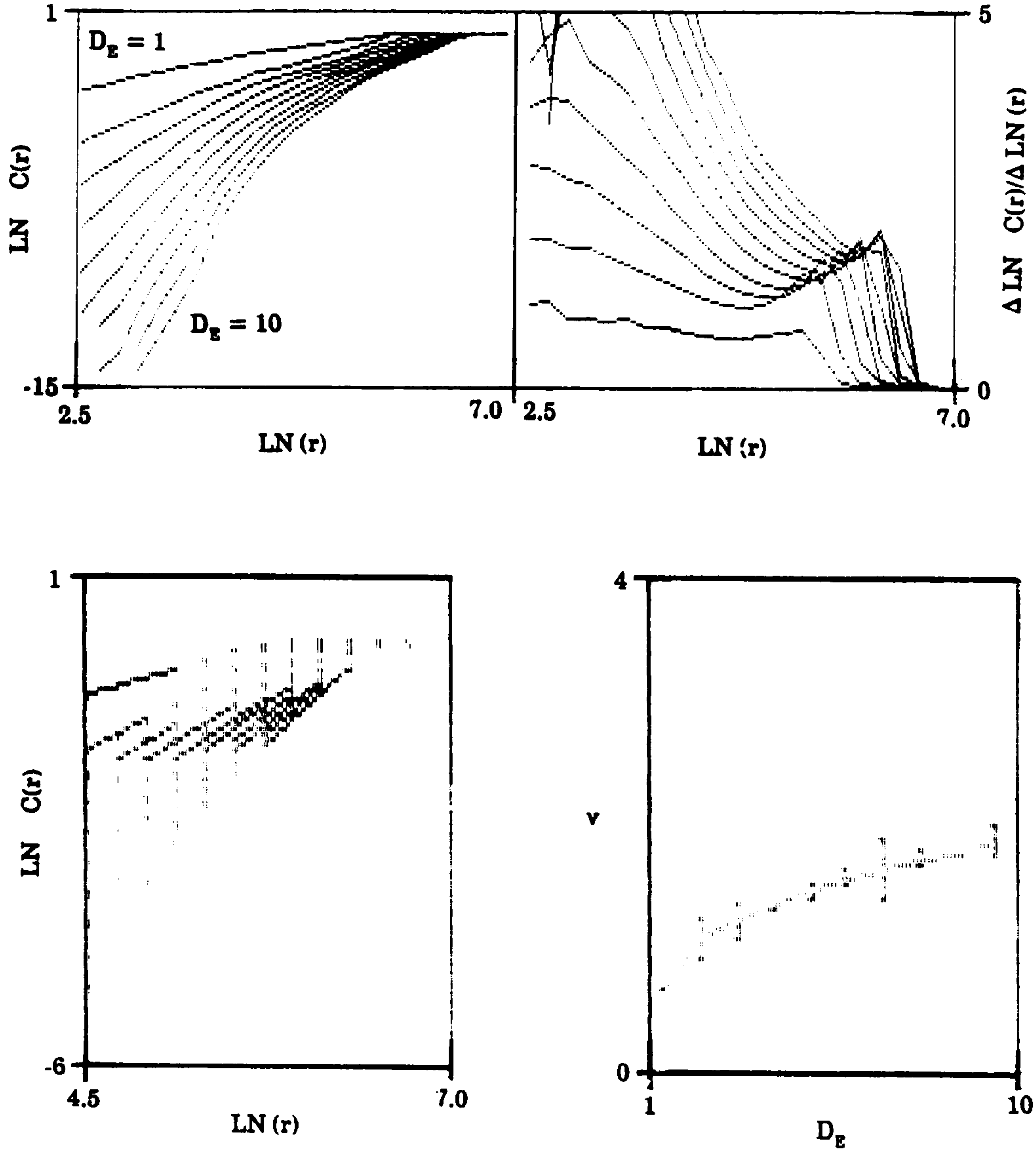

(E) $V_A = 1090$ V

Figure X-9. (Continued)

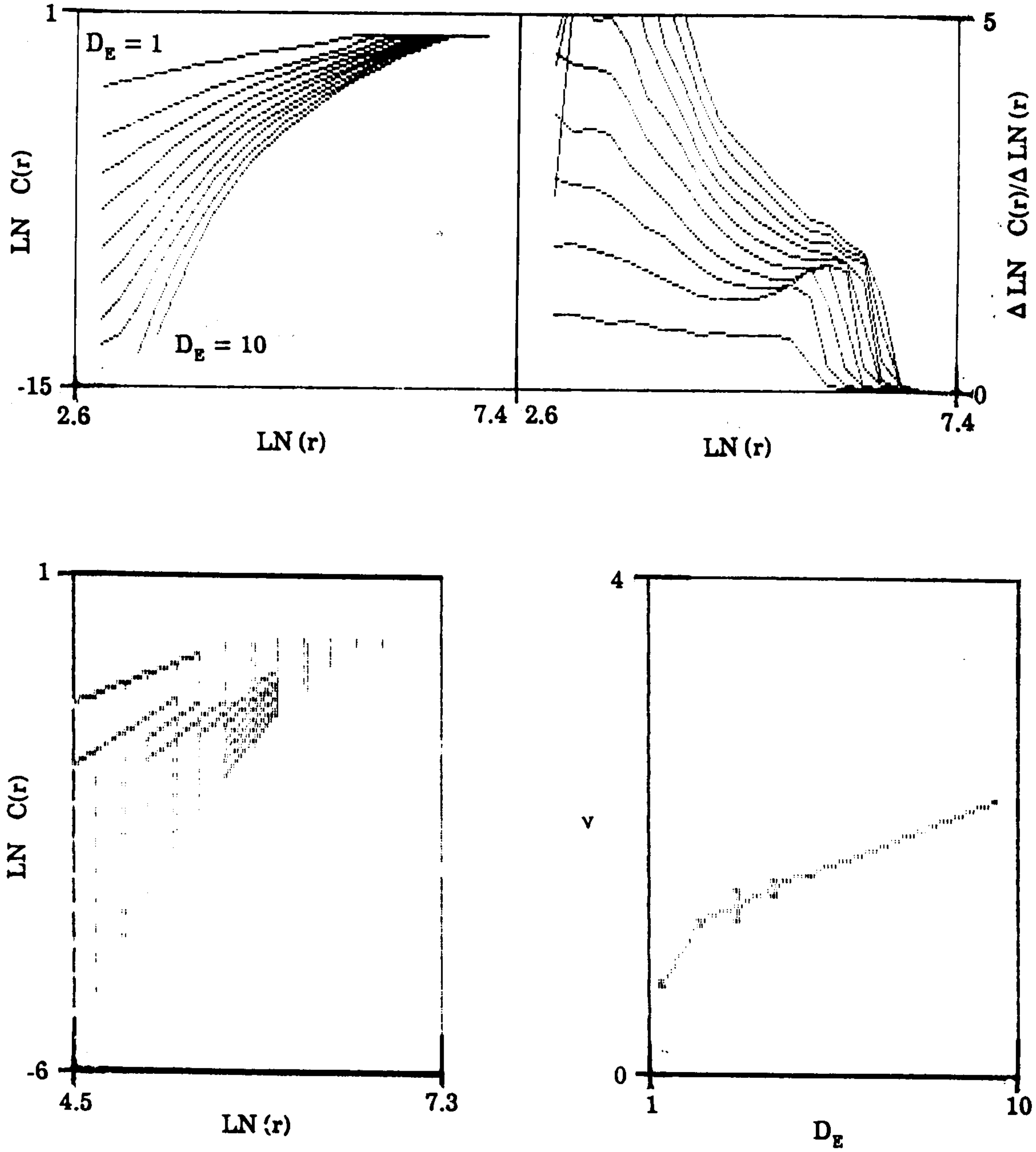

(F) $V_A = 1140$ V

Figure X-9. (Continued)

cases, there exists a very small scaling region in which the dimension may be determined. Table X-2 lists the values for each run. They are also plotted as a function of the anode voltage in Figure X-10.

C. Variation of Magnetic Field

The control parameter for the third set of data was the magnetic field strength. This was varied over a range of 0.034 T to 0.182 T. The plasma parameters measured with a Langmuir probe are plotted in Figure X-11. Figure X-12 shows the effect of the magnetic field strength on the fluctuations' power spectra. For B = 0.034 T, there is a small peak in the spectrum. This peak becomes much more prominent for the next two runs, but is then damped out when the magnetic field is increased to 0.084 T. As the field is increased further, the signal strength continues to decrease.

The reconstructed phase portraits are shown in Figure X-13. The first run exhibits a slight hint of periodicity. The trajectory becomes much more coherent over the next two runs, but this is lost as the magnetic field is increased further. By Run 6, the trajectory is filling up regions in phase space, which is characteristic of random signals. All of these observations are consistent with what was learned from the power spectra.

Figure X-14 contains the correlation plots for each run. For this set of data, one would expect that convergence would be observed in only one or two cases. As it turns out, convergence is seen only for Run 3. For this case, the correlation integral and derivative curves exhibit the two distinct regions, and once again the correlation dimension is found to be approximately 2.0. In all of the other runs of this set, the slope continues to increase with embedding dimension, implying that the fluctuations have become random.

Table X-2

Correlation Dimension for Varying Anode Voltages

Run Number	Anode Voltage (V)	Dimension
1	580	2.14
2	810	2.05
3	920	1.96
4	1010	1.68
5	1090	1.86
6	1140	2.20

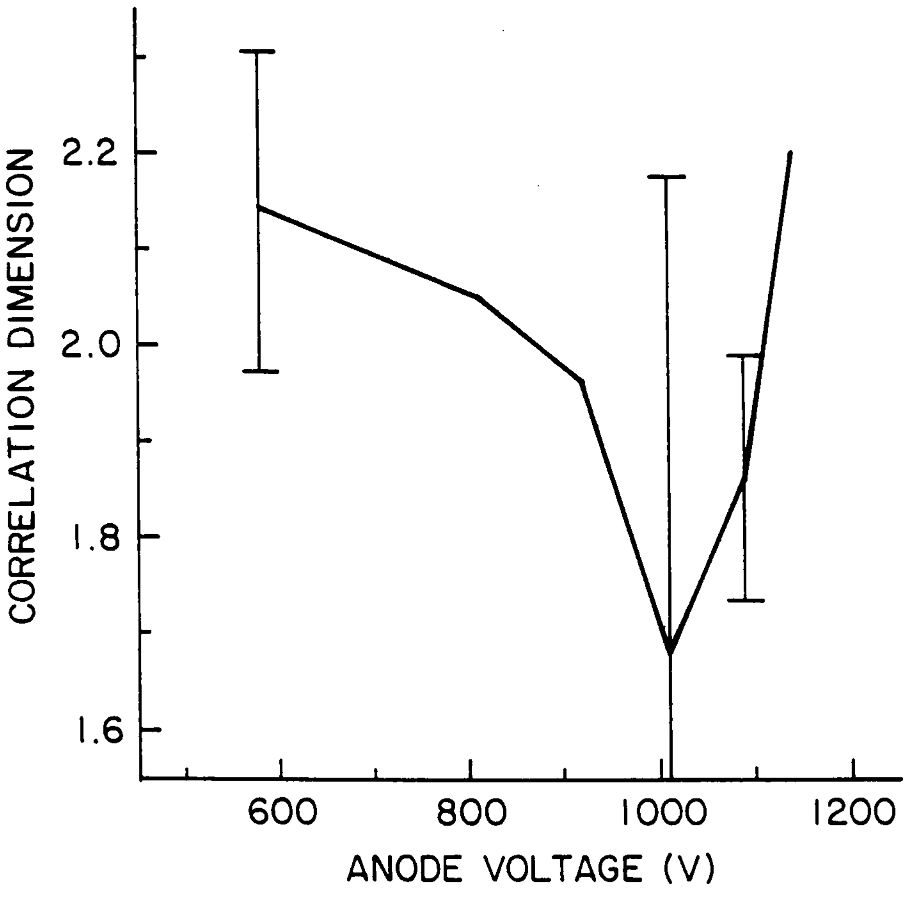

Figure X-10. Plot of correlation dimension as a function of anode voltage

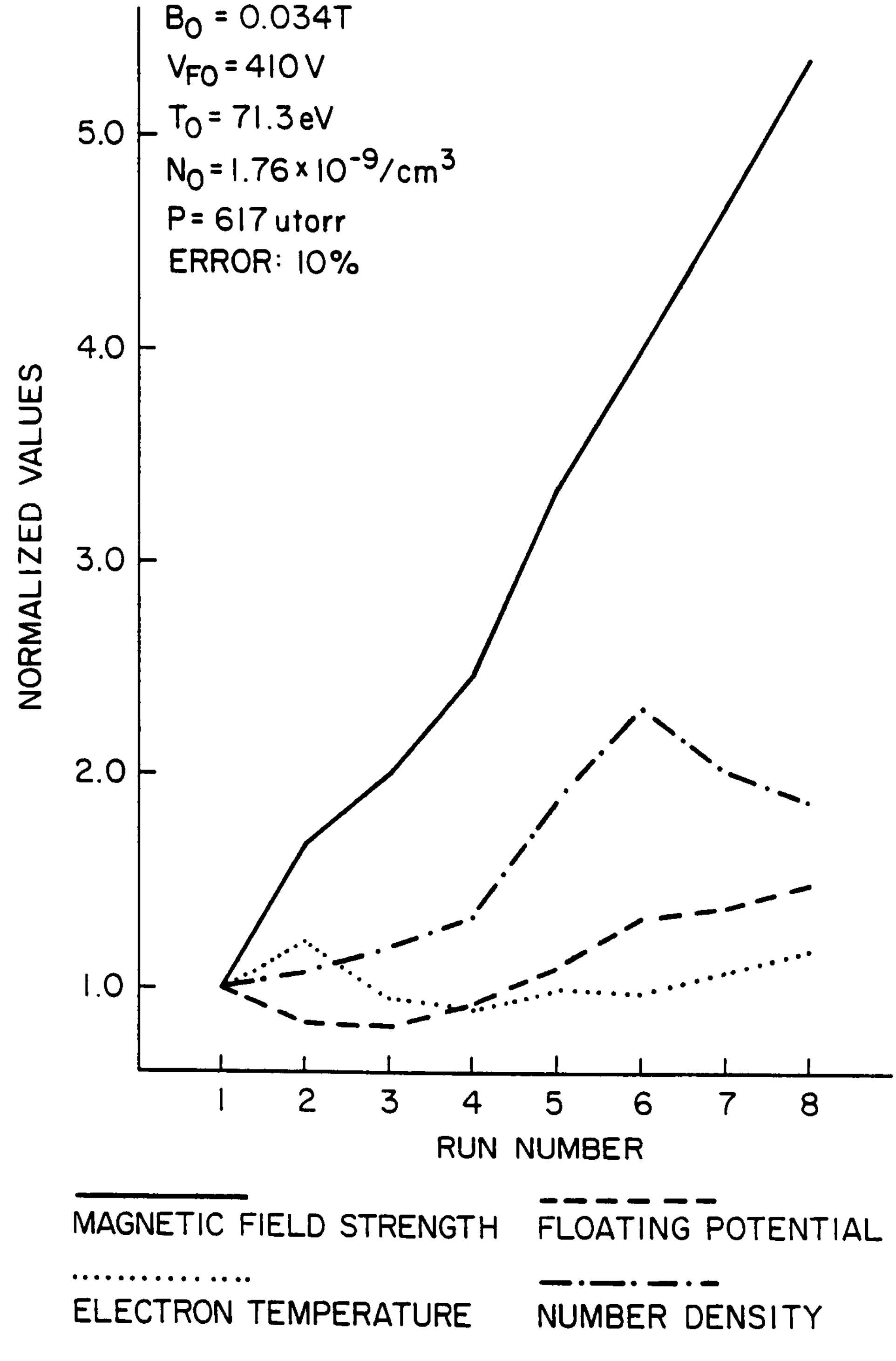

Figure X-11. Variation of plasma parameters for different magnetic field strength

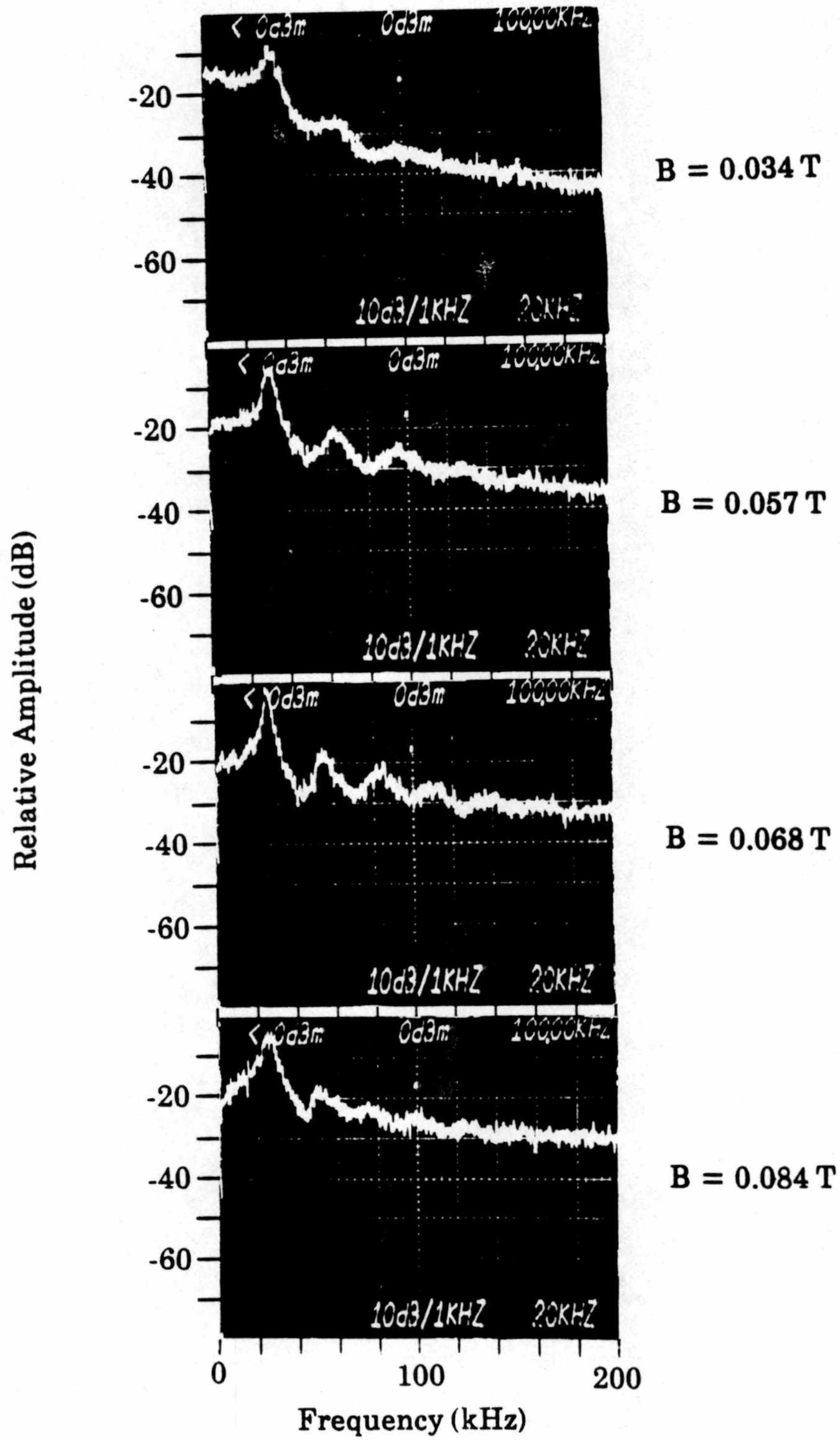

Figure X-12. Potential fluctuations for varying magnetic field strength

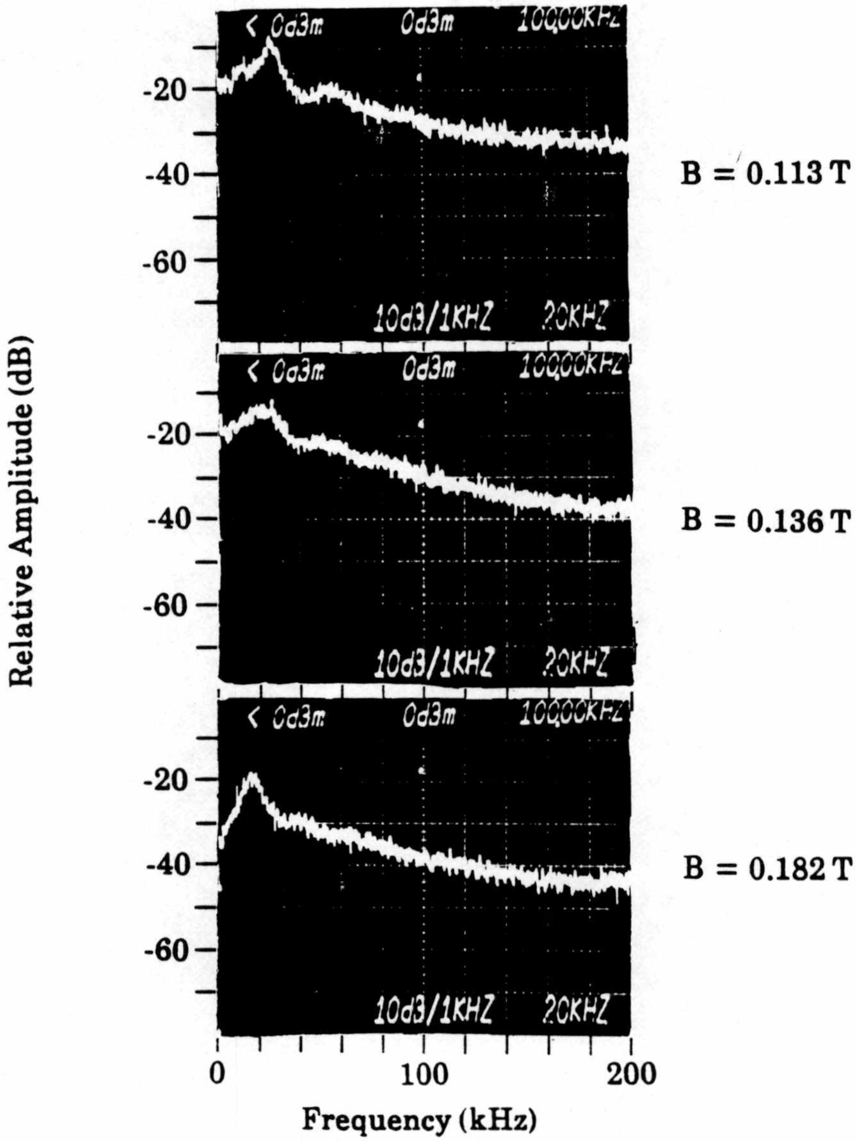

Figure X-12. (Continued)

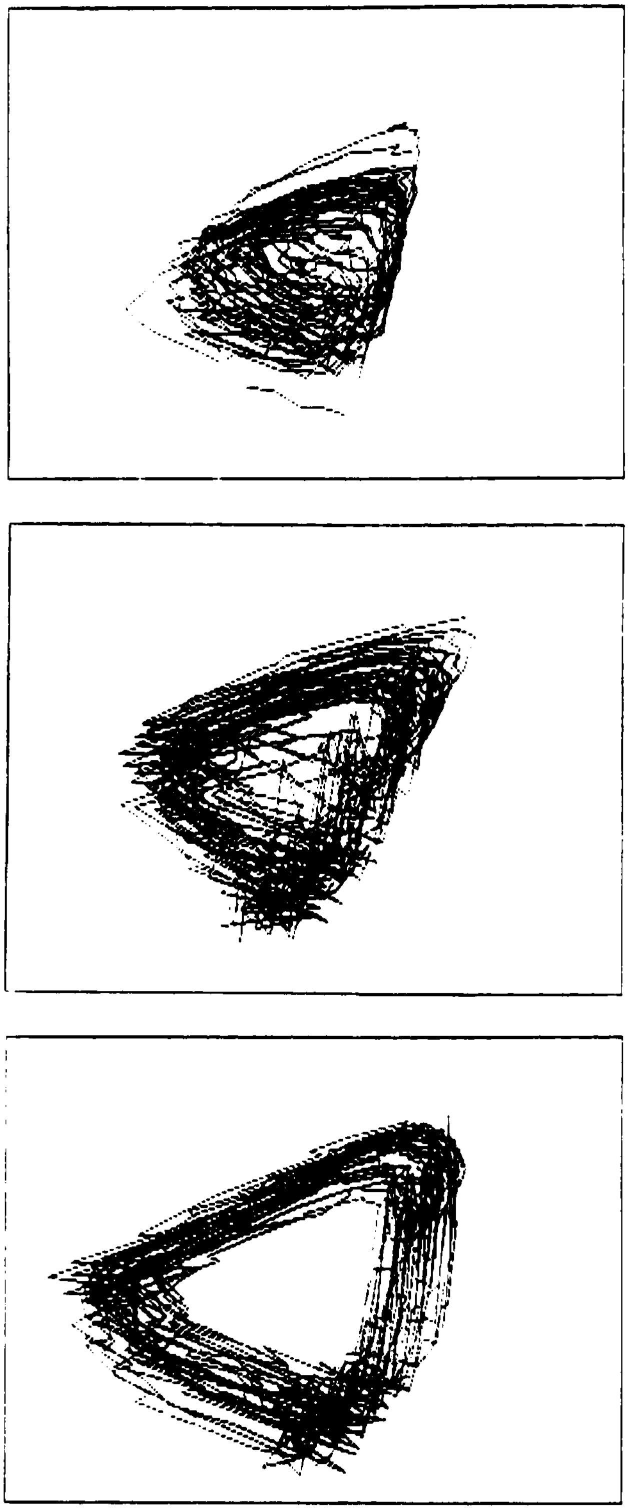

B = 0.034 T

B = 0.057 T

B = 0.068 T

Figure X-13. Reconstructed phase portraits for varying magnetic field strength

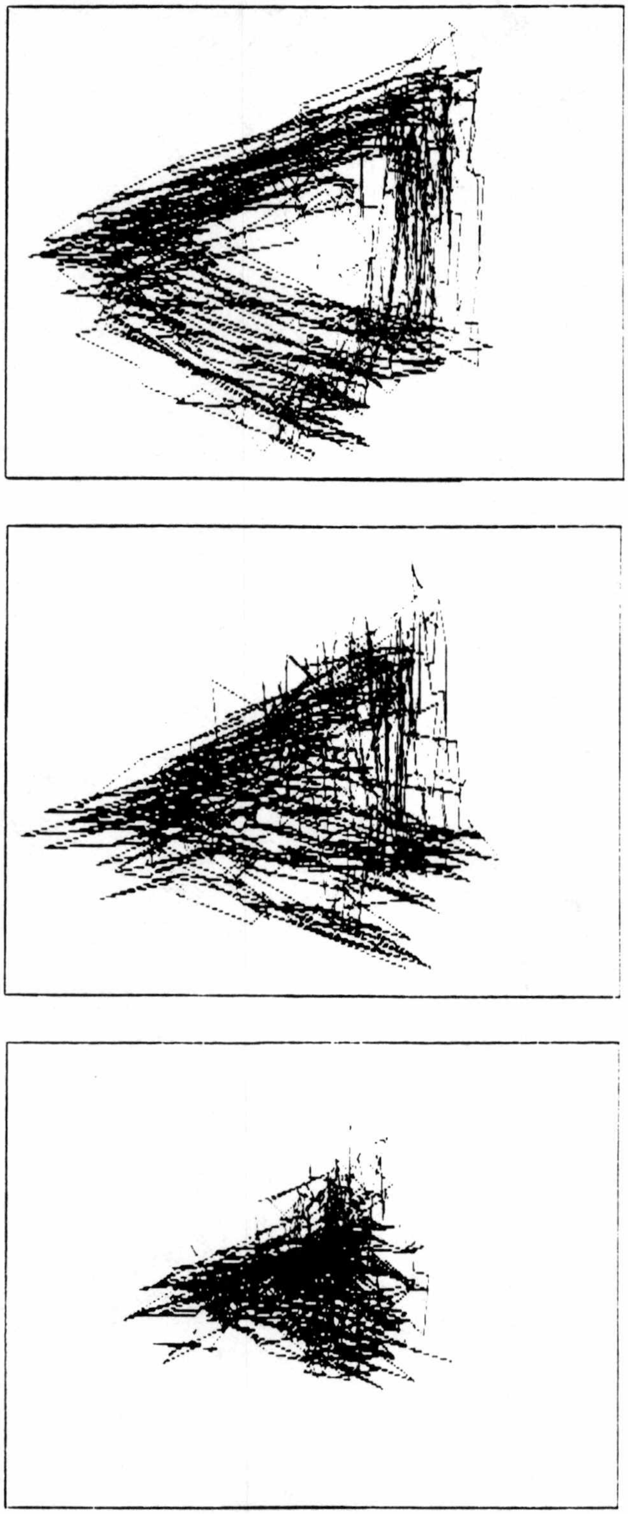

B = 0.084 T

B = 0.113 T

B = 0.136 T

Figure X-13. (Continued)

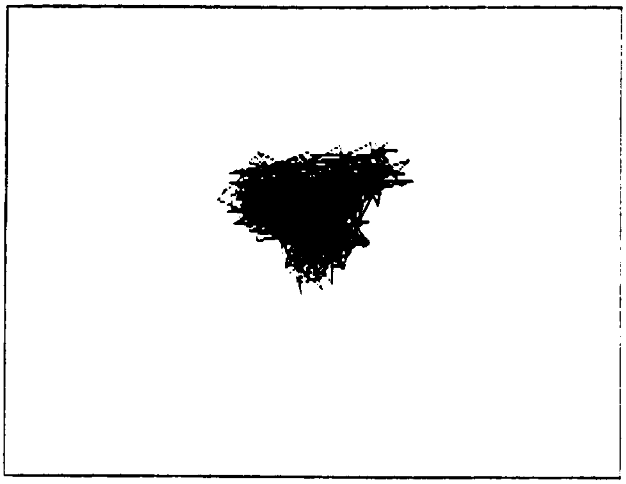

B = 0.182 T

Figure X-13. (Continued)

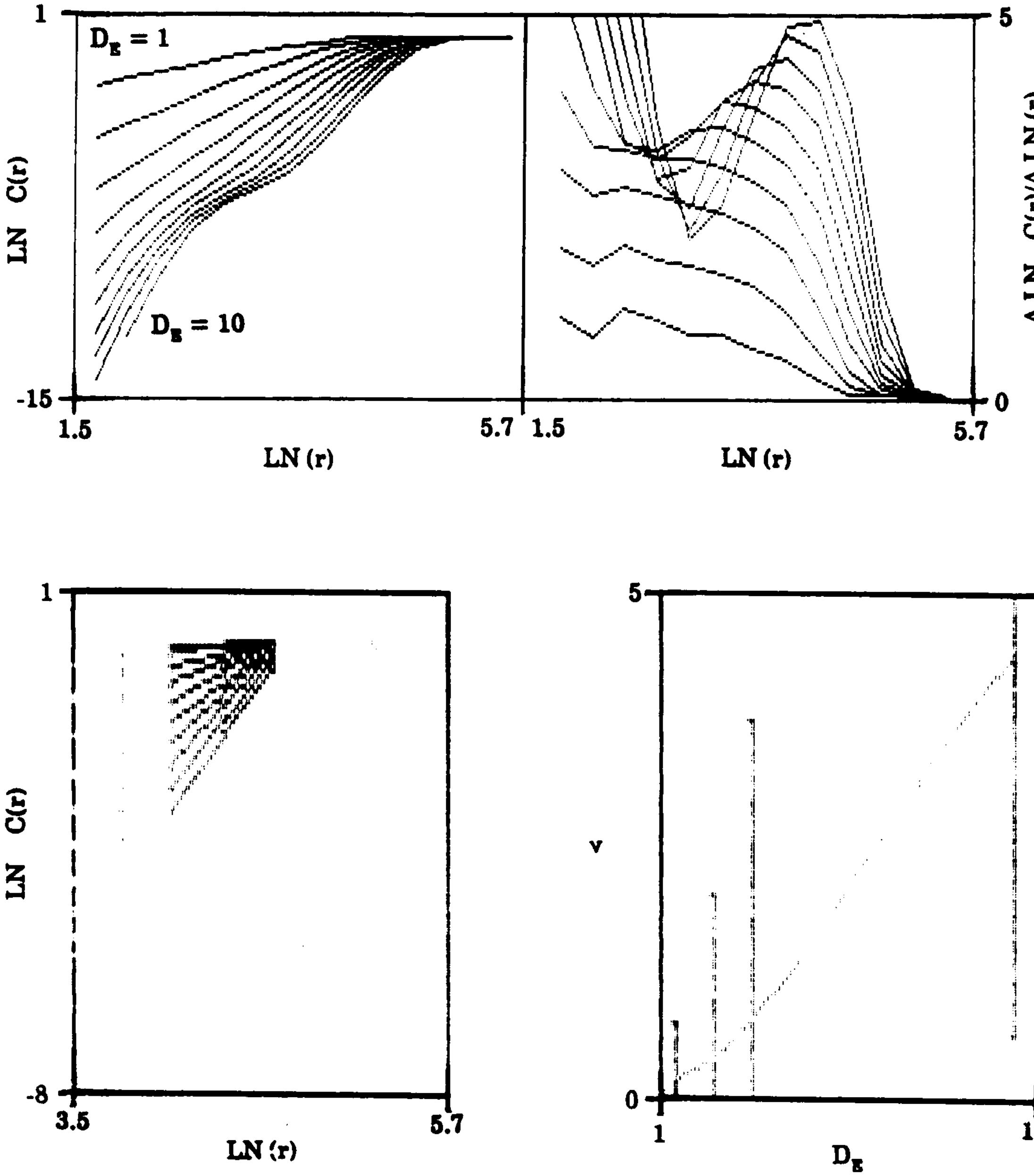

(A) B = 0.034 T

Figure X-14. Correlation plots for varying magnetic field strength

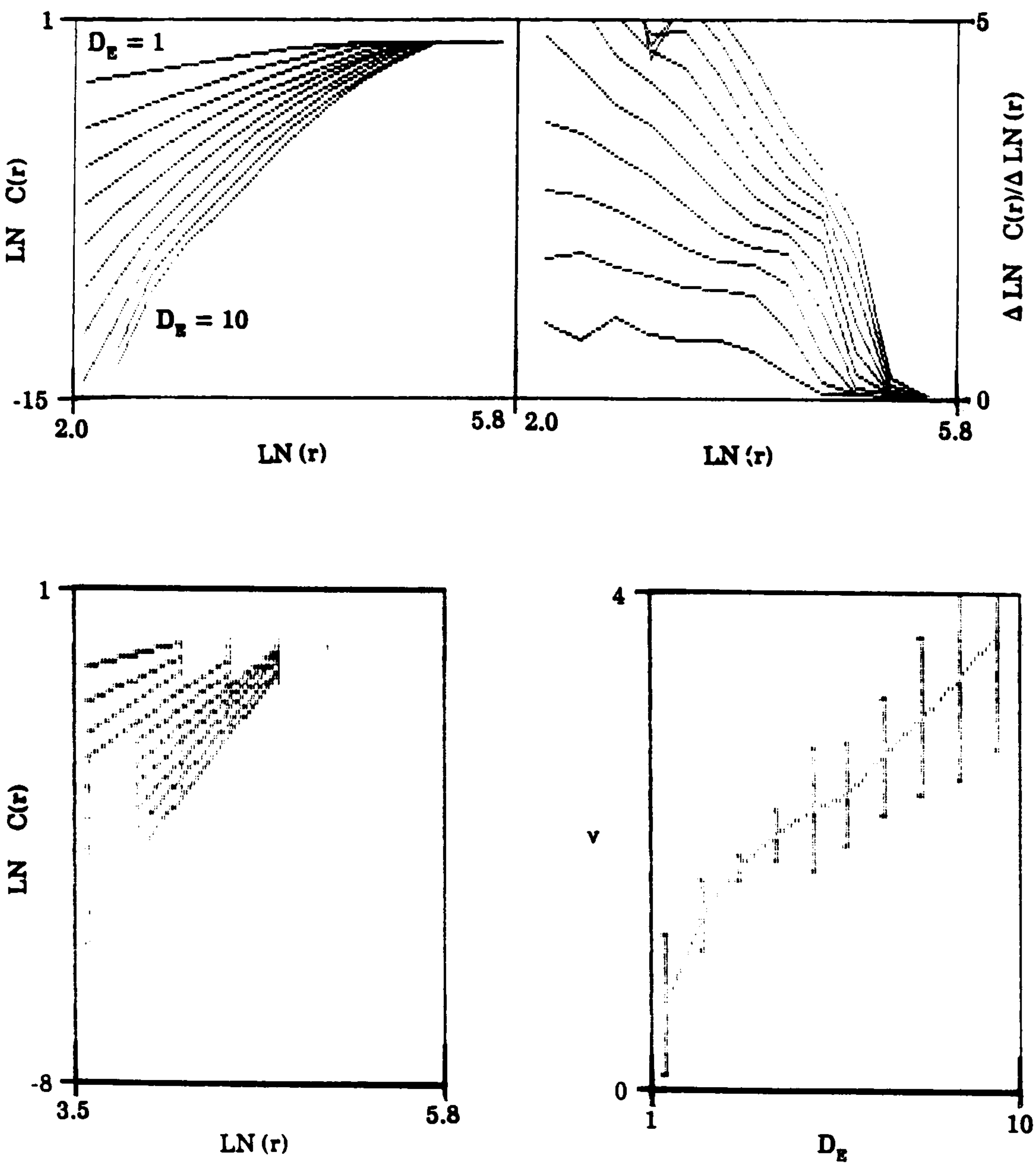

(B) B = 0.057 T

Figure X-14. (Continued)

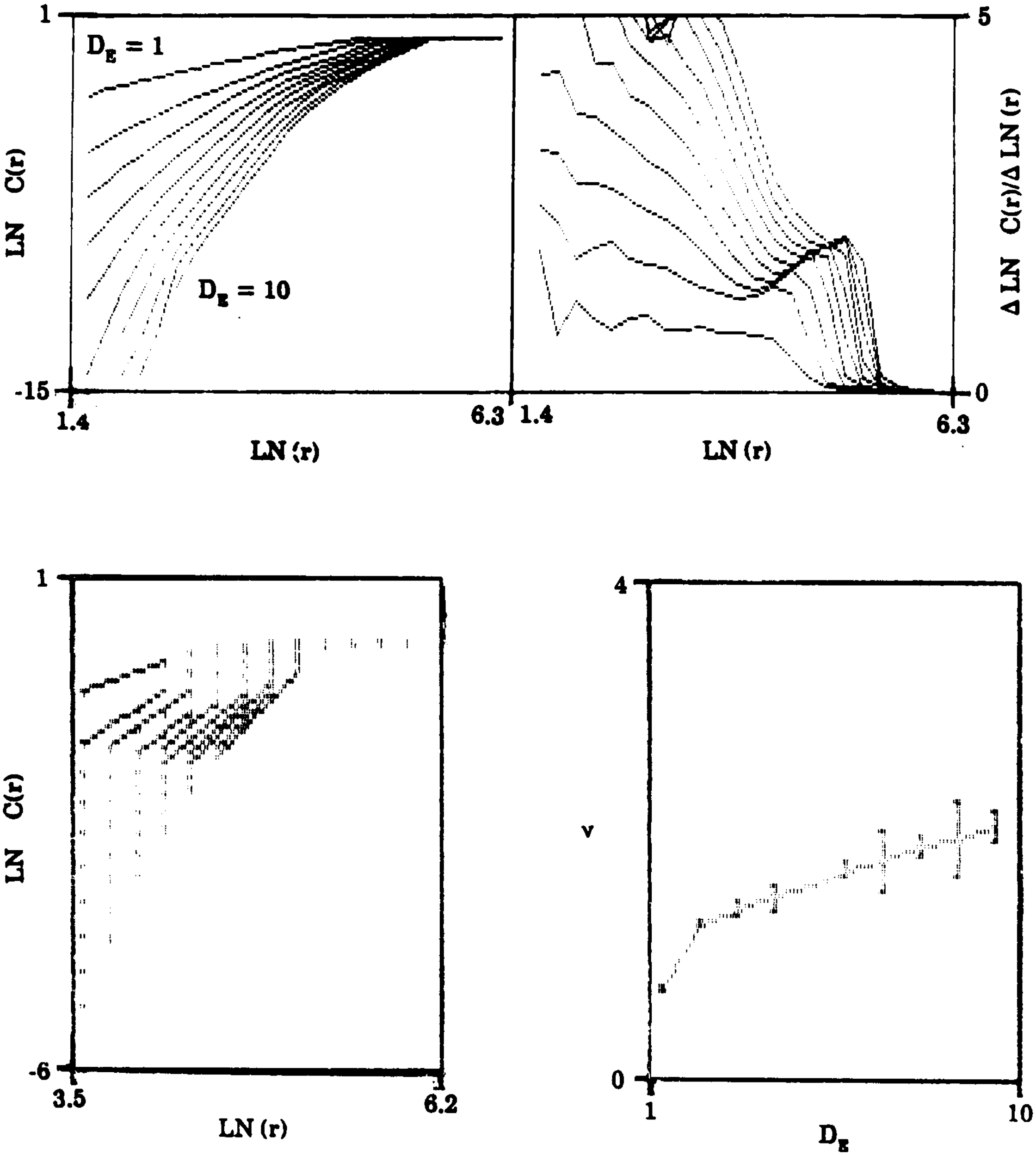

(C) B = 0.068 T

Figure X-14. (Continued)

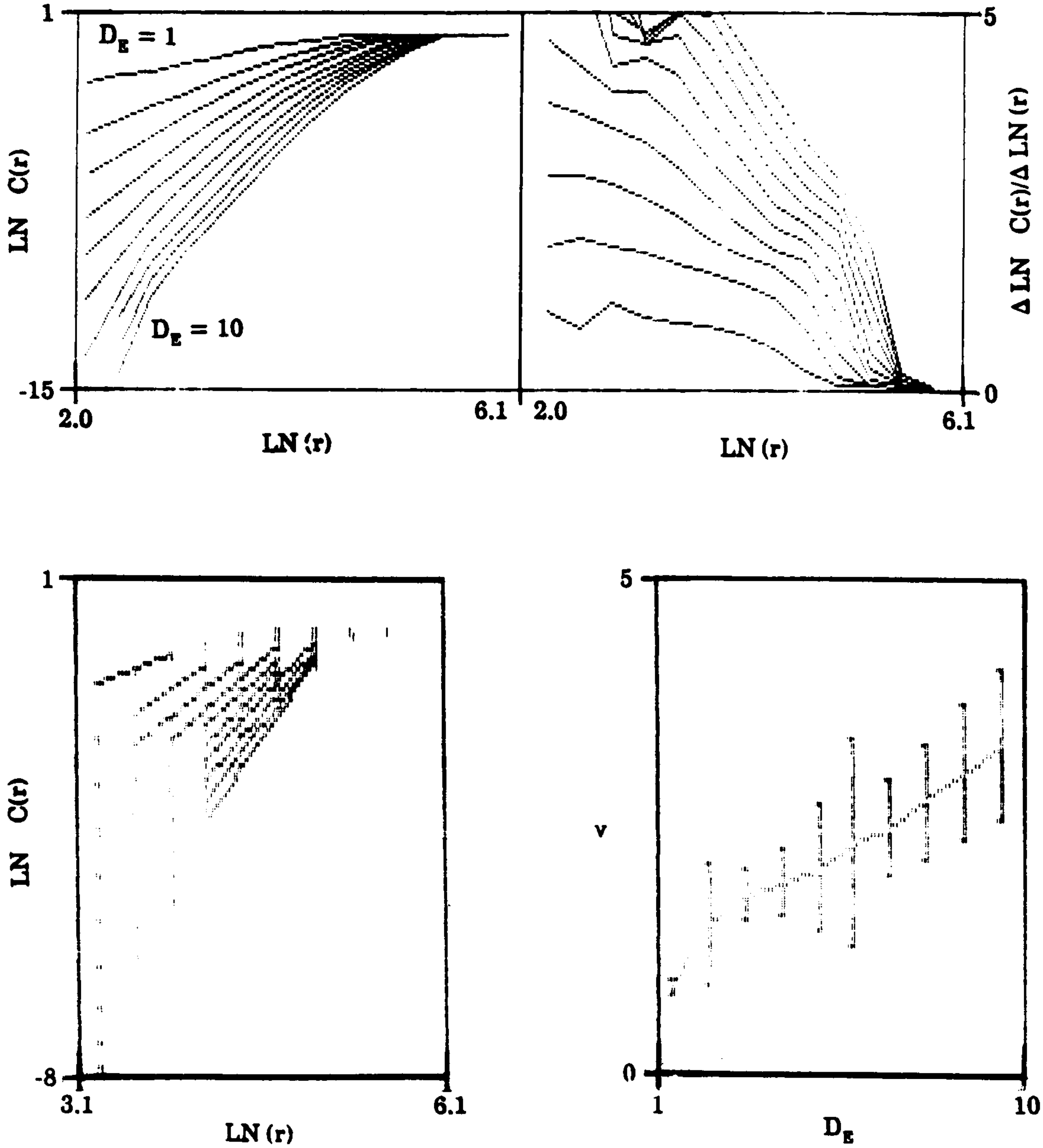

(D) B = 0.084 T

Figure X-14. (Continued)

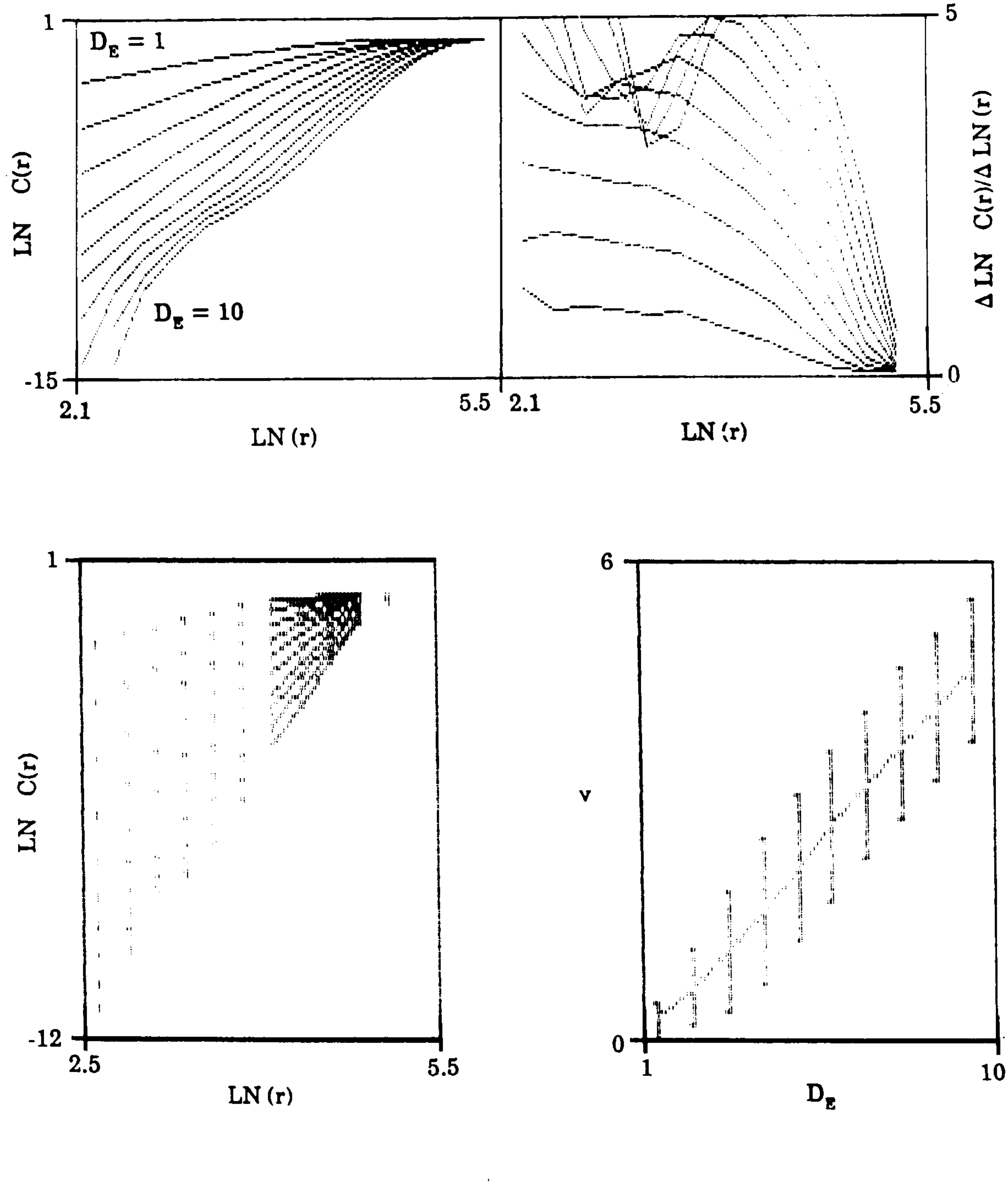

(E) B = 0.113 T

Figure X-14. (Continued)

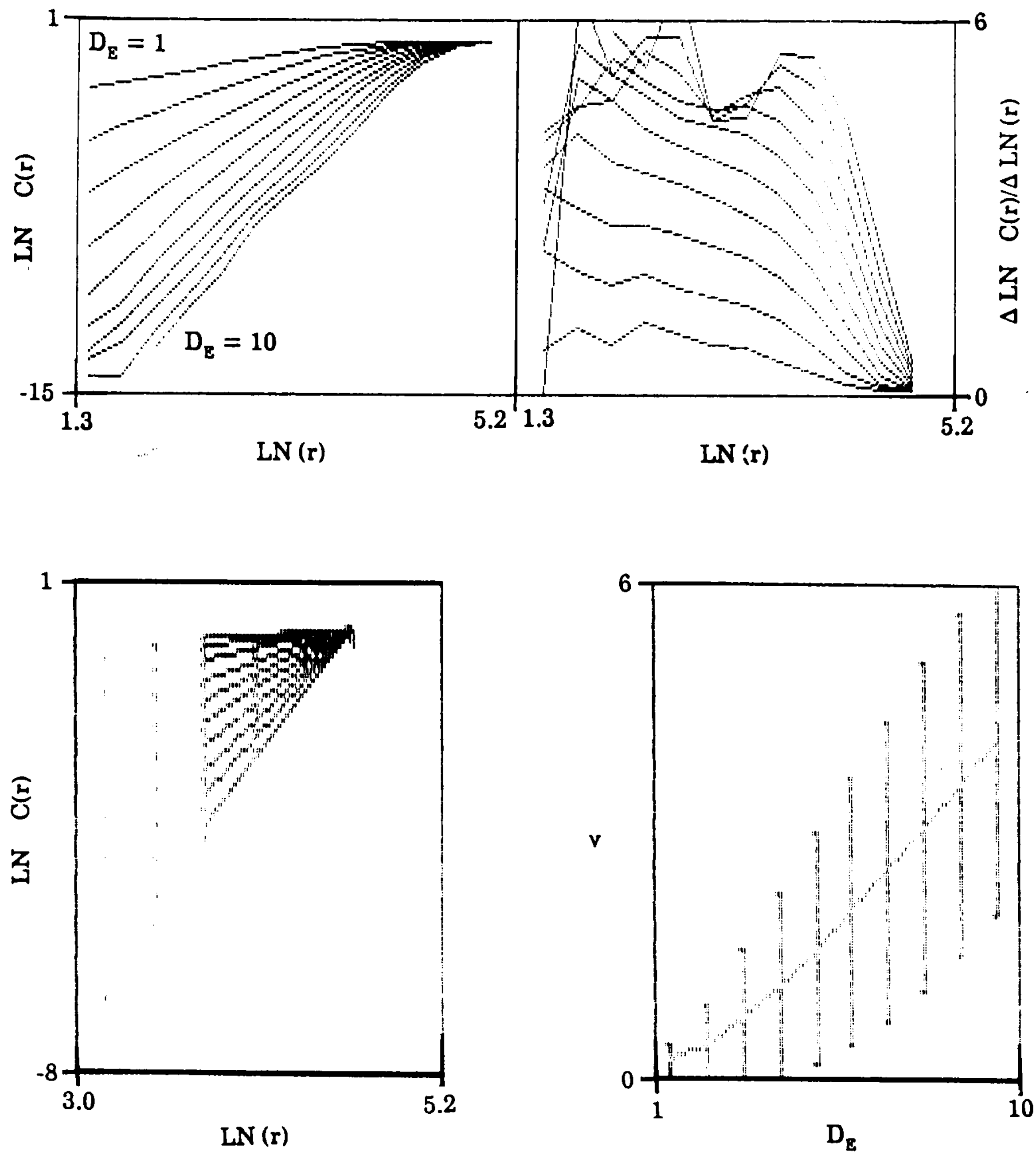

(F) B = 0.136 T

Figure X-14. (Continued)

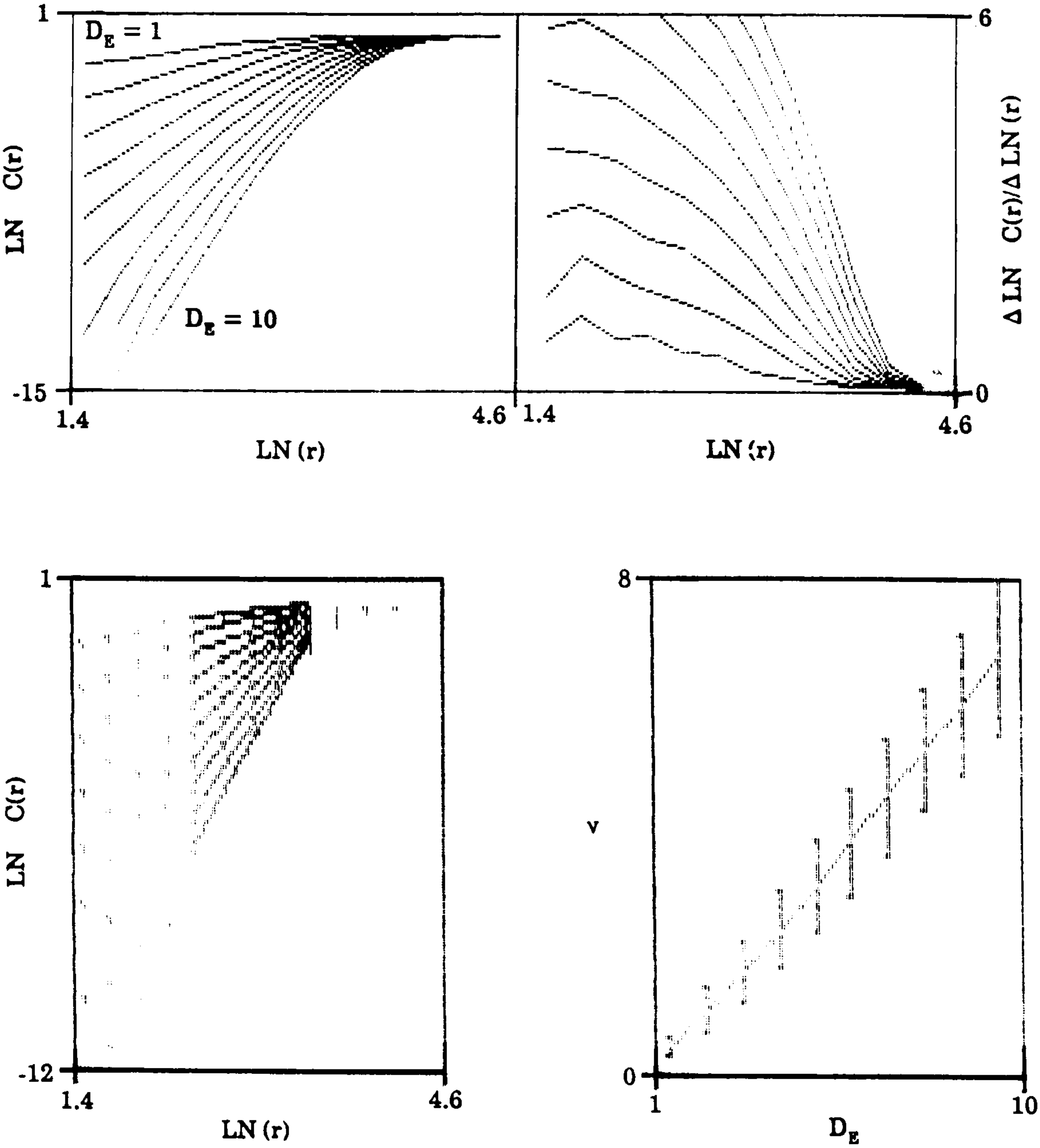

(G) B = 0.182 T

Figure X-14. (Continued)

CHAPTER XI

CONCLUSIONS

This research attempted to apply some of the tools of nonlinear dynamics to potential fluctuations in a plasma. Unfortunately, using some of these tools is more like an art than a science, and producing definite results is difficult to accomplish. While conducting this study quite a few problems were encountered. For example there was the problem of noisy data. The noise level was so high that accurately measuring the correlation dimension was very difficult. It was also observed that noise makes it practically impossible to measure the largest Lyapunov exponent from a time series. There was also the problem of the number of data points used to estimate the correlation dimension. For this study, the limiting factor is the computer time required for the computations (see Appendix A). The experimental apparatus easily allows the acquisition of 8192 data points, with the potential for more. However, this many points could tie up an IBM-AT for two weeks. This was the reason for using only 2000 data points. Though it is mathematically feasible to accurately measure correlation dimensions less than three with as little as 2000 points (Smith, 1988), there is still the problem of spurious correlations that is discussed in Appendix B.

Though numerous difficulties were encountered, some useful results were obtained from this research. As for finding evidence of chaotic behavior in the data presented, this does not appear too likely. It is possible to observe two different states of turbulence; one which appears to be regular and another which is random. However, the transition between these states was not identifiable. It was interesting to study the effects of varying the plasma parameters on the state of turbulence. For lower pressures, the fluctuations were relatively coherent, but for pressures above a millitorr they became random. The anode voltage did not have a strong effect on the fluctuations, though the attractor became slightly less noisy as the voltage was increased. The case where the magnetic field strength was varied showed that only a small range of field strengths would produce coherent oscillations for the conditions used. Interestingly enough, the value of the magnetic field for the one coherent case was 0.068 T, which was the level of the magnetic field for both of the other two data sets.

It was also interesting to see that whenever convergence for the correlation dimension was seen, the value was always approximately 2. This would imply that two oscillations are occurring, one due to the E x B drift and the other unknown. However, evidence of a second frequency was observed only in a couple of runs.

As for following up this research in the future, a few suggestions emerged from this study. In order to get more accurate results, one should use more data points; preferably 5000 or more. This of course requires the use of a much faster computer. The second recommendation would be to try inducing another oscillation into the system. This could be accomplished by periodically varying either the applied electric or magnetic fields. The electric field would be the most likely candidate, since it can be varied rather easily. This has been done previously (Spence and Roth, 1987) by applying a high voltage RF signal to an effector probe. It would be very interesting to see how this oscillation would interact with the others already present.

BIBLIOGRAPHY

BIBLIOGRAPHY

Adam, J. C., M. N. Bussac, and G. Laval (1979), "Stabilization of a Linearly Unstable Mode by Resonant Nonlinear Coupling to Damped Modes", in Intrinsic Stochasticity in Plasmas, G. Laval and D. Gresillon (eds.), Les Editions de Physique, Courtaboeuf, France, pp. 415-423.

Arter, W. and D. N. Edwards (1986), "Non-Linear Studies of Mirnov Oscillations in the DITE Tokamak: Evidence for a Strange Attractor", Physics Letters, Vol. 114A, No. 2, pp. 84-89.

Barkley, H. J., J. Andreoletti, F. Gervais, J. Olivain, A. Quemenevur, and A. Truc (1988), "Estimate of the Correlation Dimension for Tokamak Plasma Turbulence", Plasma Physics and Controlled Fusion, Vol. 30, No. 3, pp. 217-234.

Baylor, L. R., J. R. Roth, P. Dehkordi, and M. Laroussi (1984), "Anomalous Drift Waves Detected with Microwave Scattering in an Electric Field Dominated Plasma", APS Bulletin, Vol. 29, No. 8, p. 1197.

Boswell, R. W. (1985), "Experimental Measurements of Bifurcations, Chaos and Three Cycle Behavior on a Neutralized Electron Beam", Plasma Physics and Controlled Fusion, Vol. 27, No. 4, pp. 405-418.

Brandstater, A., J. Swift, H. L. Swinney, A. Wolf, J. D. Farmer, E. Jen, and P. J. Crutchfield (1983), "Low-Dimensional Chaos in a Hydrodynamic System", Physical Review Letters, Vol. 51, No. 16, pp. 1442-1445.

Braun, T. J. A. Lisboa, R. E. Francke, and J. A. C. Gallas (1987), "Observation of Deterministic Chaos in Electrical Discharges in Gases", Physical Review Letters, Vol. 59, No. 6, pp. 613-616.

Cheung, P. Y., S. Donovan, and A. Y. Wong (1988), "Observations of Intermittent Chaos in Plasmas", Physical Review Letters, Vol. 61, No. 12, pp. 1360-1363.

Cheung, P. Y. and A. Y. Wong (1987), "Chaotic Behavior and Period Doubling in Plasmas", Physical Review Letters, Vol. 59, No. 5, pp. 551-554.

Chua, L. and R. N. Madan (1988), "Sights and Sounds of Chaos", IEEE Circuits and Devices Magazine, January, 1988, pp. 3-13.

Cote, A., P. Haynes, A. Howling, A. W. Morris, and D. C. Robinson (1985) "Dimensionality of Fluctuations in TOSCA and JET", in 12th European Conference on Controlled Fusion and Plasma Physics, L. Pocs and A. Montvai (eds.), European Physical Society, Vol. 2, pp. 450-453.

Eckmann, J. P. (1981), "Roads to Turbulence in Dissipative Dynamical Systems", Review of Modern Physics, Vol. 53, No. 4, pp. 643-654.

Farmer, J. D., E. Ott, and J. A. Yorke (1983), "The Dimension of Chaotic Attractors", Physica, Vol. 7D, pp. 153-180.

Feigenbaum, M. J. (1978), "Qualitative Universality for a Class of Nonlinear Transformations", Journal of Statistical Physics, Vol. 19, No. 1, pp. 25-52.

Glass, L., X. Guevau, and A. Shrier (1983), "Bifurcation and Chaos in a Periodically Stimulated Cardiac Oscillator", Physica, Vol. 7D, pp. 89-101.

Gleick, J. (1987), Chaos, Viking, New York, pp. 20-23.

Grassberger, P. and I. Procaccia (1983), "Characterization of Strange Attractors", Physical Review Letters, Vol. 50, No. 5, pp. 346-349.

Held, G. A. and C. D. Jeffries (1986), "Characterization of Chaotic Instabilities in an Electron-Hole Plasma in Germanium", in Dimensions and Entropies in Chaotic Systems, G. Mayer-Kress (ed.), Springer-Verlag, New York, pp. 158-170.

I. L. and M.-S. Wu (1987), "Spatio-Temporal Chaos in Weakly Ionized Magneto-Plasmas", Physics Letters A, Vol. 124, No. 4 and 5, pp. 271-274.

Ikeda, K., H. Daido, and O. Akimoto (1980), "Optical Turbulence: Chaotic Behavior of Transmitted Light from a Ring Cavity", Physical Review Letters, Vol. 45, pp. 709-712.

Jingquing, F. and Z. Liulai (1988), "Plasma Instability of an Ion Source. (II) The Three Routes to Chaos in the Plasma Sheath", Chinese Physics, Vol. 8, No. 2, pp. 461-467.

Kadomtsev, B. B. and O. P. Pogutse (1970), in Reviews of Plasma Physics, M. Leontovich (ed.), Plenum, New York, Vol. 5, p. 349.

Kaplan, J. and J. A. Yorke (1978), "Chaotic Behavior of Multidimensional Difference Equations", in Functional Difference Equations and Approximation of Fixed Points, H. O. Peitgen and H. O. Walther (eds.), Springer-Verlag, New York, pp. 228-237.

Koyre, A. and I. B. Cohen (1972), Philosopiae Naturals Principia Mathematic, A. Koyre and (eds.), Harvard University Press, Cambridge.

Landau, L. D. (1944), "On the Problem of Turbulence", C. R. Dokl. Acad. Sci. USSR, Vol. 44, p. 311, Russian original reprinted in Chaos, B.-L. Hao (ed.), World Scientific Publishers, Singapore.

Laroussi, M., P. D. Spence, D. Rosenberg, R. Ghayspoor, and J. R. Roth (1985), "RF Emission Power Measurement and Anomalous Drift Wave Study in a Classical Penning Discharge"', APS Bulletin, Vol. 30, No. 9, p. 1397.

Lashinsky, H. (1979), "Transition to Turbulence in a Plasma with Discrete Unstable Modes", in Intrinsic Stochasticity in Plasmas, G. Laval and D. Gresillon (eds.), Les Editions de Physique, Courtaboeuf, France, pp. 425-437.

Libchaber, A. (1983), "Experimental Aspects of the Period Doubling Scenario", in Dynamical Systems and Chaos, L. Garrido (ed.), Springer-Verlag, New York, pp. 157-164.

Lorenz, E. N. (1963), "Deterministic Nonperiodic Flow", Journal of Atmospheric Sciences, Vol. 20, pp. 130-141.

Malraison, B., P. Atten, P. Berge and M. Dubois (1983), "Dimension of Strange Attractors: an Experimental Determination for the Chaotic Regime of Two Convective Systems", Journal of Physics Letters, Vol. 44, pp. 897-902.

Mandelbrot, B. (1983), The Fractal Geometry of Nature, W. H. Freeman, San Francisco.

Manneville, P. and Y. Pomeau (1980), "Different Ways to Turbulence in Dissipative Dynamical Systems", Physica, Vol. 1D, pp. 219-226.

Martin S., H. Leber, and W. Martienssen (1984), "Oscillatory, and Chaotic States of the Electrical Conduction in Barium Sodium Niobate Crystals", Physical Review Letters, Vol. 53, No. 4, pp. 303-306.

Mizrachi, A. B.-, I. Procaccia, and P. Grassberger (1984), "Characterization of Experimental (Noisy) Strange Attractors", Physical Review, Vol. 29A, pp., 975-977.

Moon, F. C. (1987), Chaotic Vibrations, John Wiley & Sons, New York.

Moon, F. C. and P. J. Holmes (1979), "A Magnetoelastic Strange Attractor", Journal of Sound Vibration, Vol. 65, pp. 275-296.

Packard, N. H., J. P. Crutchfield, J. D. Farmer, and R. S. Shaw (1980), "Geometry from a Time Series", Physical Review Letters, Vol. 45, pp. 712-716.

Penning, F. M. and K. Nienhuis (1949), "Construction and Applications of a New Design of the Phillips Vacuum Gauge", Phillips Technical Review, Vol. 11, No. 4, pp. 116-122.

Pettini, M., A. Vulpiani, J. H. Misguich, M. D. Leener, J. Orban, and R. Balescu (1988) "Chaotic Diffusion Across a Magnetic Field in a Model of Electrostatic Turbulent Plasma", Physical Review A, Vol. 38, No. 1, pp. 344-363.

Pomeau, Y. and P. Manneville (1980), "Intermittent Transition to Turbulence in Dissipative Dynamical Systems," Communications in Mathematical Physics, Vol. 74, pp. 189-197.

Roth, J. R. (1966), "Modification of Penning Discharge Useful in Plasma Physics Experiments", Review of Scientific Instruments, Vol. 37, No. 8, pp. 110-1101.

Ruelle, D. and F. Takens (1971), "On the Nature of Turbulence", Communications in Mathematical Physics, Vol. 20, pp. 167-192.

Sawley, M. L., W. Simm, and A. Pochelon (1987), "The Correlation Dimension of Broadband Fluctuations in a Tokamak", Physics of Fluids, Vol. 30, No. 1, pp. 129-132.

Schaffer, W. M. and M. Kot (1985), "Nearly One Dimensional Dynamics in an Epidemic", Journal of Theoretical Biology, Vol. 112, p. 403.

Schaffer, W. M., G. L. Truty, and S. L. Fulmer (1988), Dynamical Software Users Manual, Dynamical Systems, Inc., Version I.4, p. 5.16.

Schuster, H. G. (1984), Deterministic Chaos, Physik-Verlag, Weinheim (F.R.G.).

Simm, C. W., M. L. Sawley, F. Skiff, and A. Pochelon (1987), "On the Analysis of Experimental Signals for Evidence of Deterministic Chaos", Helvetica Physica Acta, Vol. 60, pp. 510-551.

Simoyi, R. H., A. Wolf, and H. L. Swinney (1982), "One-Dimensional Dynamics in a Multi-Component Chemical Reaction", Physical Review Letters, Vol. 49, pp. 245-248.

Smith, L. A. (1988), "Intrinsic Limits on Dimension Calculations", Physics Letters A, Vol. 133, No. 6, pp 283-288.

Sparrow, C. (1982), The Lorenz Equations: Bifurcations, Chaos and Strange Attractors, Springer-Verlag, New York.

Spence, P. D. and J. R. Roth (1987), "Active Modification of Plasma Turbulence with an Effector Probe", 18th International Conference on Phenomena in Ionized Gases, Vol. 2, pp 358-9.

Spence, P., S. Stafford, and J. R. Roth (1988), "Electron Collision Frequency Enhancement and Resistive Drift Wave Turbulence", Proceedings of the 1988 IEEE Conference on Plasma Science, IEEE Catalog No. 88CH2559-3, p. 36.

Sreenivasan, K. R. (1985), "Transitions and Turbulence in Fluid Flows and Low Dimensional Chaos", in Frontiers in Fluid Mechanics, S. H. Davis and J. L. Lumley (eds.), Springer-Verlag, New York, pp. 41-67.

Swinney, H. L. and H. P. Gollub (1978), "The Transition of Turbulence", Physics Today, Vol. 31, No. 8, p. 41.

Takens, F. (1981), "Detecting Strange Attractors in Turbulence" , in Dynamical Systems and Turbulence, D. A. Rand and L. S. Young (eds.), Springer-Verlag, New York.

Theiler, J. (1986), "Spurious Dimension from Correlation Algorithms Applied to Limited Time-Series Data", Physical Review A, Vol. 34, pp. 2427-2432.

Treve, Y. M. and O. P. Manley (1979), "A Possible Strange Attractor in MHD Flow", in Intrinsic Stochasticity in Plasmas, G. Laval and D. Gresillon (eds.), Les Éditions de Physique, Courtaboeuf, France, pp. 393-402.

Wang, P .K. C. (1980), "Nonperiodic Oscillations of Langmuir Waves", Journal of Mathematical Physics, Vol. 21, No. 2, pp. 398-407.

Weiland, J. and J. P. Mondt (1985), "Chaotic Behavior of Thermal Excitations in Edge Plasmas", Physics of Fluids, Vol. 28, No. 6, pp. 1735-1738.

Wersinger, J.-M., J. M. Finn, and E. Ott (1980), "Bifurcation and "Strange' Behavior in Instability Saturation by Nonlinear Three-Wave Mode Coupling" Physics of Fluids, Vol. 23, No. 6, pp. 1142-1154.

Wolf, A., J. B. Swift, H. L. Swinney, and J. A. Vastano (1985), "Determining "Determining Lyapunov Exponents from a Time Series", Physica, Vol. 16D, pp. 285-317.

Zweben, S. J., D. Manos, R. V. Budny, et al. (1987), "Edge Turbulence Measurements in TFTR", Journal of Nuclear Materials, Vol. 145-147, pp. 250-254.

APPENDICES

APPENDIX A

COMPUTATION TIME FOR CORRELATION DIMENSION ROUTINE

If one looks at the way in which the correlation dimension is defined in Chapter IV, it is apparent that many computations are necessary. In fact, when working with N data points, it is necessary to compute N(N-1) distances. This is for each value of r, and each embedding dimension. Therefore, when 2000 points are used, 40 r values, and ten embedding dimensions, it is necessary to perform 1.5992×10^9 computations. This can be fairly time consuming on any computer, and especially so on an IBM-AT, which was used throughout this research. Also, if one considers the fact that the number of computations goes up with the square of the number of data points, one can become discouraged rather quickly. One detail worth mentioning is that though this correlation dimension routine is quite time consuming, it is still more efficient than the box counting method that was used in the past.

Table A-1 lists the amount of time required to compute 39 correlation integrals with 500 points for several types of computers. These calculations were all performed with the same routine used for this research. Table A-2 lists the amount of time needed to compute ten correlation integrals on an IBM-AT for a range of data points.

Table A-1

Computation Times of Thirty-Nine Correlation Integrals for Various Computers[1]

COMPUTER	CHIP/SPEED		ACCESSORIES	TIME
	IBM COMPATIBLES / MS DOS			
IBM PC	8088/4.77	Mhz.	-	59.9 Minutes
Olivetti M24	8086/8	"	-	26.2 "
Tandy 2000	80186/8	"	Hard Disk	22.4 "
IBM XT	8088/4.77	"	HD + 8087	21.8 "
IBM AT	80286/6	"	HD	20.3 "
Tandy 2000	80186/8	"	HD + 8087	8.2 "
Wells American	80286/12	"	HD + 80287	5.1 "
	OTHER			
Definicon	68032/20	"	HD + 68881	1.2 "
Ridge	32 Bit Minicomputer			0.5 "
Cray 2	Supercomputer			1.2 Seconds

1. Source: Dynamical Software User's Manual (W. M. Schaffer et al.)

Table A-2

Time Required to Compute Ten Correlation Integrals on an IBM-AT for Varying Number of Data Points

Number of Points	Time (Min.)
500	2.5
1000	12
2000	55
3000	126
4000	229

APPENDIX B

SPURIOUS CORRELATIONS

As mentioned previously, a problem often encountered when trying to measure the correlation dimension of an experimental signal is due to what is called spurious correlations (Theiler, 1986). This effect manifests itself in the correlation integral plots as a very distinct knee. The slope appears to saturate at low r values and then increases again at higher values of r. The occurrence of this problem may inhibit a good estimate of the dimension, since it tends to reduce the scaling region. Though in most cases it is still possible to obtain the dimension, the accuracy is lessened.

These spurious correlations only occur when working with a limited number of data points, and are usually observed at the higher embedding dimensions. This is because as the embedding dimension is increased, more and more data points are needed to accurately represent the attractor. This effect is worsened when regions of phase space have very few points.

Figures B-1 through B-4 exhibit the effect of the number of data points used to estimate the correlation dimension of a particular set of plasma data. The effect is most noticeable in the derivative curves. As the number of data points increase, the dip in these curves tends to lessen. This would imply a more accurate measure of the dimension for more points. Table B-1 lists the values of correlation dimension for each case.

This probelm of spurious correlations can be avoided by using an infinite number of data points. Unfortunately, this is usually unacceptable due to a lack of time or points. In Theiler's reference, he suggests a method of modifying Grassberger and Procaccia's algorithm to evade this problem.

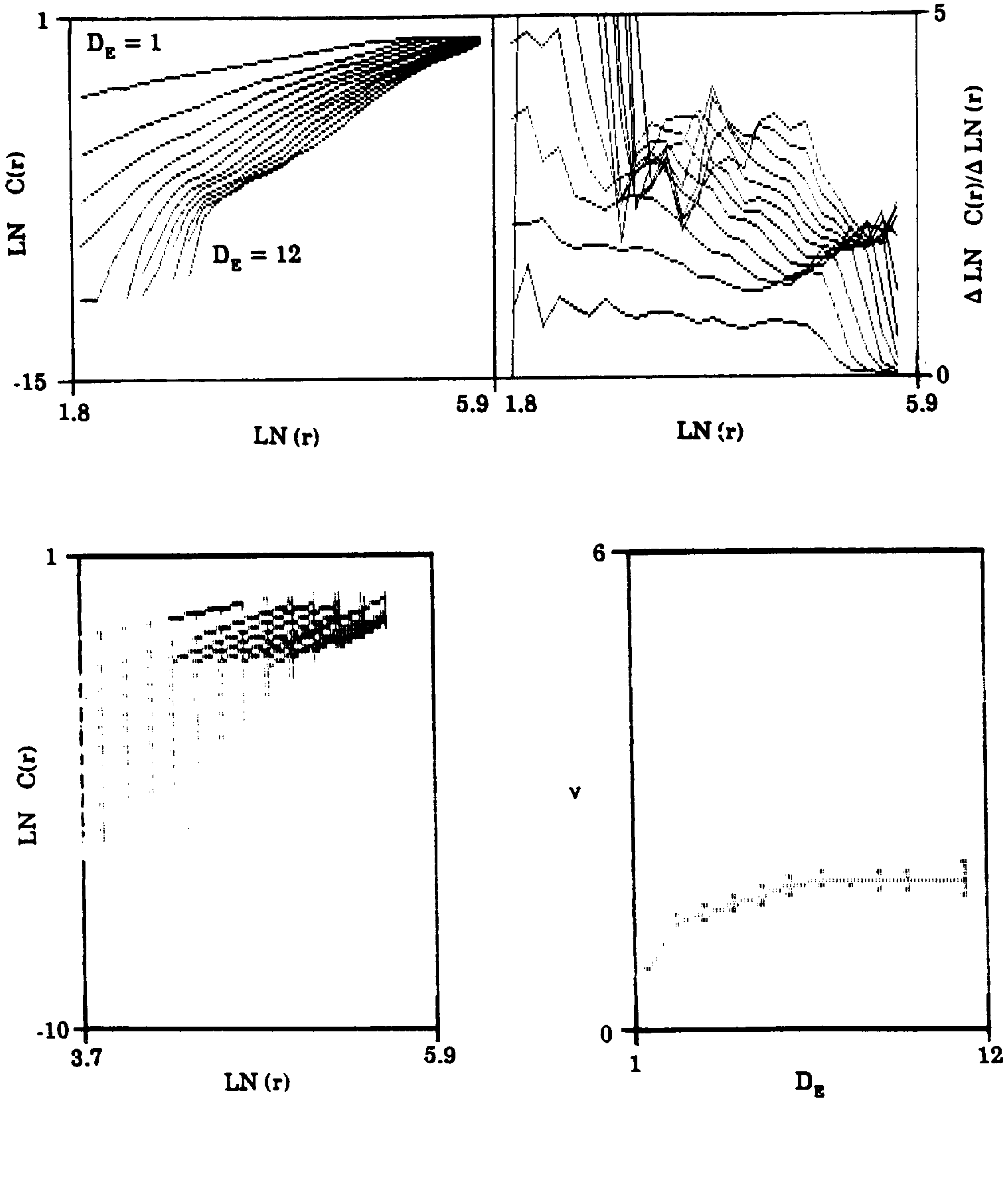

Figure B-1. Correlation plots for N = 500

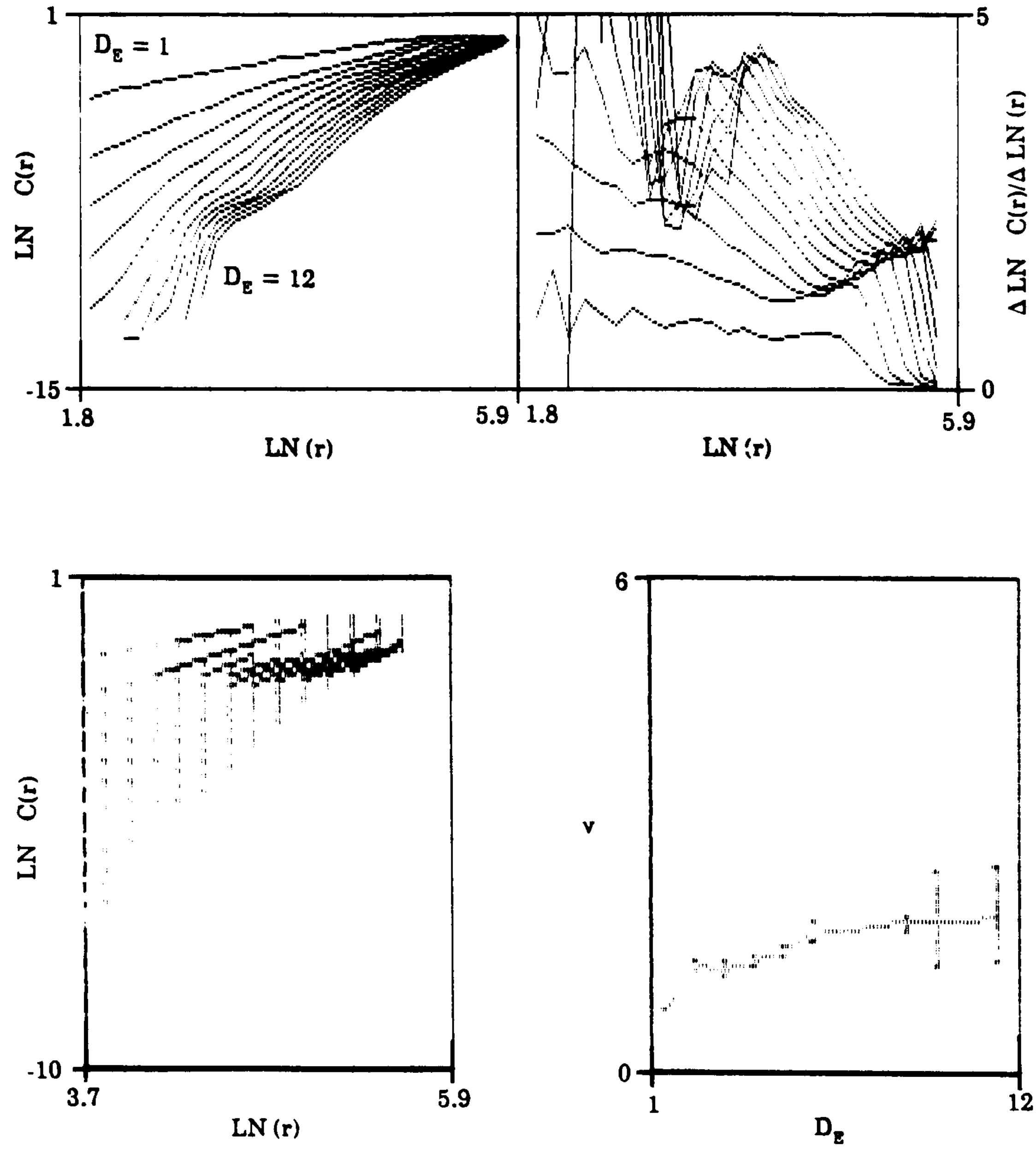

Figure B-2 Correlation plots for N = 1000

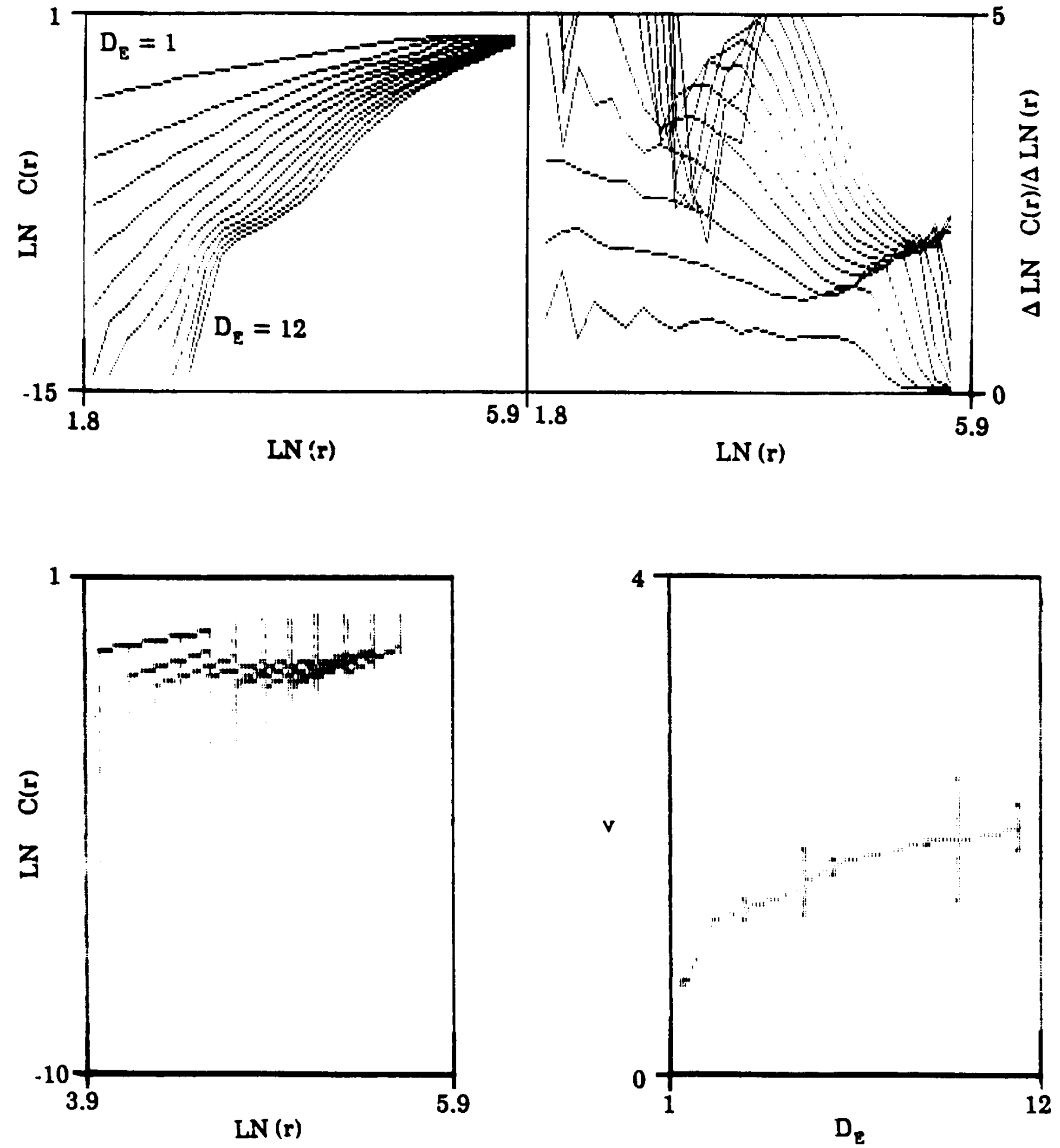

Figure B-3. Correlation plots for N = 2000

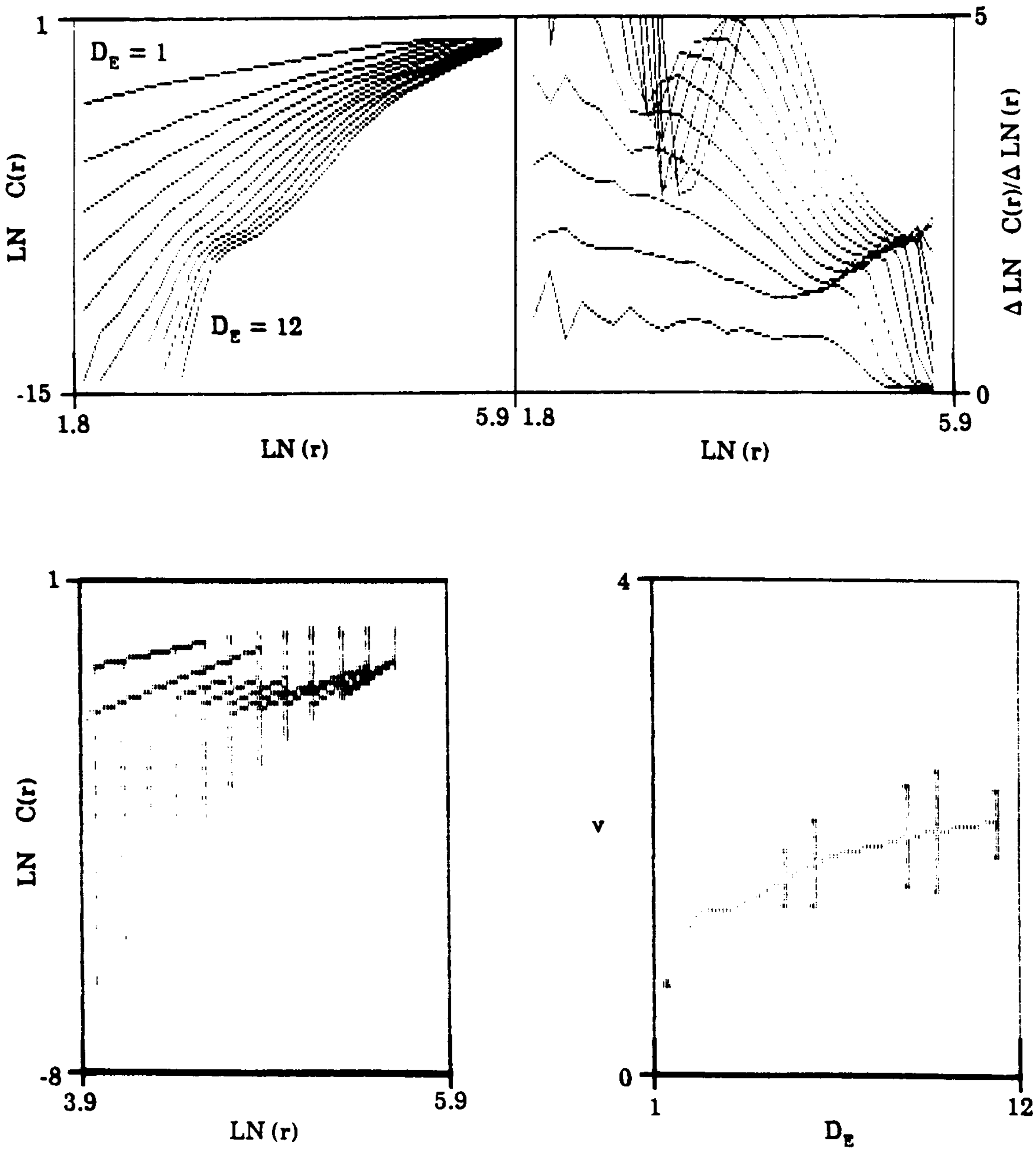

Figure B-4. Correlation plots for N = 3000

Table B-1

Correlation Dimension for Varying Number of Data Points

Number of Points	Dimension
500	1.80
1000	1.90
2000	1.94
3000	2.00

VITA

The author was born in Lynchburg, Virginia on January 28, 1963. He attended high school at Science Hill High in Johnson City, Tennessee. He obtained a Bachelor's degree in Electrical Engineering from Tennessee Technological University in March of 1986.

The author enrolled at the University of Tennessee, Knoxville in the fall of 1986 to work on his Master's degree in Electrical Engineering He received a research assistantship in the UTK Plasma Science Laboratory and performed his thesis research there. The major courses of study for the Master's degree were plasmas and electronics.

The author received his M.S. in Electrical Engineering in May 1989. He then moved to Fort Worth, Texas to work in the Research and Engineering Department of General Dynamics.